DOT/FAA/TC-22/36

Federal Aviation Administration
William J. Hughes Technical Center
Aviation Research Division
Atlantic City International Airport
New Jersey 08405

Advanced Construction Techniques for Heated Pavement Systems

March 2023

Final Report

U.S. Department of Transportation
Federal Aviation Administration

NOTICE

Technical Report Documentation Page

1. Report No.	2. Government Accession No.	3. Recipient's Catalog No.
DOT/FAA/TC-22/36		

4. Title and Subtitle	5. Report Date
ADVANCED CONSTRUCTION TECHNIQUES FOR HEATED PAVEMENT SYSTEMS	March 2023
	6. Performing Organization Code

7. Author(s)	8. Performing Organization Report No.
Hesham Abdualla, Halil Ceylan, Sunghwan Kim, Kasthurirangan Gopalakrishnan, Peter C. Taylor, and Alireza Sassani	

9. Performing Organization Name and Address	10. Work Unit No. (TRAIS)
Department of Civil, Construction and Environmental Engineering College of Engineering Program for Sustainable Pavement Engineering & Research (PROSPER) Institute for Transportation Iowa State University 813 Bissell Road Ames, IA 50011-1066	
	11. Contract or Grant No. 12-C-GA-ISU

12. Sponsoring Agency Name and Address	13. Type of Report and Period Covered
U.S. Department of Transportation Federal Aviation Administration Airport Design and Construction Branch 800 Independence Ave., SW Washington, DC 20591	Final Report
	14. Sponsoring Agency Code AAS-110

15. Supplementary Notes

The Federal Aviation Administration Airport Technology Research and Development Contracting Officer Representative (COR) was Matthew Brynick.

16. Abstract

Ice and snow accumulations on paved surfaces in airports have the potential to cause flight delays and/or cancellations, pavement deterioration, and safety concerns. In recent years, hydronic and/or electrically conductive concrete (ECON) heated pavement systems (HPS) are receiving attention for mitigating problems associated with the presence of ice/snow on roadways and paved areas of airfields. The need to investigate and/or develop new technologies to best automate and accelerate the construction of large-scale heated pavements at airports is imperative. In this study, a detailed review of advanced pavement construction techniques and practices was conducted to evaluate their efficacy and applicability to construction of HPS at airports. System requirements of ECON and hydronic HPS were identified, and laboratory experimental investigations were performed to study their efficiency and performance results, leading to the development of a design procedure for large-scale HPS at airports. Advanced construction techniques and workflows, *viz.*, precast concrete pavement, two-lift paving, and concrete overlays, for heated pavements were demonstrated through three-dimensional (3D) visualizations to provide design and construction guidance for large-scale heated pavement at airports. A 3D finite element model was developed for ECON that can be used as a cost-effective evaluation tool for examining the effects of various design parameters on the time-dependent heating performance of ECON HPS design optimization.

17. Key Words	18. Distribution Statement
Airport, Advance construction techniques, Electrically conductive concrete, Heated pavement system, Cementitious material, Conductivity	This document is available to the U.S. public through the National Technical Information Service (NTIS), Springfield, Virginia 22161. This document is also available from the Federal Aviation Administration William J. Hughes Technical Center at actlibrary.tc.faa.gov.

19. Security Classif. (of this report)	20. Security Classif. (of this page)	21. No. of Pages	22. Price
Unclassified	Unclassified	121	None

ACKNOWLEDGEMENTS

The authors would like to acknowledge the Federal Aviation Administration (FAA) Center of Excellence (COE) for the Partnership to Enhance General Aviation Safety, Accessibility and Sustainability (PEGASAS) for sponsoring this research. The authors thank the following individuals for their support and participation.

Technical guidance and administrative support:
- Mr. Peter L. Sparacino, Mr. Benjamin J. Mahaffay, Mr. Jeffrey S. Gagnon, Dr. Charles A. Ishee, and Mr. Donald Barbagallo, FAA
- Dr. William A. Crossley, PEGASAS, Purdue University
- Dr. Lori J Jarmon and Ms. Miho O. Walczak, Engineering Reseach Institute (ERI), Iowa State University (ISU)

Commercial and general aviation airports:
- Mr. Paul M. Sichko, Minneapolis-St. Paul International Airport
- Mr. Joshua Burger, John Glenn Columbus International Airport
- Mr. Bryan Belt, Des Moines International Airport
- Mr. Dave Poluga, Kent State University Airport
- Mr. David Sims, Mason City Municipal Airport

PEGASAS industrial advisory board and industry partners:
- Mr. Randy Nelson, Full Nelson Consulting
- Dr. Rod Borden, Columbus Regional Airport Authority
- Mr. Simon Caldecott, Piper Aircraft, Inc.
- Mr. Travis Cottrell, Textron Aviation
- Mr. Robbie Cowart, Gulfstream Aerospace Corporation
- Mr. Rick Crider, Kelly Field at Port San Antonio Airport Authority
- Mr. John Frasca and Mr. Bill Hogate, Frasca International, Inc.
- Mr. Jens Henning, General Aviation Manufacturers Association
- Mr. Scott Meacham and Mr. John Gausch, CAP Aviation Consulting Group, LLC
- Mr. Kevin Ohrenberger, Sikorsky Aircraft Corporation
- Ms. Gloria Liu, Continental Motors, Inc.
- Dr. Bob Tanner, Net Jets, Inc.

The authors would like to express their sincere gratitude to Mr. Gary Mitchell, American Concrete Pavement Association for his significant assistance and guidance, other research team members from InTrans's Program for Sustainable Pavement Engineering & Research (PROSPER) and other staff from ERI at Iowa State university for their assistance. The authors would also like to express thanks to Zoltek™ for providing carbon fibers, Asbury Carbons for providing the carbon powders, and The Candlemakers Store (TCS) and WR Grace & Co. for providing admixtures investigated in this study. The contents of this report reflect the views and opinions of the authors and do not necessarily reflect the views of the Federal Aviation Administration.

TABLE OF CONTENTS

LIST OF FIGURES

LIST OF TABLES

LIST OF ACRONYMS

3D	Three-dimensional
AASHTO	American Association of State Highway and Transportation Officials
AC	Alternating current
ACPA	American Concrete Pavement Association
AEA	Air entraining agent
ASHRAE	American Society of Heating, Refrigerating and Air-Conditioning Engineers
ASTM	American Society for Testing and Materials
COE	Center of Excellence
CTE	Coefficient of Thermal Expansion
DC	Direct current
ECON	Electrically conductive concrete
EHPS	Electrically heated pavement system
EMI	Electromagnetic interference
ERI	Engineering Reseach Institute
FAA	Federal Aviation Administration
FAA AC	Federal Aviation Administration Advisory Circular
FDR	Full-depth repair
FE	Finite element
FHWA	Federal Highway Administration
FOD	Foreign object debris
FWD	Falling weight deflectometer
GPS	Global positioning system
HHPS	Hydronic heated pavement system
HMA	Hot-mix asphalt
HPS	Heated pavement system
HRWR	High-range water reducer
HVAC	Heating, ventilation, and air conditioning
ICPCP	Incrementally connected precast concrete pavement
IR	Infrared
ISU	Iowa State University
JPCP	Joint plain concrete pavement
JPrCP	Jointed precast concrete pavement
JRCP	Joint reinforced concrete pavement
NAVAID	Navigational aid
OAT	One-at-a-time
PCC	Portland cement concrete
PCP	Precast concrete pavements
PE	Polyethylene
PEGASAS	Partnership to Enhance General Aviation Safety, Accessibility and Sustainability
PEX	Cross-linked polyethylene
PPCP	Precast prestressed concrete pavement
PROSPER	Program for Sustainable Pavement Engineering & Research
PVC	Polyvinyl chloride
SHRP2	Strategic Highway Research Program 2

SSD	Saturated surface dry
TCS	The Candlemakers Store
TIG	Technology Implementation Group
UTES	Underground thermal energy storage
XPS	Extruded polystyrene

EXECUTIVE SUMMARY

Airport pavement snow removal and runway deicing operations are expensive components of airport operational costs. Occasionally, these operations lead to flight delays impacting travel throughout the United States and worldwide. Chemical pavement deicing can lead to environmental issues with possible contamination of groundwater and nearby bodies of water. Use of sand/chemical mixtures has a potential for creating foreign object damage (FOD) to aircraft engines and corrosion to overall airplane structure. Heated pavement systems (HPSs) provide a potential alternative to the use of chemicals or mechanical means for removing ice and snow from the airport surfaces .

The objective of this research is to develop advanced techniques to best automate and accelerate the construction of large-scale heated airport pavements. Significant problems to be addressed include material selection, joint interfaces, new equipment necessary for installation of heating elements, time factors or construction procedures for installation, and location of ancillary equipment at the airport. This report synthesizes knowledge and experience gained from a state-of-the-art review and laboratory investigations on prototype electrically conductive concrete (ECON) and hydronic heated pavement systems (HHPSs).

Using the optimized ECON mixture recently developed at Iowa State University (ISU), a prototype small-scale ECON slab was designed, constructed, and tested to obtain the efficiency and performance results. This prototype ECON slab provided the lowest energy consumption and lowest energy cost among electrically heated pavement systems developed so far. The two-layer approach utilized in design and construction of the prototype ECON slab is cost-effective in terms of construction cost, energy consumption, and operation cost savings, and it can be implemented for large-scale ECON-based heated pavements through advanced construction techniques such as precast concrete, concrete overlay, and two-lift paving. Based on studies conducted on the prototype ECON slab, design flow and three-dimensional (3D) visualizations were developed and discussed, highlighting design and construction procedures suitable for real and large-scale applications.

Utilizing advanced construction techniques, a 3D visualization schematic and workflow for each HPS type was developed to ensure a more robust construction scheme and well-performing heated airport pavements. This method also ensures that such HPSs will perform as desired (uniform heat distribution in installed areas, effective ice and snow melting, leak-proof systems with advanced pavement joint details, etc.). In addition, 3D visualization schematics can enhance the construction process and sequence and improve communication between airport owner, consultant, and contractor. A 3D finite element (FE) modeling approach was adopted as an alternative method for evaluating ECON HPS time-dependent heating performance and thereby achieve design optimization in a timely manner. The 3D FE model for ECON slabs was developed by examining the decoupling of thermal-electrical analysis (Joule heating) using COMSOL Multiphysics software and validated though comparison with experimental test results. By employing the 3D FE modeling approach developed in this study, the sensitivity of various ECON HPS design variables to heat generation and distribution performance was identified. This could be useful for providing guidance with respect to design optimization.

1. INTRODUCTION

1.1 BACKGROUND AND MOTIVATION

In cold regions of the world where snow events occur during winter season, snow and ice on airport pavement surfaces are major concerns causing infrastructure deterioration (Xi & Olsgard, 2000), damage to concrete pavement (Sutter et al., 2008), and negative environmental impact due to the use of traditional deicing methods (Lewis, 1999). Traditional methods include chemical sprays applied to the pavement surface and large snow removal machines, such as snowplows and snow broom vehicles. These traditional methods, however, have significant drawbacks, including ineffectiveness in low temperatures, negative environmental impacts caused by the contamination of nearby water bodies, and increased labor costs. These methods are also challenging to implement in congested and small areas, such as sidewalks, aprons, and taxiways at airports, causing potential hazards to airport ground crew as well as aircraft.

Heated pavement systems (HPSs) represent alternative options for melting ice and snow and can be classified into two general categories, hydronic heated pavement systems (HHPSs) and electrically heated pavement systems (EHPSs). HHPSs melt ice and snow by circulating heated fluid through pipes embedded inside pavement structures. The cooled fluid circulates back through a heat source that reheats the fluid during each cycle. There are different types of heat sources, including geothermal waters, boilers, and heat exchangers. Geothermal water is considered to be efficient in locations with good geothermal potential (FAA, 2011). EHPSs melt ice and snow using resistive cables embedded in concrete or electrically conductive concrete (ECON). The use of resistive cables embedded inside concrete structures has been applied to deicing of snow and ice in Oregon, Texas, and Pennsylvania, where the performance of electrical cable was sometimes found inadequate due to the high-power density required (Zenowitz, 1977) and damage to electrical cables or associated sensing elements for triggering the system (Joerger & Martinez, 2006).

In recent years, ECON-based HPSs are receiving attention for mitigating the problems associated with the presence of ice/snow on roadways and paved areas of airfields. ECON works by applying a voltage to electrodes embedded in the ECON layer to deliver power to conductive materials, which then melt ice and snow. The effectiveness of the use of various conductive materials, such as steel fiber, carbon fiber, etc., added to conventional concrete to produce ECON with sufficient electrical conductivity (i.e., low electrical resistivity), and their engineering properties have been thoroughly investigated (Gopalakrishnan et al., 2015a).

ECON has been developed and tested to demonstrate the feasibility of melting ice and snow as a practical and cost-effective solution compared to other approaches (Abdualla et al., 2016). ECON system requirements for large-scale HPS construction have also been identified, along with a newly developed methodology for designing and optimizing ECON parameters to achieve sufficient heating based on the required energy (Abdualla et al., 2016).

While the concept of ECON is not new for non-structural applications, such as heating (deicing), sensing, monitoring, and electromagnetic interference shielding, the investigation of this concept for airport pavement-heating applications is limited (Gopalakrishnan et al., 2015b). Furthermore, little guidance and information exists with respect to detailed design, construction, and

performance of ECON-based HPS. Research studies on ECON application in heated pavement systems, and design and construction guidelines for large-scale ECON-heated pavements at airports are also lacking. If ECON-based HPS is to be considered an important emerging technology, it is important to address its system requirements for design, construction, and operation to enhance its efficacy, quality, and performance. Key issues including heating element requirements, detailed design and construction procedures, and operational energy requirements need to be clarified for real-scale applications.

Design and construction procedures of HPS using advanced techniques such as precast concrete pavement (PCP), concrete overlays, and two-lift paving have not previously been investigated. An important benefit of utilizing different advanced construction techniques for HPS is that they provide alternative options for constructing HPS in new or existing pavements and can accelerate construction procedures. For example, construction of an HPS as an overlay that does not require deconstruction of the existing good-condition pavement has great potential as a cost-effective approach.

1.2 RESEARCH OBJECTIVES

The objective of this research is to develop advanced techniques to best automate and accelerate the construction of large-scale heated pavements at airports. Significant problems to be addressed include material selection, joint interfaces, new equipment necessary for installation of heating elements, timing and procedures for construction and installation of elements, and location of airport ancillary equipment.

1.3 REPORT ORGANIZATION

This report presents the system requirements of heated pavements and the design and guidelines for using advanced construction techniques in a real-scale heated airport pavement system. Advanced construction techniques considered in this study include use of PCP, concrete overlay, and two-lift paving.

- Section 1: Introduction. A description of the background and objectives of this study
- Section 2: Literature Review. A comprehensive literature review of advanced construction techniques highlighting its applicability for HPS
- Section 3: System Requirements for ECON HPS. Discussion on the ECON components such as type of electrodes; ECON mixture; and design, construction procedures, and the heating performance for the prototype ECON slab, including the design procedures for large-scale ECON HPS applications for optimizing ECON parameters, such as electrodes spacing, power, voltage, etc.
- Section 4: System Requirements for HHPS. Discussions on design, construction procedures, and heating performance for the prototype hydronic heated slab
- Section 5: Three-dimensional (3D) Visualization of Advanced Construction Techniques for ECON HPS. Discussions on design and construction procedures of ECON using PCP, two-lift paving, and concrete overlays as advanced techniques to provide options for new pavements or existing pavements and to best automate and accelerate the construction of large-scale heated pavements at airports

- Section 6: 3D Visualization of Advanced Construction Techniques for HHPS. Discussions on design and construction procedures of HHPS using PCP, two-lift paving, and concrete overlays as advance techniques to provides options for new pavements or existing pavements and to best automate and accelerate the construction of large-scale heated pavement at airports
- Section 7: Feasibility Study on Development of 3D Finite Element Model for ECON HPS. Discussions on the development of a 3D FE model for evaluating the effects of various design parameters on time-dependent ECON heating performance for ECON HPS design optimization
- Section 8: Conclusions and Recommendations. A summary of the important findings and recommendations from this study

2. LITERATURE REVIEW ON ADVANCED PAVEMENT CONSTRUCTION TECHNIQUES

This section summarizes a state-of-the-art literature review of advanced construction techniques, highlighting their potential for heated pavement construction. Advanced construction techniques considered in this study include PCP, two-lift paving, and concrete overlays. Advantages and limitations of these techniques are reviewed and discussed to identify the feasibility of utilizing these techniques for large-scale HPS construction.

2.1 PRECAST CONCRETE PAVEMENT

PCP has demonstrated satisfactory performance in bridges, pavements, buildings, and airfield construction. It provides high strength, low permeability, and low cracking potential; these features are consequences of preparing the panels off-site where quality control can be more effectively implemented. Using the PCP technique instead of cast-in-place for construction of pavements expedites the construction process by eliminating the need for concrete strength-gaining time from the construction procedure (Bly et al., 2013; Merritt et al., 2004; Priddy, Bly, & Flintsch, 2013). PCP expedites rehabilitation of airfield pavements where the construction work is faster or can be done overnight because precast concrete already has gained its strength and cured at the plant (off-site); therefore, no time is needed for precast concrete to attain its strength after finishing the reconstruction work. Since flight operations must be resumed in the shortest time frame possible, often with only 4 to 6 hours available to complete repairs, the PCP technique is a good choice to minimize the downtime of airport pavement facilities (Bly et al., 2013).

Since the PCP technology enables rapid repair of pavement facilities, it can be beneficially applied where road closures can increase road congestion and result in increased lost work time, fuel consumption, and user-delay costs (Kohler et al., 2004). Merritt et al. (2004) has shown that estimated daily user-delay costs for a four-lane divided facility carrying 50,000 vehicles per day can be as high as $383,000 per day for 24-hour per day lane closure, compared to $1,800 per day for nighttime lane closure only. Because PCP is fabricated and cured in plants under controlled environments, PCP can be installed under different weather conditions. While the sensitivity of Portland cement concrete (PCC) to weather conditions does not permit cast-in-place concrete paving under all weather conditions, under weather conditions such as extremely cold or hot temperatures, using PCP would not prevent the construction work (Merritt et al., 2004). Table 1

presents the difference between PCP and cast-in-place PCC pavement (Chang, Chen, & Lee, 2004).

Table 1. Comparison Between PCP and Cast-in-Place (Chang, Chen, & Lee, 2004)

Parameter	Precast Concrete Pavement	Cast-in-Place
Speed of construction	Possible for immediate opening for traffic	Requires several days or weeks before opening for traffic
Approximate cost	$18.86/ft^2	$3.34-$4.46/ft^2
Quality control	In precast yard (plant)	Cast-in-place on-site
Useful life before the first rehabilitation	30 years	20-30 years
Manpower	Comparatively less	Regular
New equipment needed	Yes	No
Familiarity of engineers and contractors	Unfamiliar	Familiar

PCP construction in the United States began over 50 years ago, but it did not appear to be a cost-effective technique. At that time, technical information was lacking, which resulted in increased installation cost and labor requirements. The process of installing PCP can be time-consuming and require heavy equipment (Priddy, Bly, & Flintsch, 2013). The duration of repair operations is an important cost factor in highways and airports, affecting user-delay cost, road congestion, and facility reopening time. However, over the last 10 years, several U.S. highway agencies have been implementing PCP technology, and the installation price has dropped by more than 50%. The implementation of PCP systems may include both proprietary and non-proprietary systems.

Figure 1 shows the variation of intermittent repair technique with dowel bars positioned in existing concrete pavement. The Strategic Highway Research Program 2 (SHRP2) project R05 provided a guideline for design and construction of different PCP applications and developed a guideline for project selection, design, fabrication, installation, and rehabilitation of PCP systems (Tayabji, Ye, & Buch, 2013). PCP can be used to repair distressed areas of an existing pavement that represent either a small area of localized distress or an extended long-distance distress in the pavement.

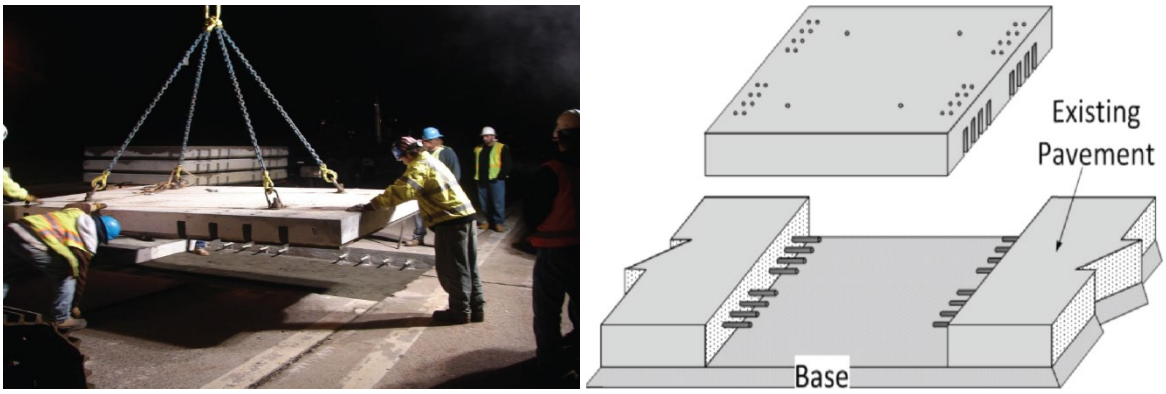

(a) (b)

Figure 1. Intermittent Repair Application for Existing Concrete Pavement

Because PCP implementation has increased, several agencies have participated in developing specifications and guidelines for such systems. The American Association of State Highway and Transportation Officials (AASHTO) established a Technology Implementation Group (TIG) in 2006 that developed a specification for fabrication and construction of PCP and guidelines for the design of PCP systems (Tayabji, Buch, & Kohler, 2009).

The application of PCP technology can be classified into intermittent repair and continuous application (Tayabji, Ye, & Buch, 2013). Full-depth repairs (FDRs) and full-panel replacement are two types of intermittent repairs. Continuous application, unlike intermittent repair of concrete pavement, uses full-scale project reconstruction or putting an overlay on existing pavements; this can apply to either PCC or asphalt cement concrete pavements. Three different types of PCP can be defined as continuous systems; (1) jointed precast concrete pavement (JPrCP) systems, (2) precast prestressed concrete pavement (PPCP) systems, and (3) incrementally connected precast concrete pavements (ICPCP) systems (Tayabji, Buch, & Kohler, 2009; Tayabji, 2019).

Various PCP types have been assessed in comparison to conventional concrete pavement systems; these include joint plain concrete pavement (JPCP) and joint reinforced concrete pavement (JRCP) in terms of design concepts, field installation procedures, advantages, limitations, and costs (Chang, Chen, &Lee, 2004). The PCP methods evaluated included the Super-slab® system, FDR, and the URETEK Method™ (Chang, Chen, & Lee, 2004). The Super-slab system designed by the Fort Miller Co. is intended for use in rapid construction work such as highways, ramps, taxiways, and in heavy traffic areas. Furthermore, it can be used to reduce user cost and to shorten the duration of construction operation. Precast panels of super-slab can be used either for intermittent repairs or continuous paving. The length of each panel can range up to 25 feet, and width can range from a minimum of four feet to a maximum of 12 feet. Precast pavement panels have dowel bars and tie bars on two sides and slots on the other sides. Dowel bars are used to transfer loads to adjacent panels and to connect precast panels. A precast panel has two grout ports, one for bedding the grout ports and the second to fill the dowel slots. Bedding grout ports are used to fill voids between the panels and the graded bedding base. A high-strength grout material is poured through the bedding grout port to provide good interlock with adjacent slabs.

The Super-slab system was selected for installation in the Tappan Zee Bridge toll plaza in Rockland County, New York. Super-slab was chosen so that the construction work could be conducted during night-time hours and allow lane openings during morning rush hours, thereby avoiding excessively high user costs. The project sponsor was satisfied with the construction results, including the appearance and the quality of the precast panels. The capital cost of this project was about $\$26/ft^2$ including fabrication, delivery, and installation. While using PCP cost more than conventional concrete pavement, it dramatically reduced user costs resulting from traffic delay caused by pavement rehabilitation operations.

FDRs, also known as the Michigan method, are used only for intermittent paving, not in continuous paving. The panel size is typically 6 ft x 12 ft (1.8 m x 3.6 m), and each panel contains three dowel bars in each wheel path with the dowels embedded in the precast concrete at the transverse joints. The FDR does not require curing after the placement of PCP as it is prepared and cured off-site.

The URETEK method uses small, drilled holes to allow a polymer resin to lift the panels and fill the underside voids between the panels and the graded bedding base. This method can be used for repairing differential settlements and void conditions underneath concrete or asphalt pavements in both highways and airports. Instead of using dowels, as in the Super-slab system, the URETEK method utilizes a stich-in-time system, a procedure that places a composite-reinforced resin blade (fiberglass tie) to transfer load into an adjacent panel. Once the blade is inserted, the remaining space in the slot is filled with a high-density polymer resin. The advantage of the stich-in-time method is that it is less expensive than the procedure of inserting dowels. Other PCP types (Bly et al., 2013) recently applied in airfield applications include "Soviet-style" slabs and "U.S. Air Force Methods."

2.2 TWO-LIFT CONCRETE PAVING

Two-lift concrete paving (also referred to as two-layer construction or dual-layer paving technology) has become a common construction practice in Europe; in this method, the lower lift can be optimized to enable the use of locally available or recycled materials, while the top lift is optimized for long life and functionality (see Figure 2). Two-lift concrete paving involves the placement of two wet-on-wet layers of concrete or bonding wet to dry layers of concrete where the bottom layer is relatively thicker, and the top layer is relatively thinner (Cable, 2004). One of the benefits of two-lift paving includes using recycled aggregate, which leads to cost reduction and production of more sustainable pavements; this method also provides a high-quality and durable surface, improves skid resistance, and reduces noise (Cable, 2004). These benefits could compensate for the required use of two slipform pavers needed for each layer, and the extra labor and trucking costs associated with them. The use of two-lift concrete pavement is currently under investigation by several agencies in the United States.

Figure 2. Two-lift Construction of Concrete Pavement in Progress (Hu et al., 2014)

Two-lift concrete paving is not a new concept and has been around almost as long as concrete paving itself (Cable, 2004). Two-lift concrete paving was conceptually developed and first constructed in the United States, but it later became more prevalent in Europe (Cable, 2004; Cable & Frentress, 2004). In the early 1950s, the common practice of two-lift paving included placement of a mesh layer between the bottom layer and top layer of concrete; but recently in the U.S., a single, homogenous layer of concrete has typically been used, along with reducing the pavement slab joint length, thereby reducing the application of two-lift paving (Cable, 2004). However, two-lift paving has been implemented in the United States since 1970 in Iowa, Florida, and Michigan, and since the 1930s in European countries, including Austria, Belgium, Germany, and the Netherlands (Cable & Frentress, 2004).

2.2.1 Two-lift Concrete Paving in the United States and Europe

The first use of two-lift concrete pavement was in 1891 in Bellefontaine, Ohio by the Buckeye Portland Cement Company, and the method was patented in 1906 in Chicago, Illinois (Cable, 2004; Cable & Frentress, 2004). Two-lift concrete paving was implemented in the United States with a top-layer concrete thickness in the range of 1.6–4 inches and a bottom layer concrete thickness range of 6–11.8 inches (based on a survey from 1976 to 2012) (Hu et al., 2014). Two-lift concrete paving was constructed in Lyon County, Iowa to demonstrate the feasibility of using recycled aggregate at the bottom lift while the top lift was made with high-quality aggregates. In 1978, Florida constructed a test section of two-lift pavement to investigate the performance of pavement with two different flexural strengths in which the top lift had higher flexural strength than the bottom lift due to the use of low-quality or recycled materials for the bottom lift. The pavement constructed in both the Iowa and Florida projects was reported as being in good condition (Cable, 2004). Because of the availability of local low-quality aggregate in Kansas, a two-lift paving approach was adopted there using the local aggregate for the bottom lift and imported high-quality aggregate for the top lift to provide longevity and functionality. In Michigan,

since pavement surface noise was an issue, two-lift pavements were built with high-quality aggregates in the top lift, the exposed surface, to reduce noise. Application of two-lift paving will help agencies to reduce paving costs and the environmental impact of pavements.

In Europe, two-lift concrete paving was implemented in different countries where, according to a survey from 1989 to 2008, the top-layer thickness of concrete was in the range of 1.6–5.5 inches, and the bottom layer thickness of concrete was in the range of 6–10 inches (Hu et al., 2014). Two-lift paving was used in Germany to reduce noise, increase friction, and achieve a smooth profile by building the top lift of pavements with high-quality aggregate that was also resistant to freeze-thaw effects (Cable & Frentress, 2004). Two-lift concrete paving was used at the Munich airport, with a bottom lift thickness of 9.5 inches and a top lift thickness of 5.5 inches. Locally available aggregates were used in the bottom lift, and high-quality aggregates were used in the top lift. One of Germany's largest companies, Wirtgen GmbH, manufactures slipform pavers capable of paving with a width between 16.4 feet and 50 feet and a depth of up to 17 in. (Cable, 2004). The Austrian government enforced regulations on any upcoming new construction of highway to utilize site materials such as recycled aggregates in concrete mixture; as a result, two-lift paving was used to fulfill the new regulations (Cable & Frentress, 2004). For example, a deteriorated pavement on Freeway A1, a connecting road between Vienna and Salzburg, was demolished, and its materials were recycled to be used for building new pavement. The recycled aggregate was used for the 8.5-inch-thick bottom lift, since the bottom lift is not as sensitive as the 1.6-inch-thick top lift, which contained high-quality aggregate to reduce noise and increase friction.

2.2.2 Construction of Two-lift Concrete Paving

There are no guidance or standards available to specify minimum requirements (e.g., strength, durability) for the characteristics of bottom concrete lift nor are there guidelines for how to achieve durability, safety, and noise reduction on the top lift (Hu et al., 2014).

Two-lift paving requires additional paving machines, mixing plants, belt placers, extra trucks, and labor for the second paver, as shown in Figure 3 (Hu et al., 2014). Since two types of concrete are used in two-lift construction, inspection of incoming concrete loads is required to identify the different concrete mixtures for each layer. Two-lift paving was used in I-70 highway construction in Saline County, Kansas in 2008. Figure 3(a) depicts the construction work showing a two-lift paving-equipment train that includes a spreader with a belt placer, a slipform paver, a burlap drag, and the curing/texturing equipment. The belt placer and slipform paver for the bottom lift are shown in Figure 3(b). The bottom lift was placed with the spreader and the first slipform paver, and the bottom lift concrete mixture was stiffened by adding viscosity-modifying admixtures to it; Figure 3(c) shows inhibit deformation of the bottom lift during placement of the top lift. In addition, a grid was placed under the concrete discharge spreader of the top lift to mitigate the deformation of the bottom lift while placing the concrete for the top lift. Dowel baskets were placed prior to paving, and tie bars were inserted in front of the bottom lift paver. Figure 3(d) illustrates the paving procedures of the top lift using the second belt spreader and slipform paver.

(a) (b)

(c) (d)

Figure 3. Two-lift Construction of Concrete Pavement in Progress: (a) Two-lift Paving Equipment Train, (b) Bottom-lift Belt Placer/Spreader and Paver, (c) Demonstration of the Concrete Stiffness of the Bottom Lift, and (d) Top-lift Belt Placer/Spreader and Paver (Hu et al., 2014; Gerhardt, 2013)

The recommended time for placing the top-lift concrete is between 30–60 minutes after the placement of the bottom-lift concrete to mitigate combining the two concrete mixtures and to obtain a sufficient bond in the wet-on-wet procedure (Cable, 2004). Additional equipment demands, such as slipform paver, belt placer, bath plant, extra labor, and land for placing the equipment have increased the cost of two-lift paving to about twice that of single-lift paving (Gerhardt, 2013). This cost could be reduced by using low-quality or recycled materials at the bottom lift and by utilizing only one slipform to cast both lifts. To reduce the construction cost of two-lift paving, the American company, GOMACO, and the German company, Wirtgen, developed a slipform paver to facilitate the two-lift paving using one slipform paver for both lifts.

2.3 CONCRETE OVERLAYS

Concrete overlay systems have been proposed as cost-effective maintenance and rehabilitation solutions for a wide range of combinations of existing pavement types, conditions, desired service lives, and anticipated traffic loading. Although in the past they have been referred to as ultrathin whitetopping, conventional whitetopping, bonded overlays, unbonded overlays, etc., they have more recently been classified into two broad types (see Figure 4): the bonded resurfacing family and the unbonded resurfacing family (Harrington et al., 2007; Torres et al., 2012). Concrete overlays are discussed in detail in the National Concrete Pavement Technology Center (NCPC), *Guide to Concrete Overlays Solutions 2007* (Harrington et al., 2007) and ACI 325.13R-06 *Concrete Overlays for Pavement Rehabilitation* (ACI Committee 325, 2006).

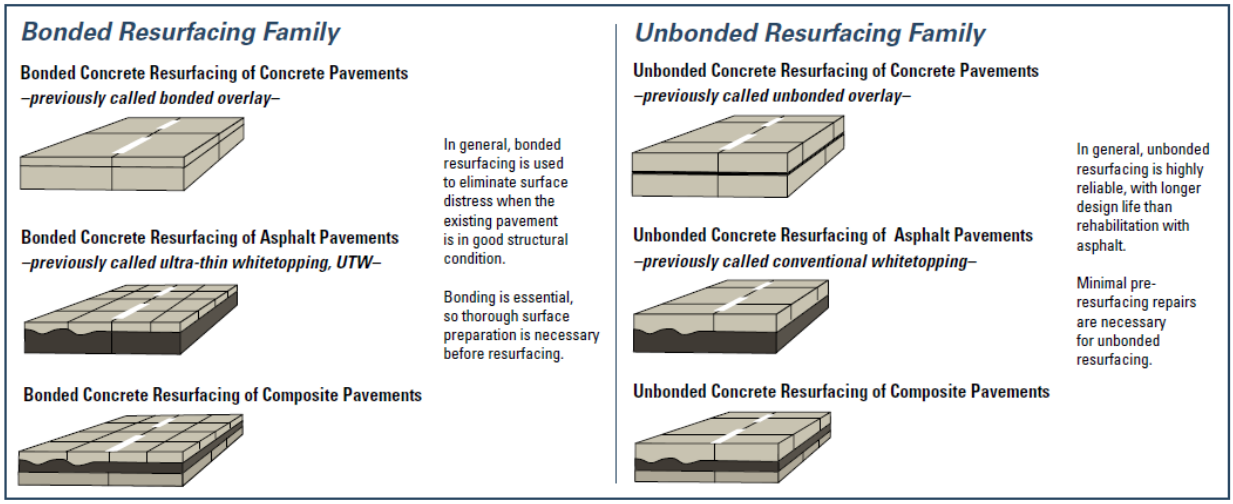

Figure 4. Two Families of Concrete Overlay System (Harrington et al., 2007)

2.3.1 Unbonded Resurfacing Family

Unbonded resurfacing has been used to restore the structural capacity of existing pavements that are in poor or deteriorated condition. Due to the isolated layer, unbonded resurfacing and the existing pavement act independently of one another to mitigate reflective cracking. Since unbonded resurfacing is structurally isolated from the existing pavement, dowel bars should be used to transfer load when the thickness of the pavement is greater than 8 in. (20.3 cm) and when loads are heavy.

2.3.1.1 Unbonded Concrete Resurfacing of Concrete Pavements

In the past, unbonded resurfacing of concrete pavements was called unbonded overlay. The recommended thickness of unbonded resurfacing of concrete pavement is in the range of 4–11 in. (10.2–27.9 cm) depending on the anticipated traffic load and condition of the existing pavement. Unbonded resurfacing of concrete pavements has been successfully implemented with good to excellent performance in many states, including California and Iowa. The crucial parameters that affect the performance of unbonded concrete resurfacing are separator layer design, resurfacing

thickness, joint spacing, and load transfer, as well as the condition of the subgrade that may pose failure to the surface, shoulder, and clearance.

2.3.1.1.1 Design

The design thickness of unbonded concrete resurfacing placed on existing concrete pavement may be calculated using a design procedure similar to that for designing a new concrete pavement on a rigid base with consideration of the separated layer. The design procedures for highway roads include the 1993 AASHTO design guide (AASHTO, 1993) or the Portland Cement Association (Packard, 1984) design guideline (Mallick & El-Korchi, 2013). The FAA Advisory Circular (FAA AC) 150/5320-6F provides guidance on the design and evaluation of pavements used by aircraft at civil airports (FAA, 2016). The joints of unbonded resurfacing may be matched or mismatched with the existing concrete pavement; this is because some states enforce matching the joints of the unbonded resurfacing, while others deliberately mismatch the joints. According to previous specifications, mismatching joints of unbonded resurfacing with existing pavement increases the efficiency of load transfer (Mallick & El-Korchi, 2013). The load transfer performance has been recognized as better than a new concrete pavement because of the support provided by the underlying pavement. Dowels are recommended when unbonded resurfacing must support high volumes of traffic. In general, if the unbonded resurfacing thickness exceeds 8 in. or more, dowels should be used. Short joint spacings are recommended to mitigate the effect of curling stresses. Joint spacing is typically 6–15 ft depending on the unbonded resurfacing thickness.

Since unbonded resurfacing relies on the absence of bonding between the resurfacing and the existing pavement, the design of the separator layer can have a dramatic effect on pavement performance. The separator layer prevents reflective cracking and isolates the concrete resurfacing from the existing pavement so that both layers move individually. A fine-grade asphalt mixture has been recommended as a separator layer and this provides excellent results compared to others, such as polyethylene sheeting, liquid asphalt, and chip seal; these are not recommended due to poor performance (Mallick & El-Korchi, 2013;ACI Committee 325, 2006). The thickness of the separator layer is typically 1–1.5 in. depending on the existing pavement condition. The separator layer also does not enhance the pavement's structural capacity. The drainage condition of the existing pavement also has a significant effect on the separator layer performance, increasing the risk of stripping in the separator layer. The separator layer has the potential to cause early-age shrinkage in unbonded resurfacing if the weather temperature exceeds 120 °F (48.9 °C), so proper curing should be used to reduce the surface temperature before placing concrete resurfacing.

2.3.1.1.2 Construction

The construction procedure for unbonded concrete resurfacing of concrete pavement is similar to that of placing, spreading, consolidating, and finishing conventional concrete. The construction of unbonded resurfacing may entail constructing a new shoulder because the grade elevation might increase, typically in the range of 10–12 in. (25–30 cm) (Mallick & El-Korchi, 2013); so, if a shoulder is needed, a tied shoulder should be used to widen the unbonded resurfacing pavement. The benefits of a tied shoulder are to reduce edge stresses and longitudinal cracking. The depth of transverse and longitudinal saw-cuts is typically between one-fourth and one-third of the resurfacing concrete thickness.

2.3.1.2 Unbonded Concrete Resurfacing of Asphalt Pavements

Unbonded concrete resurfacing of asphalt pavements has been used in different states as a rehabilitation and maintenance solution providing good to excellent performance. In the past, unbonded concrete resurfacing of asphalt pavements was called conventional whitetopping. Unbonded concrete resurfacing has the potential to increase the life of pavements that exhibit extensive deterioration, include rutting, shoving, potholes, and pumping (see Figure 5). While distressed asphalt pavement areas do not have to be repaired before placing concrete resurfacing, milling may be required if the existing asphalt has extensive deterioration.

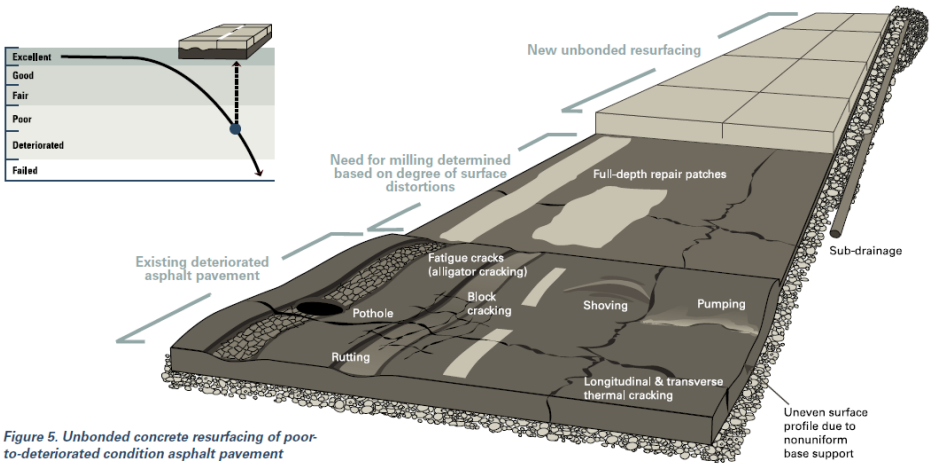

Figure 5. Unbonded Concrete Resurfacing of Asphalt Pavement (Harrington et al., 2007)

The crucial factor affecting the performance of concrete resurfacing of existing asphalt or composite pavement is uniformity of the base support that can contribute to enhancing pavement performance. Although this resurfacing type does not rely on bonding, some partial bonding between the resurfacing and existing asphalt pavement can contribute to better pavement performance.

2.3.1.2.1 Design

The thickness of unbonded resurfacing of asphalt pavement is typically 4–11 in. (10.2–27.9 cm) depending on desired life, anticipated traffic loading, and the condition of the existing pavement. The thickness of unbonded resurfacing can be designed using conventional concrete pavement procedures, such as those given in the 1993 AASHTO design guide (AASHTO, 1993) and the American Concrete Pavement Association (ACPA) StreetPave software program. The ACPA StreetPave software utilizes new engineering analyses to produce optimized designs for city, municipal, county, and state roadways. According to rigid pavement analysis and design guideline published by the Federal Highway Administration (FHWA), joint spacing may be estimated in feet as twice the slab thickness in inches (Heinrichs et al., 1989). Short joints are recommended to reduce curling and warping stresses due to high k-values. There is discrepancy regarding whether dowel bars should be used. In previous experiences reported by different agencies, unbonded resurfacing without dowel bars was used and its performance was reported satisfactory (Mallick & El-Korchi, 2013). On the other hand, other agencies reported highway faulting problems

attributed to the absence of dowels in unbonded resurfacing (Mallick & El-Korchi, 2013). Nonetheless, doweling of joints is recommended if the unbonded pavement resurfacing undergoes high-volume traffic. To accelerate early-age strength gains of concrete pavement to significantly reduce the downtime of the traffic lane, accelerating admixtures should be used to achieve early opening and reduce road user cost.

2.3.1.2.2 Construction

Before placing unbonded concrete resurfacing of asphalt pavements, the existing pavement should be smooth and free of extensive rutting and surface distortion (see Figure 6). High surface asphalt temperature also has the potential to cause early-age shrinkage in unbonded resurfacing if the weather temperature exceeds 120 °F (48.9 °C), so proper curing should be used to reduce the surface temperature before placing unbonded concrete resurfacing. The construction procedure of unbonded concrete resurfacing of asphalt pavement is similar to placing, spreading, consolidating, and finishing conventional concrete. The depth of transverse and longitudinal saw-cut is typically between one-fourth and one-third of the resurfacing concrete thickness.

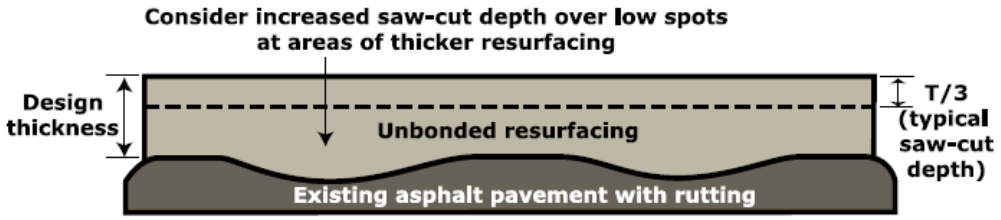

Figure 6. Asphalt Rut Depth When Determining Saw-cut Depth (Harrington et al., 2007)

2.3.2 Bonded Concrete Resurfacing Family

Bonded concrete resurfacing, in contrast to unbonded concrete resurfacing, can be used when the existing pavement is in good or better structural condition, perhaps with some surface distress. Bonded resurfacing can be used to extend the life of existing pavements by eliminating structural and functional deficiencies such as rutting, pothole problems, surface friction, noise, ride quality, etc.

Bonded concrete resurfacing has been successfully used in existing concrete pavements. When bonded resurfacing is placed on concrete pavements, i.e., JPCP, joints should match with the underlying pavement to prevent reflective cracking and to behave as a monolithic pavement. Moreover, the aggregate properties of the bonded surfacing should be compatible with those of the underlying pavement to mitigate shear stress. When bonded resurfacing is to be placed on asphalt concrete, it is important to ensure that the pavement surface is uniform and free of surface distortion to provide a sufficient bond. Since bonded resurfacing is thin, dowel bars cannot be used; however, the dowel bars in the existing pavement can provide load transfer.

2.3.2.1 Bonded Concrete Resurfacing of Concrete Pavements

In the past, bonded resurfacing of concrete pavements was called bonded overlay. The recommended thickness of bonded concrete resurfacing of concrete pavement is in the range of 2–5 in. (5.1–12.7 cm), and it can be selected based on desired life, anticipated traffic loading, and the condition of existing pavement.

2.3.2.1.1 Design

The design concept of bonded resurfacing assumes that the bonded resurfacing and the existing pavement behave monotonically to reduce stresses and deflections. If the bonded resurfacing and existing pavements are not adequately bonded, chances are that an early age cracking will occur due to the increase of curling and loading stresses in the concrete resurfacing.

Before applying bonded concrete resurfacing of concrete pavements, the existing concrete pavements should be in good or better structural condition with some surface distress as shown in Figure 7, so an evaluation of existing pavement is significantly important in determining the feasibility of applying bonded concrete resurfacing as the best candidate for a rehabilitation solution. The evaluation of existing concrete pavements includes falling weight deflectometer (FWD), visual inspection, and coring of the existing pavement. The design thickness of bonded resurfacing can be calculated using the 1993 AASHTO design guide (AASHTO 1993) or the Portland Cement Association (Packard, 1984) design guideline (Mallick & El-Korchi, 2013). The required thickness of bonded resurfacing—using the AASHTO approach—is the difference between the structural capacity of a new concrete pavement and the effective thickness of the existing pavement. The joints of bonded resurfacing of concrete pavements should be matched with existing pavements to eliminate reflective cracking and behave as a monolithic pavement. Since the thickness of bonded resurfacing is thin, dowels cannot be used; however, the dowels in the existing pavement can transfer the loads to the adjacent slabs.

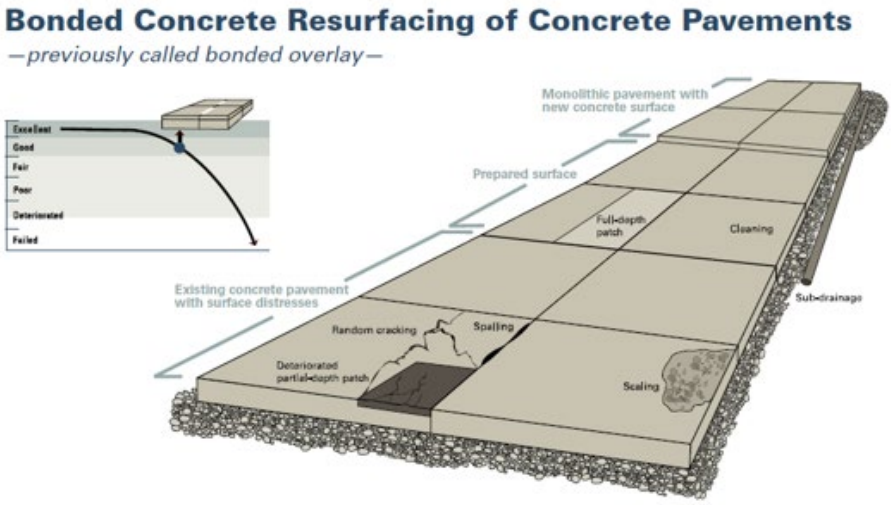

Figure 7. Bonded Concrete Resurfacing of Good Condition Concrete Pavement (Harrington et al., 2007)

2.3.2.1.2 Construction

The concrete mixture of bonded concrete resurfacing should be compatible with the existing concrete pavement. This recommends using rapid-strength materials to quickly gain strength, as well as considering the effect of thermal expansion, contraction, and shrinkage to minimize stresses at the bonding layer. A slump value in the range of 2–3 in. (5.1–7.6 cm) is suggested to provide sufficient bonding grout. Fibers added to the bonded resurfacing mixture reduce plastic shrinkage cracking and improve toughness and post-cracking behavior. The aggregate coefficient of thermal expansion of the resurfacing concrete should be comparable to that of the existing concrete to reduce thermal stresses at the bond interface. To ensure sufficient bond between bonded concrete resurfacing and existing concrete pavement, an assortment of approaches to surface preparation may be implemented, including shot-blasting, milling, and sandblasting. The most common practice for surface preparation is to use shot-blasting followed with air blasting, then placing the resurfacing concrete. A bonding agent is not recommended for use as a bonding material because a bonding agent may cause debonding between the layers if it dries before placing the resurfacing concrete (Delatte, 2014). After paving the resurfacing concrete, the recommended sawing time is in the range of 4–12 hours, as long as the concrete pavement gains its strength to prevent spalling or raveling at joints (Mallick &El-Korchi, 2013; Delatte, 2014). The suggested saw-cut joint depth is half the overlays thickness, although others have recommended a saw-cut extending through the entire depth of the overlay.

2.3.2.2 Bonded Concrete Resurfacing of Asphalt Pavements

Bonded concrete resurfacing was previously known as ultra-thin whitetopping. The recommended thickness of bonded concrete resurfacing of asphalt pavements is in the range of 2–5 in. (5.1–12.7 cm) depending on desired life, anticipated traffic loading, and the condition of the existing pavement. Good performance of bonded resurfacing of asphalt pavement has been successfully implemented in many states. The existing asphalt pavement should be in good to fair structural condition, and asphalt pavements with severe surface distress such as rutting, shoving, or alligator cracking may be milled to provide better bonding (Delatte, 2014). A proper evaluation of asphalt pavement is significantly important to ensure the bond quality between the resurfacing concrete and the asphalt pavement and to help in evaluating the design thickness of the resurfacing concrete. The evaluation of asphalt pavement can be performed using visual inspection, core samples for testing, and a falling-weight deflectometer (FWD).

2.3.2.2.1 Design

The design thickness of bonded concrete resurfacing of asphalt pavements can be calculated using design procedures of the American Concrete Pavement Association (ACPA, 1998).

The joint spacing for bonded resurfacing of asphalt pavements ranges from 3–8 ft (0.9–2.4 m), and generally, the joint spacing in feet is typically 1–2 times the pavement thickness in inches; the resurfacing concrete is saw-cut into squares. Use of the recommended joint spacing helps to reduce the stresses due to curling and warping. Joints should be located so as to avoid the wheel path, or the aggregate interlock may be unable to withstand and transfer heavy truck loads (Delatte, 2014). In this case, there would be no need for sealing the joints. The depth of the saw-cut for longitudinal

joints and transverse joints should be one-third and one-fourth of the resurfacing concrete thickness, respectively.

2.3.2.2.2 Construction

Before placing the bonded concrete resurfacing of asphalt, the distresses in the existing pavement should be removed. Milling can be used to repair the surface of the existing pavement from significant surface distortions and to enhance the bond between two layers. Either fixed-form or slipform paving can be used to place the bonded concrete once the existing surface has been prepared. Fixed-form is suggested for pavement with short length, complicated geometry, or variable width. On the other hand, in the case of high production paving, slipform would be more appropriate (Delatte, 2014).

2.3.3 Concrete Overlays and ECON Requirements

Tables 2 and 3 summarize the characteristics of bonded and unbonded concrete overlays and compare them against ECON requirements. The recommended ECON thickness is in the range of 2–4 in., similar to the thickness of bonded concrete overlays. ECON using a bonded concrete overlay will meet the requirements for the bonded overlay thickness. The ECON mixture includes conductive materials and other admixtures to reduce the electrical resistivity from that of bonded or unbonded concrete mixture as shown in Tables 2 and 3. Embedding dowel and/or tie bars in the ECON layer is not recommended.

Table 2. Summary of Bonded Concrete Overlays and ECON Requirements

Items	Bonded Concrete Overlay Options			ECON Requirements
	On Asphalt Pavements	On Concrete Pavements	On Composite Pavements	ECON
Old name	Ultra-thin whitetopping	Bonded overlays	Not Applicable	ECC
Thickness	2–6 in	2–6 in.	2–6 in.	2–4 in.
Mixture design				
Fiber	Optional	Optional	Optional	Carbon fiber
Aggregate property (CTE)	Similar or lower than the existing pavement	Similar or lower than the existing pavement	Similar or lower than the existing pavement	Similar or lower than the existing pavement
Accelerated mixtures	Optional	Optional	Optional	Optional
Joints				
Maximum joint spacing (ft)	1.5 times thickness (in.)	Match existing cracks and joints and cut intermediate joints	1.5 times thickness (in.)	Flexible
Transverse joint spacing	3–8 ft	Match existing joints	3–8 ft	Flexible
Longitudinal joint spacing	3–8 ft	Match existing joints	3–8 ft	Flexible
Transverse joint saw-cut depth	T/3	Full depth plus 0.50 inch	T/3	Flexible
Longitudinal joint saw-cut depth	T/3	T/2 (at least) or (Full depth plus 0.50 inch)	T/3	Flexible
Joint pattern	Square	Joints must match with existing pavement (to reduce curling stresses, smaller overlay panels might be used)	Square	Flexible
Transverse dowel bars	No	No	No	Prefer not to have dowel or tie bars
Longitudinal tie bars	No	No	No	Prefer not to have dowel or tie bars
Separator layer—HMA	No	No	No	No
Joint sealing	Contraction and construction joints should be filled with hot-poured joint sealant (backer rod is not recommended)	Yes, hot-poured joint sealant	Contraction and construction joints should be filled with hot-poured joint sealant (backer rod is not recommended)	Flexible

ECC = Electrically conductive concrete
CTE = Coefficient of Thermal Expansion
T = Thickness
HMA = Hot-mix asphalt

Table 3. Summary of Unbonded Concrete Overlays and ECON Requirements

Items	Unbonded Concrete Overlay Option			ECON Requirements
	On Asphalt Pavements	On Concrete Pavements	On Composite Pavements	ECON
Old name	Conventional whitetopping	Unbonded overlay	Not Applicable	
Thickness	4–11 in.	4–11 in.	4–11 in.	2–4 in.
Mixture design				
Fiber	Optional	Optional	Optional	Carbon fiber
Aggregate property (CTE)	Similar or lower than the existing pavement	Similar or lower than the existing pavement	Similar or lower than the existing pavement	Similar or lower than the existing pavement
Accelerated mixtures	Optional	Optional	Optional	Optional
Joints				
Maximum joint spacing (ft)	T < 6 in. — spacing 2 times T (in.) T ≥ 6 in. — spacing 2 times T (in.) T > 7 in. — spacing 15 ft	T < 5 in. — spacing 6 x 6 ft T 5-7 in. — spacing 2 times T (in.) T > 7 in. — spacing 15 ft	T < 6 in. — spacing 2 times T (in.) T ≥ 6 in. — spacing 2 times T (in.) T > 7 in. — spacing 15 ft	3—6 ft
Transverse joint saw-cut depth	T/4 min - T/3 max	T/4 min - T/3 max	T/4 min - T/3 max	Flexible
Longitudinal joint saw-cut depth	T/3	T/3	T/3	Flexible
Joint pattern	Square	It is not critical to mismatch overlay joints to the underlying joints. Mismatch joints enhance the benefit of load transfer	Square	Flexible
Transverse dowel bars	Yes, when T ≥7 in.	Yes, when T ≥7 in.	Yes, when T ≥7 in.	Prefer not to have dowel or tie bars
Longitudinal tie bars	Yes, when T ≥6 in.	Yes, when T ≥6 in.	Yes, when T ≥6 in.	Prefer not to have dowel or tie bars
Separator layer—HMA	No	Typically, 1 in. asphalt or geotextile fabric	No	Not Applicable
Joint sealing	Yes, hot-poured joint sealant	Yes, hot-poured joint sealant	Yes, hot-poured joint sealant	Flexible

CTE = Coefficient of Thermal Expansion
T = Thickness
HMA = Hot-mix asphalt

2.4 SUMMARY: ADVANTAGES AND LIMITATIONS OF ADVANCED CONSTRUCTION TECHNIQUES FOR HEATED PAVEMENT APPLICATIONS

Table 4 summarizes advantages and limitations of use of advanced construction techniques for heated pavement applications in comparison to use of cast-in-place in HPS construction (Chang, Chen, & Lee, 2004; Tayabji, Ye, & Buch, 2013; Hu et al., 2014; Harrington et al., 2007).

Table 4. Advantages and Limitations of Use of Advanced Construction Techniques for Heated Pavement Applications

	Advantages	Limitations
Precast concrete pavement	• Better concrete quality • Better curing conditions at fabrication plant • Minimal weather dependency of concrete placement • Reduced delay prior to opening to traffic—no onsite curing of concrete • A mature, but still evolving technology	• Expensive • Still relatively new • Difficult to achieve smooth surface
Tow-lift paving	• Economic paving sections can be achieved • Many choices available for surface texture • Reduced tire/pavement noise • Improved sustainability by recycling	• Not a time-efficient process • Lacking sufficient data to support long-term performance • Majority of the contractors in the U.S. have perceived concerns on two-lift concrete paving • Fewer contractors in the U.S. have completed two-lift paving project • Extra permits and land space needed for additional equipment
Concrete overlays	• Can be designed to achieve a service life in the range of 15 to over 40 years • Can be constructed rapidly and with effective construction traffic management • Can be applied to a wide variety of existing pavements exhibiting a wide range of performance issues • Cost effective	• Lack of consideration of the structural contribution of the interlayer and its interaction with the overlay and the existing pavement in terms of friction or bonding • Overestimation of the existing pavement effective thickness when the existing slab is relatively thick • Not sufficient data to support long-term performance • Lack of consideration of curling and joint spacing in the concrete overlay

3. SYSTEM REQUIREMENTS FOR ECON HPS

3.1 SCOPE AND OBJECTIVES

The system requirements for ECON-based HPS are related to material selection, design, construction, and operational performance. To identify these system requirements, a prototype ECON slab was constructed and tested for its efficiency and performance. A design flow chart was developed to clarify the design procedures and to optimize the ECON variables such as electrode spacing, required voltage and current values, and an ECON's geometry for large-scale HPS applications.

3.2 CONSTRUCTION MATERIALS

The main components of the ECON HPS include conductive materials (heating elements) for ECON, electrodes, insulation layers, a power supply, and temperature sensors. An ECON-based HPS works by applying an electric current through electrodes embedded in a conductive concrete layer. Because it has lower electrical resistivity than normal concrete, ECON behaves like a conductor of electricity.

The ability of an ECON HPS to melt snow and ice depends on the electrical resistivity (i.e., the reciprocal of electrical conductivity) of conductive materials; the value required for deicing applications should be less than 1,000 Ω·cm (Gopalakrishnan et al., 2015a; Yehia et al., 2000). The electrical resistivity of conventional concrete varies according to whether it was air dried, oven dried, or not dried at all. The electrical resistivity values of air-dried conventional concrete range from 600 to 1,000 kΩ·cm; oven-dried values are about 10^8 kΩ·cm. When not dry, conventional concrete is considered a semiconductor with a resistivity value of about 10 kΩ·cm (Gopalakrishnan et al., 2015a).

Previous studies have investigated the addition of conductive materials to conventional concrete as heating elements (Xie et al., 1995; Tuan, 2004). Such materials typically include steel fibers, graphite powder, and carbon particles, and they are incorporated into concrete in proportions from 1% to 20% by volume; reported electrical resistivity values range from 400 to 2.4×10^5 Ω·cm.

Researchers at Iowa State University (ISU) recently developed a new ECON mix that includes carbon fiber-based materials (Ceylan, 2015; Sassani et al., 2015). Table 5 shows the ECON mix proportion developed by the ISU research team. The mix contains 0.75% of 6-mm-long carbon fiber by volume of the total concrete mix. It also utilizes methylcellulose as a fiber-dispersive agent to make carbon fiber particles well-distributed and consequently to improve the electrical conductivity property. Its electrical resistivity value was in the range of 50–200 Ω·cm at room temperature (i.e., 20 °C ambient temperature), consistent with electrical conductivity magnitudes reported by previous studies (Yehoa et al., 2000; Heymsfield et al., 2013; Tuan, 2008; Tuan, Nguyen, & Chen, 2010; Tuan, 2004a; Xie & Beaudoin, 1995; Zuofu, Zhuoqiu, & Jianjum, 2007; Wu, Huang, Chi, & Weng, 2013; Tuan, 2004b). The 28-day compressive strength of the developed ECON mix was 40 MPa, translating into a 28-day flexural strength value of 4.0 to 5.0 MPa using various strength conversion equations included in the ACPA strength converter web application (ACPA, 2015). These strength properties meet the minimum strength requirements mentioned in the FAA specification (FAA, 2016). These results imply that the developed ECON has better

electrical properties with adequate mechanical properties, representing improvement over mixtures reported in the literature.

Table 5. Mix Proportion for ISU ECON

Components		Type	Content
Basic	Coarse aggregate	Limestone	1,010 kg/m^3
	Fine aggregate	River sand	634 kg/m^3
	Fly ash	Class F	72 kg/m^3
	Cement	Holcim Type I/II	289 kg/m^3
	Water	Tap water	162.5 kg/m^3
Admixtures	Methylcellulose	Dispersive agent	1.4 kg/m^3
	AEA	MasterAir AE 90	324 ml/ m^3
	HRWR	MasterGlenium 7500	2.5 kg/m^3
	Carbon fiber 6-mm	Synthetic carbon fiber	0.75 (% Vol.)

AEA = Air entraining agent
HRWR = High-range water reducer
Note: Aggregate contents presented are in saturated surface dry condition (SSD).

Table 6 summarizes the electrode types reported in the literature for application of ECON for ice and snow melting purposes. Most metallic materials identified as electrodes could provide sufficient electric current flow results since the electrical conductivity of ECON is lower than any metal. However, an important lesson learned from previous studies is that a good bond between the electrodes and the conductive concrete is very essential to ensure adequate heating performance. The use of embedded steel plates was unable to provide desirable heating performance due to smooth bonding between the conductive concrete and the electrodes (Tuan, 2004a). Conductive adhesive was suggested for use in obtaining a sufficient bond between the electrodes and conductive concrete, but this solution is reported to be not very cost-effective (Xie & Beaudoin, 1995). The use of perforated steel and perforated stainless-steel plates with gaps larger than the maximum aggregate size are also recommended to ensure that conductive concrete can be bonded with the electrode (Tuan, 2004a; Zuofu, Zhuoqiu, & Jianjum, 2007; Chen & Gao, 2012).

In the design and construction of the prototype ECON-heated slab for this study, by considering its advantages, perforated galvanized steel with a gap size larger than the maximum aggregate size was selected as an electrode. Although perforated stainless steel provides similar results, it is not cost-effective in comparison with perforated galvanized steel.

Table 6. Summary of Electrode Materials and Shapes Reported in Literature

Material Type	Shape	Result Reported	Reference
Steel	Circular bar	Ineffective bonding and affected by corrosion	Heymsfield et al., 2013
Perforated steel	Angle plate	Effective bonding	Tuan, 2004a
Perforated stainless steel	Plate	Effective bonding and resisted corrosion	Zuofu, Zhuoqiu, & Jianjum, 2007; Chen & Gao, 2012
Galvanized iron	Not reported	Effective bonding and resisted corrosion	Tian & Hu, 2012

As a cost-effective solution, a thin, thermal insulation layer could be used to minimize heat loss and reduce the total heat required to melt ice and snow. The percentage of back and edge heat loss can be defined as follows: 0% heat loss if both bottom and edges are insulated, 4% of heat loss if only the bottom is insulated, 10% heat loss if both perimeter and edge are isolated, and 20% heat loss if no insulation is used at all (Viega, 2005). The materials reported in use for the insulation layer include epoxy coating and mortar, sawdust mortar consisting of equal parts of cement, sand, and sawdust (Yehia & Tuan, 1999), and the extruded polystyrene (XPS) insulation board (Yang et al., 2012). However, epoxy coating and mortar did not provide good insulation, so this material is not recommended for thermal insulation. The results indicated that using XPS foam board insulation as thermal insulation was sufficient to prevent heat loss, thereby minimizing cost of energy consumption; so, in the design and construction of the prototype ECON-heated slab in this study, XPS foam board insulation was utilized to prevent heat losses.

The resistivity of conductive concrete will decrease with increasing voltage while using either alternating current (AC) or direct current (DC). The resistivity values of conductive concrete are lower when using AC in comparison to DC (Chen & Gao, 2012). When using AC to power ECON, AC takes different paths, passes through the slab in more distributed fashion, and consequently provides good heat distribution (Tuan, 2004a). When using DC to power ECON, the DC takes one path and has the possibility of creating hot spots, i.e., localized heating spots (Tuan, 2004a). While use of photovoltaic system as a source of energy to power ECON was investigated (Heymsfield et al., 2013), the photovoltaic energy system utilized could not provide enough power to melt snow and ice through ECON.

3.3 ELECTRICAL CIRCUIT AND SNOW/ICE MELTING MODELS

The model shown in Figure 8 represents the electrical circuit model for ECON HPS. The heating element (conductive material) equivalent circuit is represented by a set of resistors and capacitors, with the resistors and capacitors symbolized as “R” and “C” in Figure 8. A distributed model is selected to represent the evenly spread conductive material under the snow and ice area. The circuit is fed with an AC power supply to power the conductive material to generate heat to melt snow and ice. A temperature sensor could be used in the control circuit to monitor the temperature of the pavement surface and control the voltage.

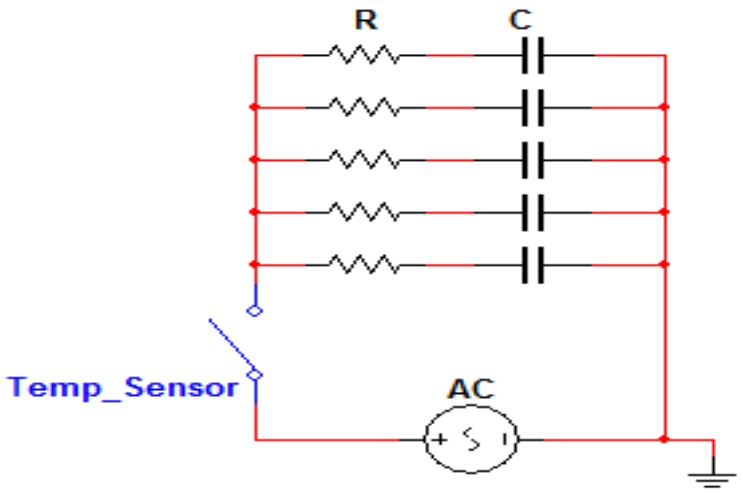

Figure 8. Electrical Circuit Model for ECON Heated Pavement System

Figure 9 illustrates changes in voltage applied to the ECON through the embedded electrodes during the snow/ice melting process. After turning on the electrical power, the voltage will increase until a time (t_1) when the sensor temperature reaches a previously set temperature. This period is represented as T_a in Figure 9. At t_1, the sensor will trigger the control circuit to make the voltage rate constant and maintain the set temperature. The period of constant voltage rate, represented as T_b in Figure 9, will allow the surface to be evenly heated and melt snow and ice together. After the temperature and constant voltage period (i.e., T_b) has elapsed, the sensor will trigger the control unit to turn off the power. During this period, represented as T_c in Figure 9, the charges gained by the capacitors will start discharging and the snow and ice will completely melt using heat from temperature drops without need for any electrical power source.

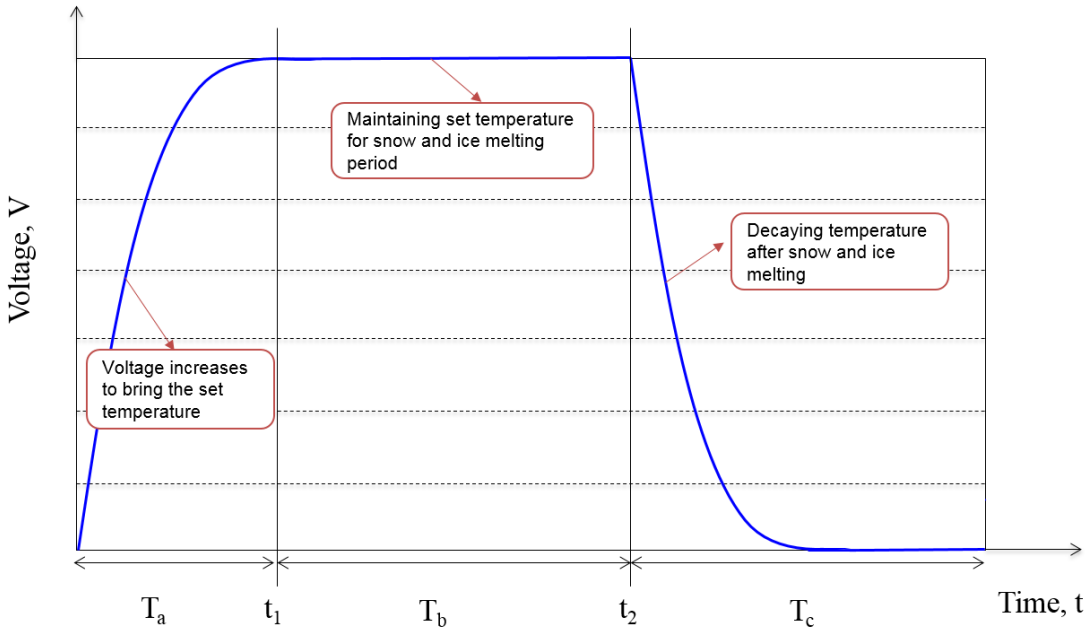

T_a: Time period to reach set voltage and temperature
t_1: Time when the temperature reaches targeted temperature
T_b: Time period to maintain set temperature to allow heating to be equally spread into snow and ice melting by providing constant voltage rate
t_2: Time when the sensor triggers the control circuit to turn the power off
T_c: Time period after which the snow and ice is expected to completely melt

Figure 9. Voltage Changes in Snow and Ice Melting Process

3.4 DESIGN FLOW OF ELECTRICALLY CONDUCTIVE CONCRETE HEATED SLAB

The design flow for a large-scale ECON-heated slab is developed and illustrated in Figure 10. The first step involves determination of design criteria, including snow/ice melting time, amount of snow/ice melted, and associated power density requirements. The design parameters to be determined include slab dimension, distance between electrodes, electrical resistance, and voltage. The slab dimension (i.e., L, W, and T) should be selected accounting for actual concrete design and construction practices. The distance between electrodes (L_s) can be calculated by subtracting the distances between slab edge to and electrode embedded (d) from the length of the slab. The electrical resistance (R) can be calculated using the resistivity (ρ) of ECON material, the cross-sectional area parallel to the electrodes (A_c), and L_s. By selecting an electric voltage (V) value, the electric current (I) and the power density (P_d) can be calculated using other design parameter values previously selected. If the calculated P_d does not meet the power density requirement, the selected design parameter values should be revised to meet the power density requirement and additional design criteria as needed.

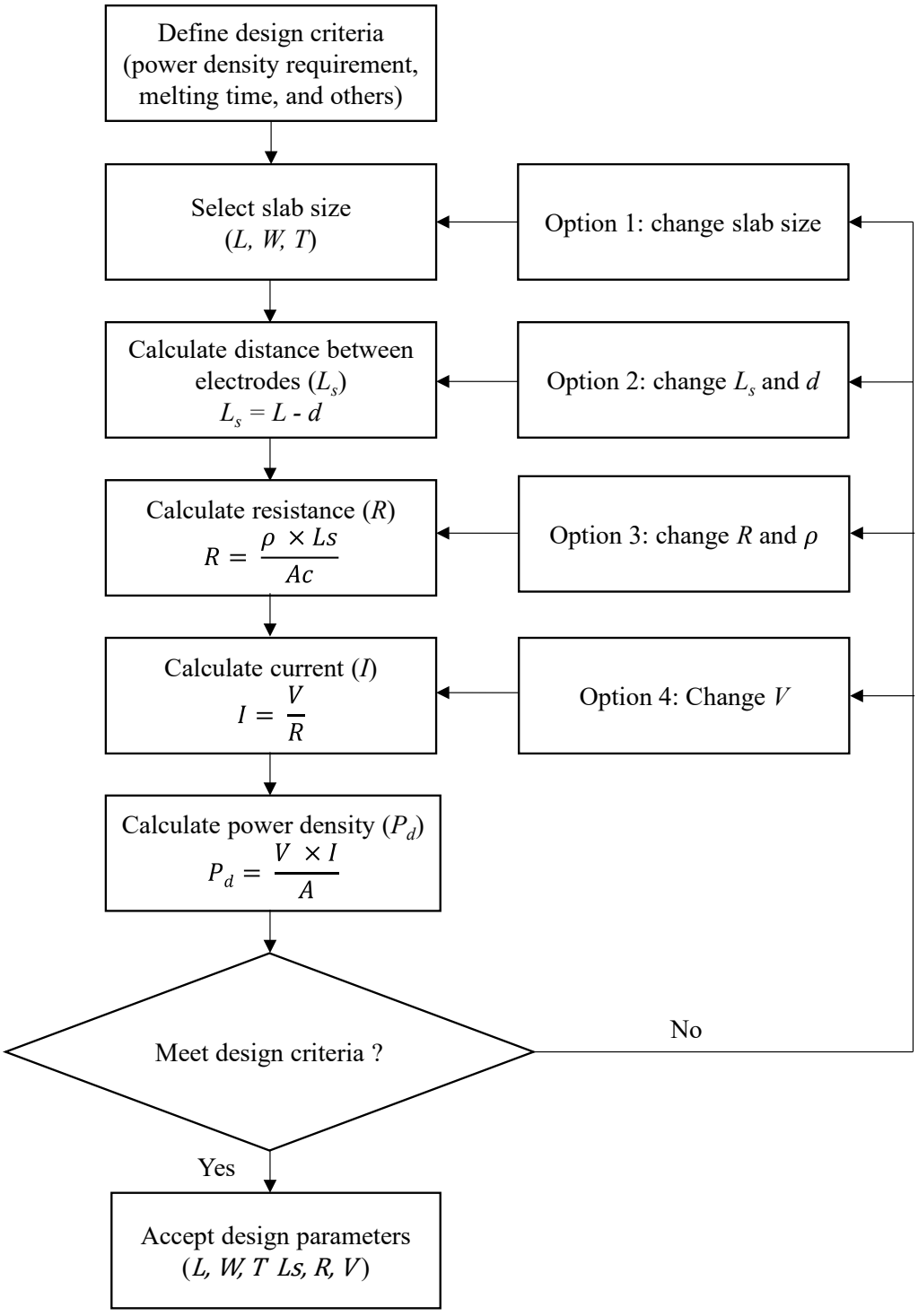

Figure 10. Design Flow for a Large-Scale ECON-Heated Slab

To provide better understanding of this design procedure, a design example is herein presented. The design criteria selected in this example is to have similar snow/ice melting performance to that of the prototype ECON slab discussed previously. Note that 880 w/m^2 of P_d is required to melt 2.5-cm-thick snow in 35 minutes for the prototype ECON slab with 1.22 (L) × 0.86 (W) × 0.1 (T)

m small-scale slab dimensions. Slab dimensions of 4.6 m (L) × 4.6 m (W) × 35.5 cm (T) were selected for the large-scale ECON-heated slab. These dimensions are close to those of concrete slabs used in airport pavement construction. This ECON-heated slab consists of two layers; the top layer is a 10-cm-thick conductive concrete, and the bottom layer is a 25.5-cm-thick conventional concrete.

Following the steps described in Figure 10, the other design parameters, including L_s, R, and V, can be selected. By selecting a d value of 40 cm for two electrodes (i.e., 20 cm of d per electrode), the L_s value of 4.2 m is derived. By using 50 Ω·cm of ρ from ECON materials used in the prototype ECON slab, 4.2 m of L_s, and 0.46 m^2 (= 4.6 m (W) × 0.1 m [T of ECON layer]) of A_c, the R value of 4.6 Ω can be calculated. By selecting V to be 300 V, an I value of 65 A and a P_d value of 920 w/m^2 are calculated for the large-scale ECON-heated slab dimension previously selected. The calculated P_d value of 920 w/m^2 is higher than the 880 w/m^2 of the P_d required to melt 2.5 cm of snow in 35 minutes. This implies that accepting the design parameters determined in this example will provide quicker melting of snow than the selected design criteria (i.e., 35 minutes). Of course, the design parameters determined in this example can be revised if additional design criteria for each of design parameters are required.

3.5 PROTOTYPE ISU ECON SLAB DESIGN, CONSTRUCTION, AND EVALUATION

3.5.1 Design

A prototype ECON slab, 122 (Length, L) cm × 86 (Width, W) cm × 10 (Thickness, T) cm, was designed for construction at the ISU PCC laboratory to identify any construction and operational issues (see Figure 11). The 10-cm slab thickness was divided into two layers with a 5-cm ECON top layer and a 5-cm conventional concrete of bottom layer. The purpose of a thin ECON layer was to lower the cost and to heat the surface as required to melt snow and ice. The concept of implementing two layers of concrete placed on one another other is not new and is being used as a sustainable construction technique for placement of concrete as in concrete overlay and two-lift concrete paving.

Two perforated galvanized steel angles, 3.175 cm (L) × 3.175 cm (W) × 0.32 cm (T), were embedded 65 cm apart in the ECON layer. Each hole in the perforated galvanized steel was larger than the maximum aggregate size to ensure that conductive concrete could be bonded with the electrode. The electrodes were connected to an AC supply to power the conductive concrete. Temperature sensors were installed in both the ECON and the conventional concrete layers. Insulation layers 2.5 cm thick were placed at the edges and bottom of slab to minimize heat losses.

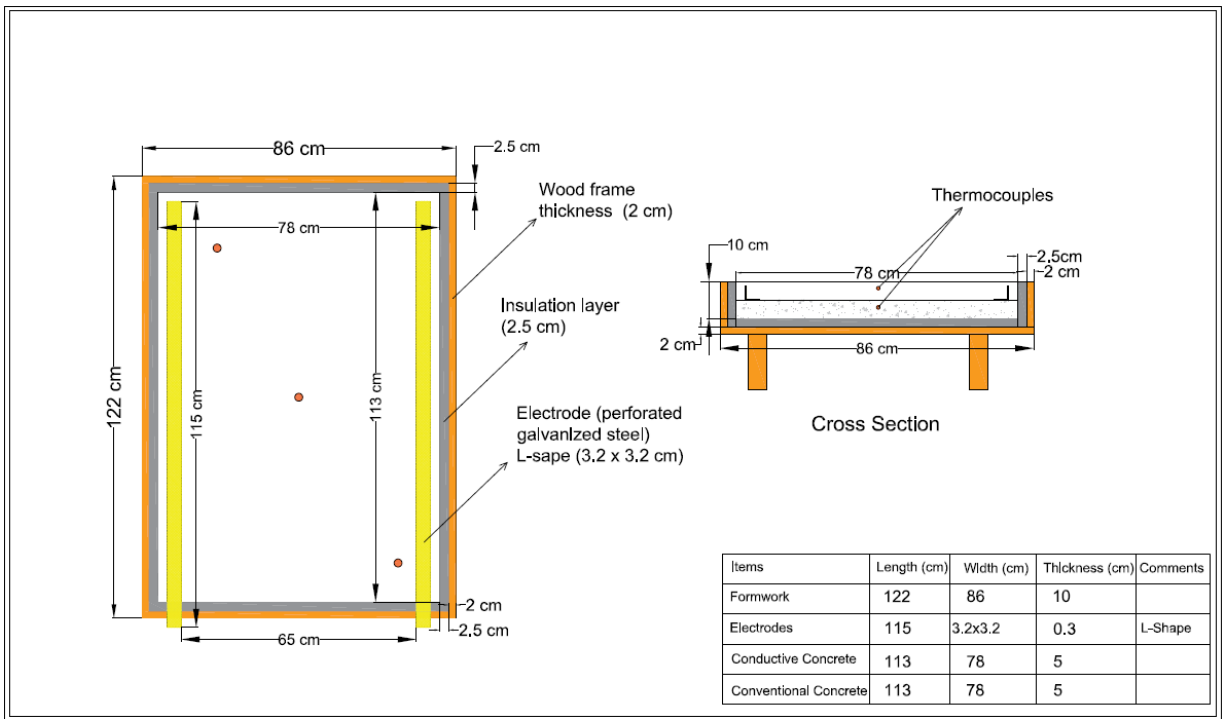

Items	Length (cm)	Width (cm)	Thickness (cm)	Comments
Formwork	122	86	10	
Electrodes	115	3.2x3.2	0.3	L-Shape
Conductive Concrete	113	78	5	
Conventional Concrete	113	78	5	

Figure 11. Detailed Design of the Prototype ECON-Heated Slab

3.5.2 Construction

Figure 12 shows the process of constructing the prototype ECON-heated slab at the ISU PCC laboratory. XPS foam, 2.5 cm thick, was placed inside the slab formwork as insulation layers to prevent heat losses before paving (Figure 12(a)). The ECON slab was constructed in two stages.

First, a 5-cm-thick conventional concrete layer was placed into the slab formwork. The top surface of the conventional concrete layer was screened and then grooved to provide an effective bond between conventional concrete and ECON layers (Figure 12(b, c, and d)). Two angle-shaped perforated electrodes were also placed on the top surface of conventional concrete layer (Figure 12(c)).

Second, a 5-cm-thick layer of ECON was placed on top of a conventional concrete layer (Figure 12(e)). Note that the ECON mixture used in this study is a newly developed mix design at ISU containing 0.75% of 6-mm-long carbon fiber by volume and providing about 50 Ω·cm of electrical resistivity with about 40 MPa of 28-day compressive strength.

During the ECON placement, attention was given to ensuring good bonding between ECON and perforated electrodes (Figure 12(f)). Temperature sensors were installed in both ECON and conventional concrete layers as designed (Figure 12(g)). A total construction cost of $130 was estimated for producing the final prototype ECON-heated slab (Figure 12(h)). The construction cost is dependent on the heating element cost and its potential to provide desirable heat radiation to melt the snow with an efficient energy consumption.

Figure 12. Construction of the Prototype ECON-Heated Slab

3.5.3 Evaluation

Following the ECON slab construction, a set of experimental tests was executed to evaluate the snow-melting performance of the ECON slab in melting 2.5-cm-thick snow on the ECON slab surface. An AC power supply (80 V and 11A) was used in the ECON slab operation to provide electricity via electrodes. The ambient temperature was -1 °C and the wind speed was 10 mph. Figure 13 illustrates the snow-melting process of the ECON slab when 2.5-cm-thick snow was placed on it. More than half of the snow on the ECON slab surface was melted after 25 minutes of slab operation (see Figure 13(b)). Most of the snow on the ECON slab was completely melted after 35 minutes of ECON slab operation (see Figure 13(d)).

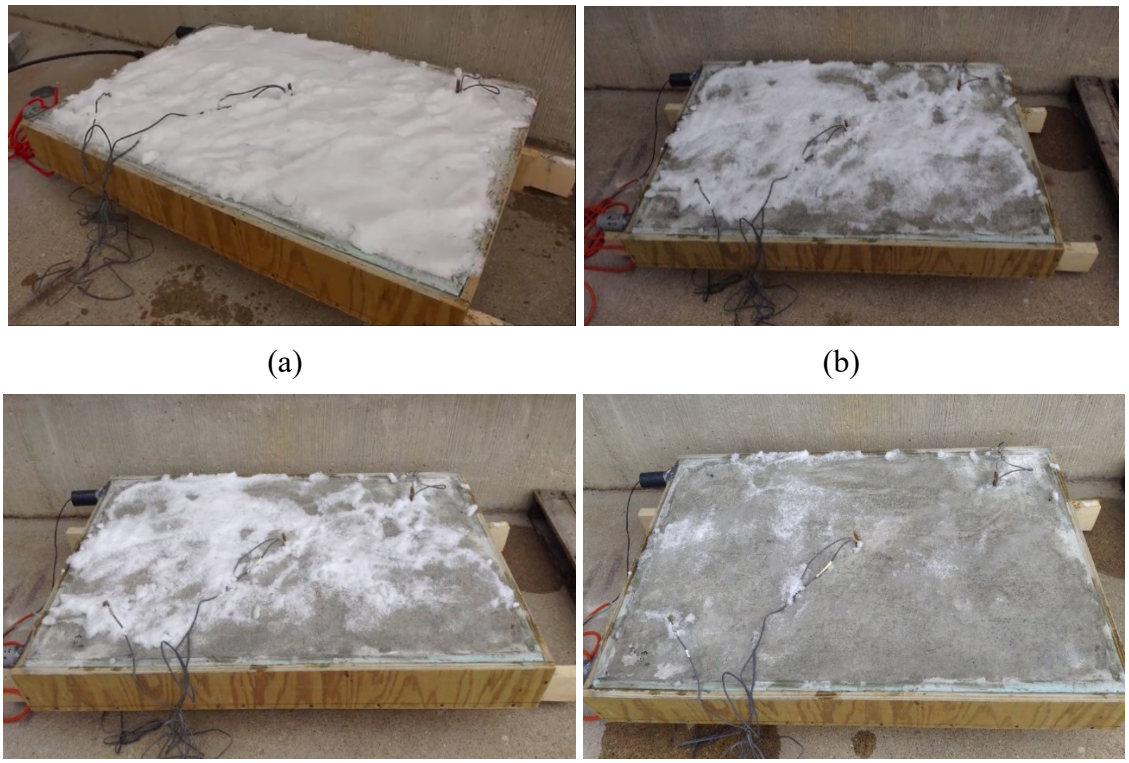

(a) (b)

(c) (d)

Figure 13. Snow Melting Performance Test on Prototype ECON Slab: (a) Placement of 2.5-cm-thick Snow on the Heated Slab, (b) After 25 Minutes, (c) After 30 Minutes, and (d) After 35 Minutes

An AC power supply (80 V and 11A) was used to melt 2.5-cm-thick snow on 1 m^2 of ECON slab surface in about 35 minutes. An energy density of 880 w/m^2 was reported (multiplying 80 V by 11A for 1 m^2 of ECON slab surface). Note that the energy density is correlated with the snow-melting time. As the energy density increases, the melting time will decrease.

Figure 14 is a snapshot of the heat distribution taken using an infrared (IR) thermographic camera about 30 minutes after the ECON was set into operation. The IR heat map demonstrates that, while the ECON slab can generate enough heat to melt snow and ice simultaneously on the entire slab surface, slightly different heating zones are observed on the surface due to the nonhomogeneous

structure of the ECON mixture consisting of the cementitious materials, fibers, aggregate, moisture, and pores.

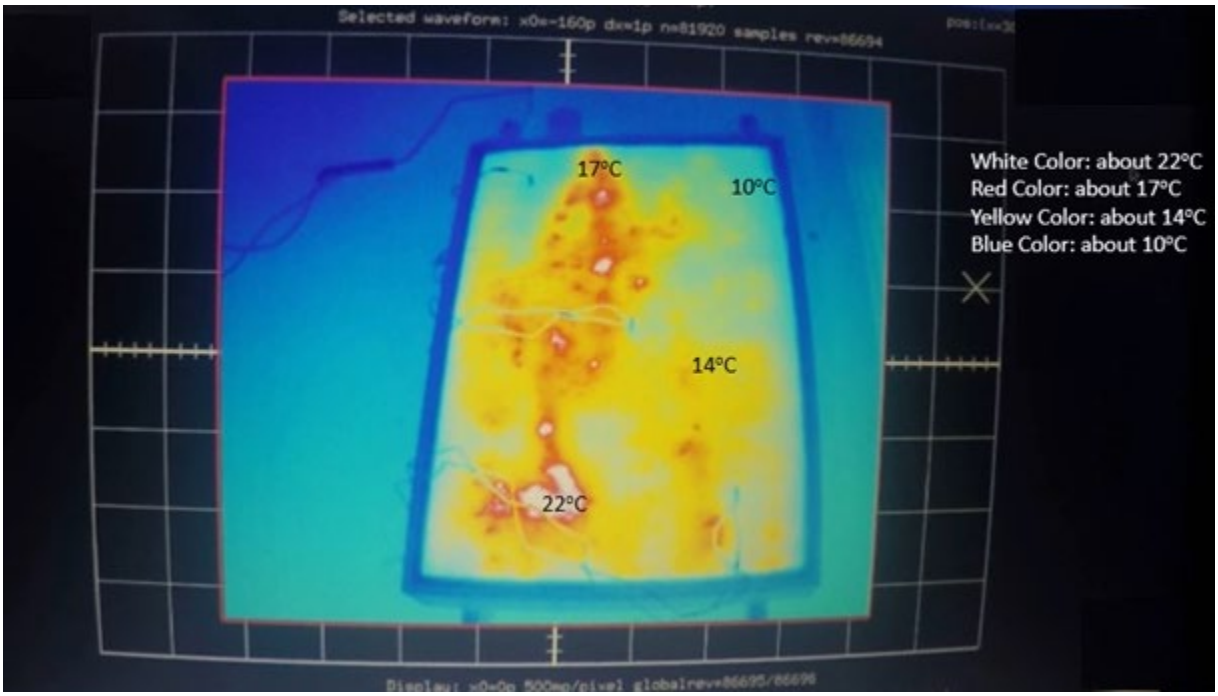

Figure 14. Infrared Thermographic Image Snapshot of the ECON Slab in Operation

The energy consumption and cost of the ECON slab in melting 2.5-cm-thick snow were estimated and compared with electrical HPS previously developed and reported in the literature (see Table 7). For the sake of one-to-one comparison, the energy consumption was calculated through the energy density (W/m^2) and melting time (hours) using information directly from the literature. Energy cost was estimated by multiplying the energy consumption (kW-h/m^2) by ¢12/kW-h of average electrical cost assumed based on 2015 average costs.

Table 7 shows that the prototype ECON slab developed in this study provides the lowest energy consumption (0.54 kw-h/m^2) and lowest energy cost (¢6.5/m^2) among electrical HPS developed and reported in the literature. In previously developed HPS (Zuofu, Zhuoqiu, & Jianjum, 2007; Yang et al., 2012; Tuan & Yehia, 2002), the estimated energy consumption ranged from 0.70 to 2.28 kw-h/m^2, and estimated energy costs ranged from ¢8.4/m^2 to ¢27.4/m^2. The improved operational performance of the ECON slab in this study results from the fact that the newly developed ECON provides higher conductivity resulting from uniform heating in the entire surface to melt snow and ice quickly.

Table 7. Energy Consumption and Cost Comparisons of Electrically HPSs

Deicing System	Ambient Temperature (°C)	Melting Time (min.)	Snow Thickness (mm)	Energy Consumption[a] (kW-h/m^2)	Energy Cost[b] (¢/m^2)	Reference
Conductive concrete steel fiber and steel shaving	2	300	50	2.28	27.4	Tuan & Yehia, 2002
Carbon-fiber tape heating panel	-11	558	15	1.14	13.6	Yang et al., 2012
Carbon-fiber grille	-1	120	27	0.70	8.4	Zuofu, Zhuoqiu, & Jianjum, 2007
ISU ECON Slab	-1	35	25	0.54	6.5	NR

NR = No reference

[a]Energy consumption of each system was calculated for comparison purposes.
[b]Average electricity cost assumed ¢12/kW-h based on average 2015 cost.

3.6 SYSTEM REQUIREMENTS FOR ECON HPS: SUMMARY, FINDINGS, AND RECOMMENDATIONS

Materials, design, construction, and operational requirements for the cost-effective performance of ECON HPSs were identified. A prototype ECON-heated slab was designed and constructed using a newly developed ECON mix designed at ISU. Based on the performance evaluation results of the prototype ECON-heated slab, design flow and three-dimensional (3D) renderings were developed to aid in the design and construction procedures for real and large-scale HPS applications. The major conclusions drawn from this study are summarized below:

- The prototype ECON slab developed in this study provided the lowest energy consumption and the lowest energy cost among electrically heated pavement systems developed and reported so far in the literature (Zuofu, Zhuoqiu, & Jianjum, 2007; Yang et al., 2012; Tuan & Yehia, 2002). Such excellent operational performance is because the newly developed ECON materials provide higher conductivity (about 50 Ω·cm of electrical resistivity) resulting in uniform heating on the entire surface to melt snow and ice quickly.

- The two-layer approach utilized in the design and construction of the prototype ECON slab places a thin ECON layer (top layer) on a conventional concrete layer (bottom layer). This approach is cost-effective in terms of materials cost, energy consumption, and operation cost savings. It can be implemented for large-scale ECON HPSs using precast concrete technique, concrete overlay, and two-lift paving.

- The design parameters to be determined for the large-scale ECON HPS include slab dimension, distance between electrodes, electrical resistance, and voltage. The design flow developed in this study can be utilized to determine these parameters for given design criteria.

- Key construction materials required for well-performing ECON HPSs are low-resistivity (i.e., high-conductivity) ECON materials, electrodes to be well bonded with ECON, and cost-effective thermal insulation.

- Use of AC to heat ECON can provide more spread-out heat distribution by enabling the electrons take different paths into conductive materials inside ECON than DC taking one path.

4. SYSTEM REQUIREMENTS FOR HHPSs

4.1 SCOPE AND OBJECTIVES

This section discusses the development of assessment frameworks and a design flow chart for HHPSs. HHPSs are widely used to provide heating and cooling in residential buildings and/ or to melt ice and snow to prevent ice accumulation on paved surfaces.

4.2 CONSTRUCTION MATERIALS

The components of an HHPS include heat transfer fluid, piping, fluid heater, pumps, and controls, as shown in Figure 15 (American Society of Heating, Refrigerating and Air-Conditioning Engineers, 2015). An HHPS melts ice and snow by circulating heated fluid through pipes embedded inside concrete structures. The cooled fluid runs through a heat source that reheats the fluid for each cycle. A common practice is the use of propylene glycol as a heat transfer fluid due to its moderate cost, high specific heat, and low viscosity. Pipes can be made of metal, plastic, or rubber. The drawback of using steel pipes is their susceptibility to rusting, so, the use of steel embedded in pavement is not a common practice. An alternative to steel pipe is plastic pipes such as polyethylene (PE) or cross-linked polyethylene (PEX) because it has resistance to corrosion and lower material cost. PE and PEX withstand fluid temperatures up to 60 °C and 93 °C, respectively.

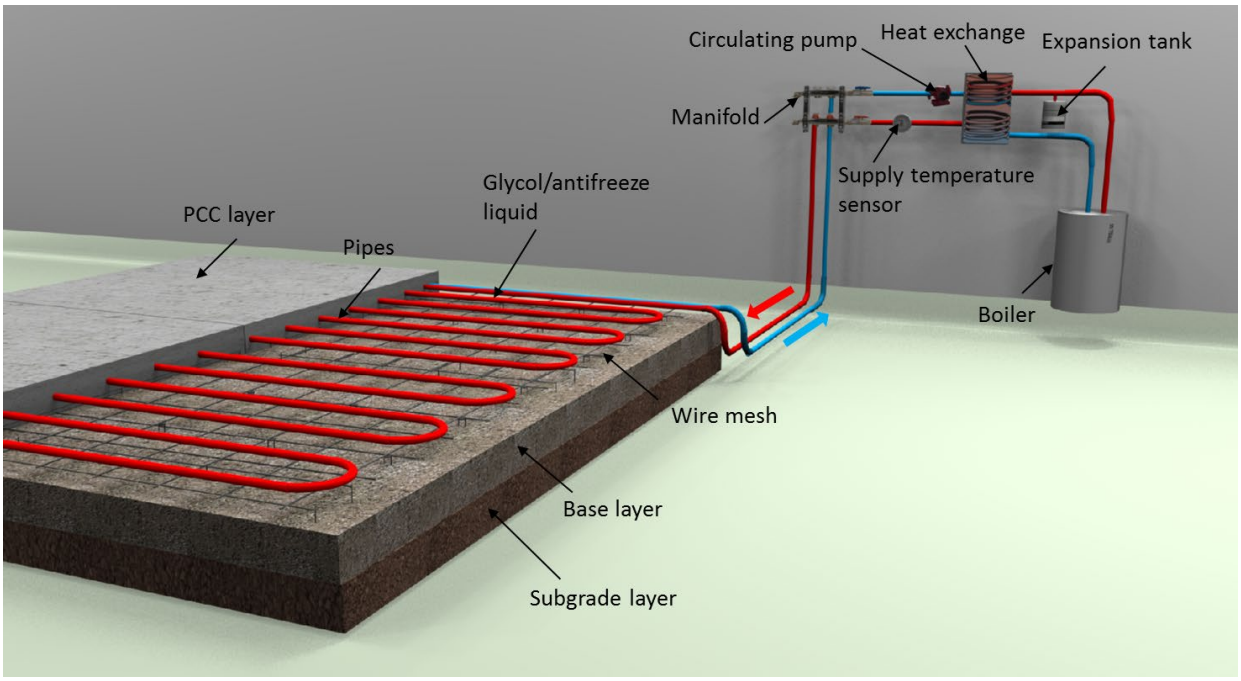

Figure 15. Detail of an HHPS

The different types of fluid heaters include geothermal hot water, underground thermal energy storage (UTES), boilers, and heat exchangers (FAA, 2011). The fluid heater can be selected based on availability at the project site. Geothermal water is considered efficient in locations with good geothermal potential (Joerger & Martinez, 2006). The efficiency of hydronic HPS in melting ice and snow significantly depends on different factors (Ceylan, Kim, & Gopalakrishnan, 2014), including fluid temperature, pavement conductivity, pipe depth, and pipe spacing. The thermal conductivity of PCC is higher than for hot-mix asphalt (HMA), so PCC has the potential to conduct more heat.

4.3 PIPING DETAILS AND SNOW/ICE MELTING MODELS

A hydronic slab's pipes can be arranged in different patterns, e,g., serpentine or slinky, to provide uniform heat on the hydronic slab surface to prevent ice and snow accumulation. The serpentine pattern (see Figure 16) is commonly used in melting snow and ice on paved surfaces (Spitler & Ramamoorthy, 2000). In the serpentine pattern, straight pipes are placed on equal centers and connected to a manifold using U-shaped pipes. The slinky pattern is placed in a circular shape with each circle overlapping the other one. A hydronic heated system was constructed into a 44.5-m-long and 17.7-m-wide bridge deck in Amarillo, Texas, and a serpentine pipe pattern was selected (Minsk, 1999). The geothermal well was used as the energy source to heat the fluid, resulting in a reduction in operation cost.

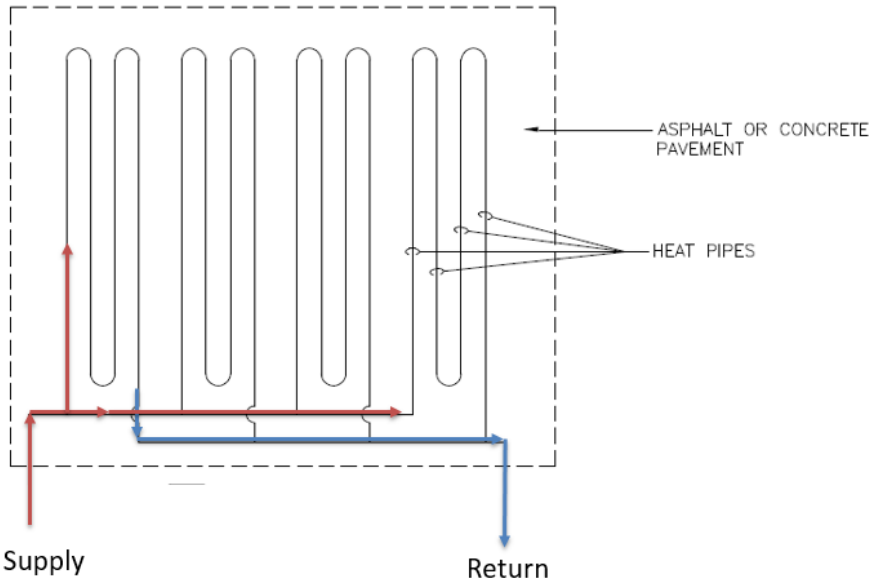

Figure 16. Hydronic Pipes Pattern (FAA, 2011)

The pipe pattern can be designed using industrial software, such as LoopCAD® 2016. LoopCAD can generate circuit layout drawings and zones for the project site and perform detailed hydronic calculations such as energy density based on American Society of Heating, Refrigerating and Air-Conditioning Engineers (ASHRAE) methods (see Figure 17). LoopCAD software has the flexibility to adjust the pipe layout drawings, and loop lengths are generated by the program.

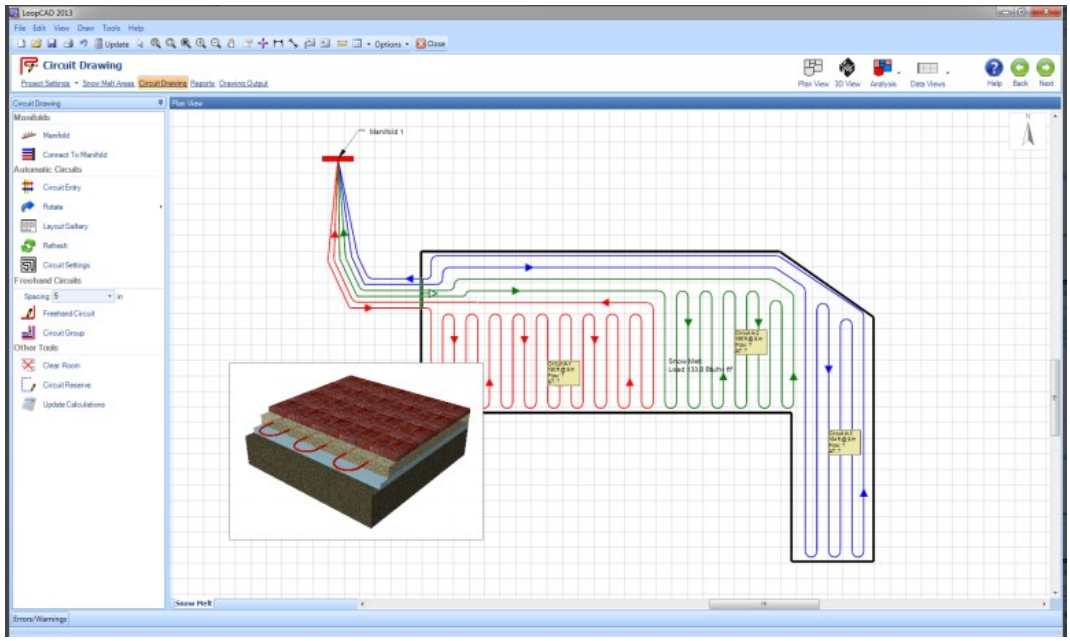

Figure 17. Snowmelt Design LoopCAD Software

4.4 DESIGN FLOW OF A HYDRONIC HEATED SLAB

Figure 18 shows design flow for an HHPS that considers the various options for advanced construction techniques described in this study, i.e., PCP, concrete overlay, and two-lift paving. The steps required to design HHPSs include defining the pavement surface temperature, determining heat requirements, determining supply fluid temperature, defining tubing layouts, choosing glycol percentage, and determining flow rate, pressure loss, and pump selection. The flow chart was developed based on ASHRAE (2015) and FAA AC 150/5370-17 (FAA, 2011), and an industry manual of Uponor®.

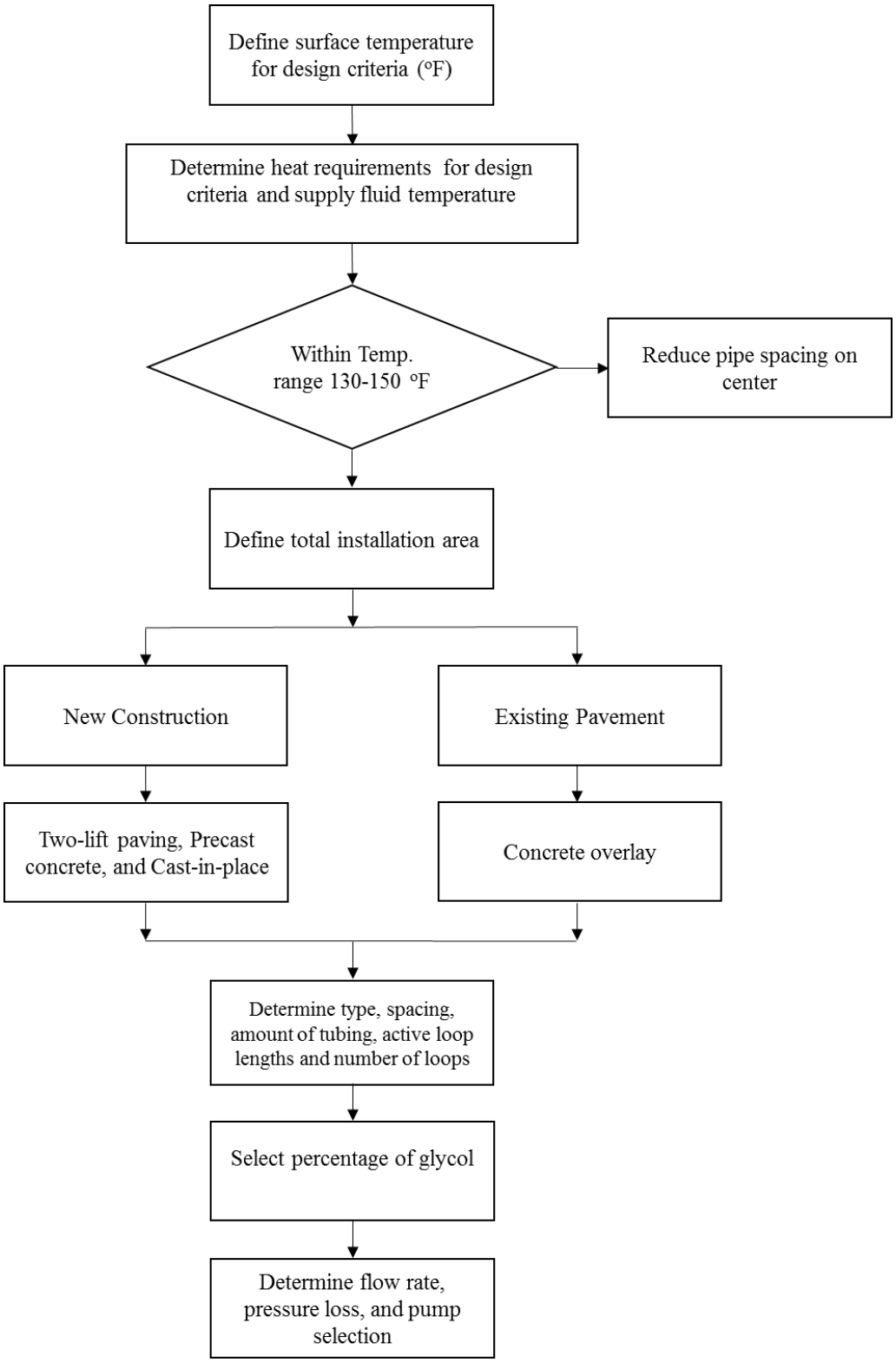

Figure 18. Design Flow Chart for HHPS

4.4.1 Define Temperature of Pavement Surface

A temperature range of about 35 °F to 45 °F at the pavement surface can be selected as a design criterion to maintain the pavement surface above the freezing point.

4.4.2 Determine Heat Requirements

The minimum design requirement of an HPS is that it must be capable of keeping a surface condition of "no worse than wet" (FAA, 2011) and maintaining a surface temperature above the freezing point before and during the snow accumulation. The heating requirement to melt snow depends on the rate of snowfall, air temperature, relative humidity, and wind speed. The steady-state energy balance equation for required heat flux (q_o) in (W/m^2) is presented below:

$$q_o = q_s + q_m + A_r(q_h + q_e) \quad (1)$$

where, q_s, q_m, A_r, q_h, q_e are sensible heat flux (W/m^2), latent heat flux (W/m^2), snow-free area ratio, convective and radiative heat flux from a snow-free surface (W/m^2), and heat flux of evaporation (W/m^2), respectively. The detailed equation definition and parameters are available in the ASHRAE 2015 Heating, Ventilation, and Air Conditioning (HVAC) handbook (ASHRAE, 2015) and the FAA AC 150/5370-17 (FAA, 2011). The heat flux q_o, equation (1), does not account for the back and edge heat losses that increase the total heat slab output (q_o), that can vary from 4% to 20% depending on factors such as pavement construction, operating temperature, ground temperature, or back exposure (Viega, 2015).

The heat requirement for a snow-melting installation is based on classification systems I, II, or III:

- Class I (minimum): residential walks or driveways
- Class II (moderate) commercial sidewalks and driveways
- Class III (maximum) toll plazas of highways and bridges, aprons and loading areas of airports, and hospital emergency entrances

These classifications are correlated to snow-free area A_r values. Class I has a snow-free area ratio of 0, and the surface is allowed to be covered with sufficient thickness of snow before beginning to melt the snow. Class II has a snow-free area ratio of 0.5, and the surface must be kept clear of snow accumulation, while a wet surface is acceptable. Class III has a snow-free area ratio of 1, and the surface must melt snow quickly while it is falling, and the surface must remain dry.

4.4.3 Determine Supply Fluid Temperature

The value of fluid temperature required to achieve the total heat flux output (q_o) can be calculated based on equation 2:

$$t_m = 0.5q_o + t_f \quad (2)$$

where:
t_m = average fluid temperate, °F

t_f = water film temperature (°F), taken as 33 °F

The recommended temperature of the supplied fluid should be within a range of 130 °F to 150 °F due to the limitation of the pipe's temperature resistance and other construction materials. If the average fluid temperature surpasses the recommended temperature for achieving a designed heat flux (q_o), the pipe spacing should be reduced.

4.4.4 Define the Total Installation Area

The total installation area on an HHS should be defined by estimating the capacity of the fluid heater (boiler size) and the required amount of tubing using the total heat flux (q_o). The value of snow melting heat flux includes back and edge losses, usually in the range of 630 to 950 W/m^2.

4.4.5 Define Pipe Design

The pipe spacing can be determined based on the required classification systems previously mentioned. The recommended on-center pipe spacing for classes I, II, III are up to 30 cm, 23 cm, and 15 cm, respectively, although these spacings can be reduced for some areas that experience severe weather conditions. The amount of tubing can be selected based on tube type, size, and other relevant information from tubing suppliers or manufactures. In addition, the numbers and lengths of active loops depend on the total installation areas and the manifold specifications provided by the manufacturer.

4.4.6 Define Glycol Percentage

Glycol is widely used as a heating liquid solution in HHSs because it has high specific heat along with reasonable cost. The glycol percentage can be selected based on weather condition (temperature). The recommended percentage of glycol is in the range of 40% to 60% water solution by volume.

4.4.7 Determine Flow Rate, Pressure Loss, and Pump Selection

Fluid flow rate depends on the energy requirement and differential temperature. The recommended differential temperature between the supply and return fluid is 25 °F. Pressure loss per foot can be determined by considering the fluid flow rate and fluid temperature. The required pump can be selected by considering the fluid flow rate, the energy requirements of the piping system, the specific heat of the fluid, and the viscosity of the fluid.

4.5 PROTOTYPE HYDRONIC HEATING SLAB DESIGN, CONSTRUCTION, AND EVALUATION

4.5.1 Design

A prototype hydronic heated slab of dimensions 112 cm (Length, L) × 84 cm (Width, W) × 12 cm (Thickness, T), was designed for construction at the ISU PCC laboratory to identify construction and operational issues (see Figure 19). Copper pipe was embedded in conventional concrete to circulate heat transfer fluid in a closed loop between the hydronic heated slab and the heating

source. An antifreeze agent, such as propylene glycol, was used to heat the hydronic heated slab surface to melt ice and snow. The pipe spacing had 20-cm centers and a 2-cm diameter. The pipe was placed 5 cm below the concrete surface. The pipe should be covered with a minimum 5 cm of concrete above and below (ASHRAE, 2015). Thermocouples were installed at different depths to measure the temperatures within the slab as shown in Figure 19. Insulation layers 2.5 cm in thickness were placed at the edges and bottom of the slab to minimize heat losses.

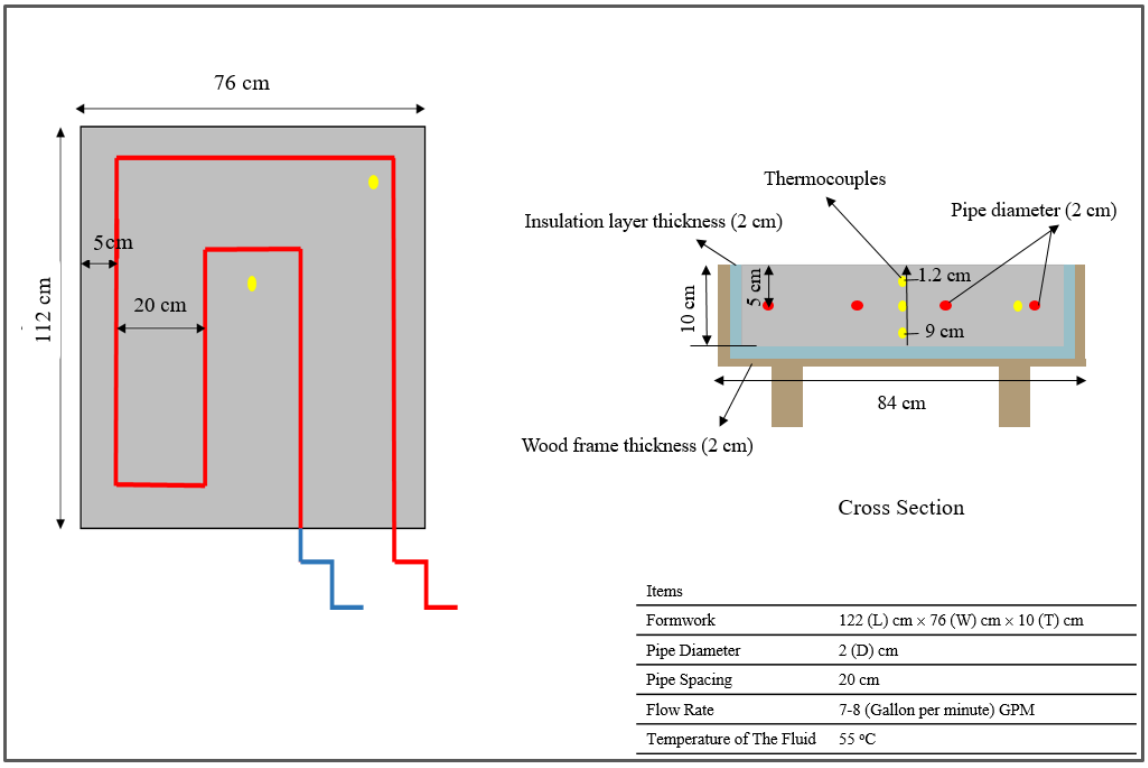

Items	
Formwork	122 (L) cm × 76 (W) cm × 10 (T) cm
Pipe Diameter	2 (D) cm
Pipe Spacing	20 cm
Flow Rate	7-8 (Gallon per minute) GPM
Temperature of The Fluid	55 °C

Figure 19. Detailed Design of the Prototype Hydronic Heated Slab

4.5.2 Construction

The construction sequence of the prototype hydronic heated slab at the ISU PCC laboratory is shown in Figure 20. XPS foam layers 2.5-cm thick were placed inside a slab formwork as insulation layers to prevent heat losses before paving (Figure 20(a)). The ECON slab was constructed in two stages.

First, a rebar chair was placed into the slab formwork to raise the wire mesh 5 cm off the bottom. Copper pipe was then placed on top of the wire mesh and tied to the wire mesh to keep it from moving while pouring the concrete. Thermocouples were then placed using a sensor tree in the center of the slab and near the copper pipe (see Figure 20(a)). Two holes were made in the formwork to allow the copper pipes to connect with the heat source (see Figure 20(c)).

Second, conventional concrete was placed into the formwork (see Figure 20(b)). The compressive and flexural strengths at an age of 28 days were 36 MPa and 5.5 MPa, respectively. A vibrator was used to achieve sufficient bonding between the copper pipe and the concrete. After screening and

finishing the concrete surface, the copper pipes were connected to the boiler and the pump so that fluid could be circulated in a closed loop, in which the cold fluid could be reheated using the boiler (see Figure 20(d)). Thermometers were attached to the boiler's inlet and outlet copper pipe to measure the temperature of the fluid during the operation. A total construction cost of $1,100 included the prototype hydronic heated slab, the water heater, and pump shown in Figure 20(d).

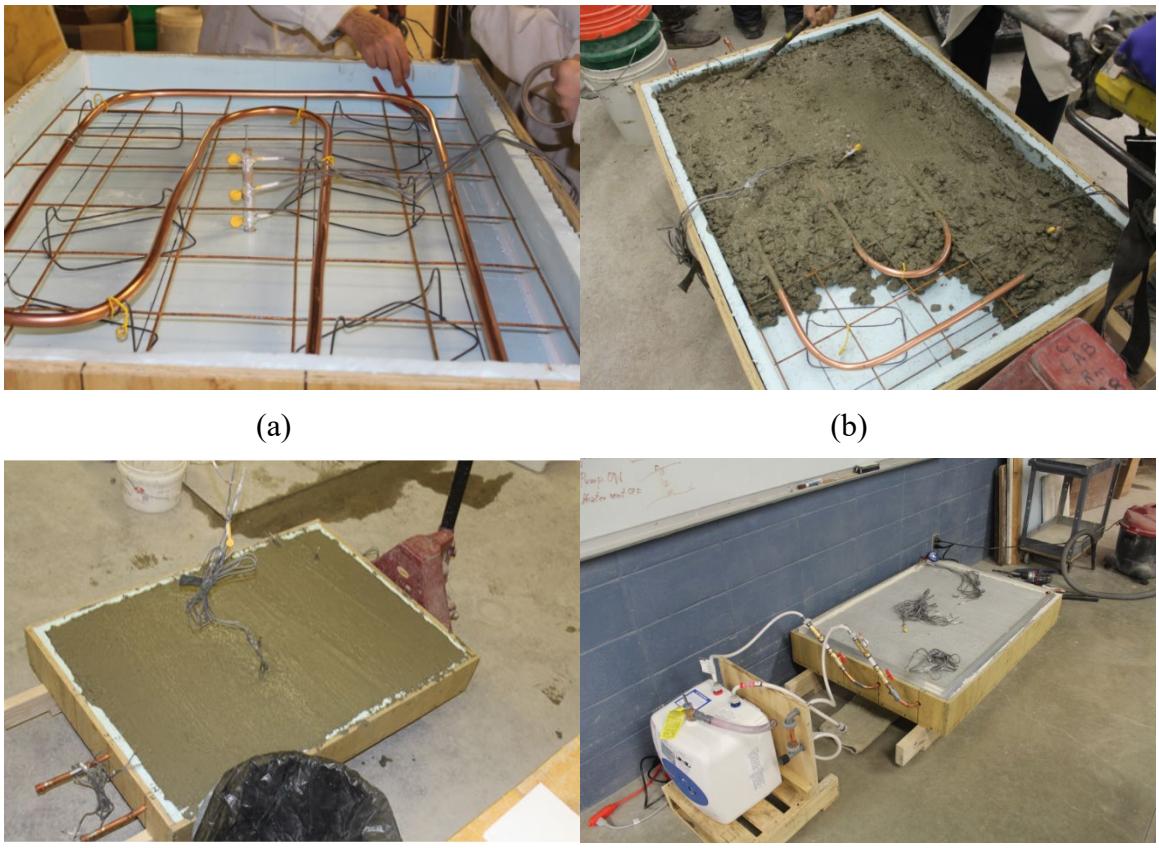

(a) (b)

(c) (d)

Figure 20. Construction of the Prototype Hydronic Heated Slab

4.5.3 Evaluation

The prototype hydronic heated slab was placed into a chamber room to evaluate snow-melting performance by melting 2.5-cm-thick snow on the slab surface (see Figure 21(a)). The chamber room temperature was set at -5 °C during the experimental test, and the fluid was heated using the water boiler and circulated using a pump. Figure 21 shows images of the snow melting process.

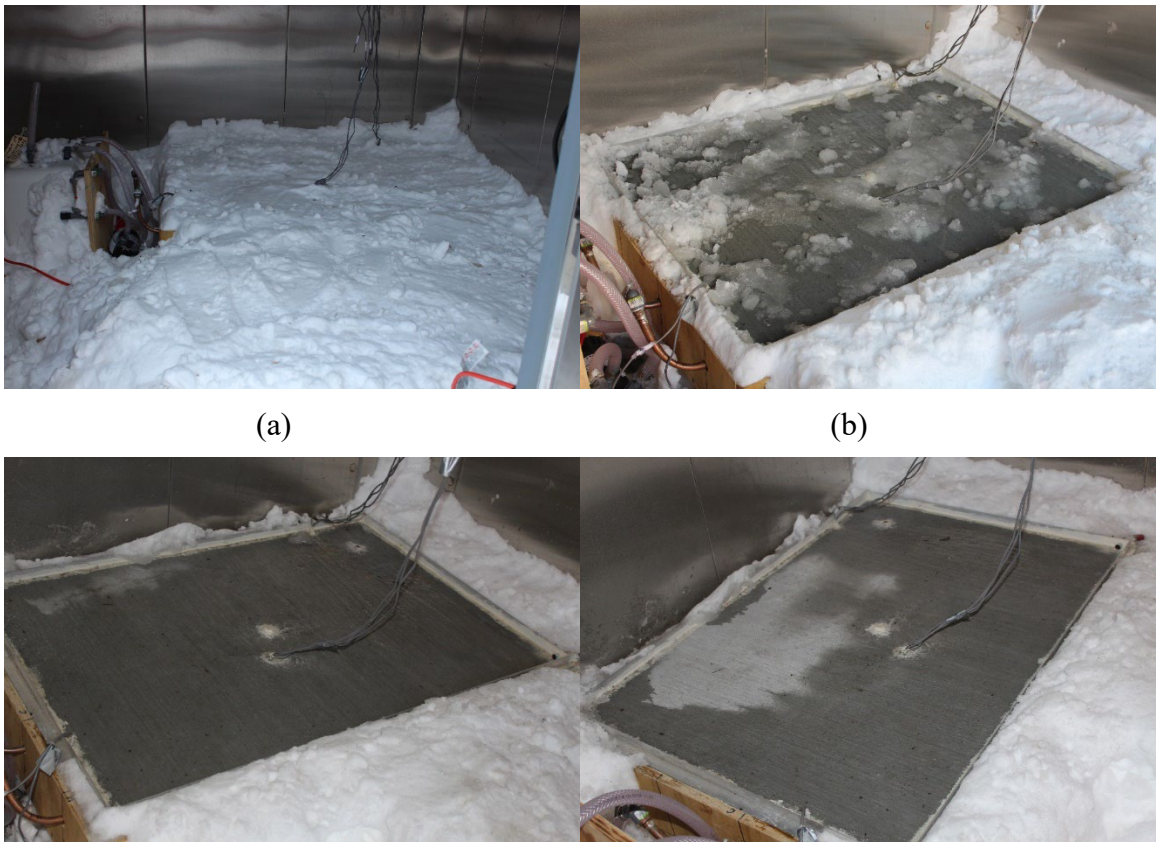

(a) (b)

(c) (d)

Figure 21. Snow Melting Performance Test on Prototype Hydronic Heated Slab: (a) Placement of 2.5-cm-thick Snow on the Heated Slab, (b) After 35 Minutes, (c) After 40 Minutes, and (d) After 45 Minutes

The 2.5-cm-thick snow layer was placed on 0.9 m^2 of the hydronic slab surface before turning the system on (see Figure 21(a)). Within 35 minutes after turning on the hydronic slab, nearly half of the snow was melted (see Figure 21(b)), and the snow was completely melted after 40 minutes (see Figure 21(c)). The hydronic slab surface was partially dry after 45 minutes due to evaporation from the wet surface (see Figure 21(d)). The energy consumption of the hydronic slab was 1,400 W and the estimated energy density was 1550 W/m^2 (1,400 W/ 0.9 m^2).

Figure 22 shows a snapshot of the heat distribution taken using an IR thermographic camera about 30 minutes after the hydronic slab was set into operation. The IR heat map demonstrates that the hydronic slab can generate enough heat to melt snow and ice simultaneously on the entire slab surface—although the heat initially started on top of the copper pipe and then dissipated onto the entire surface.

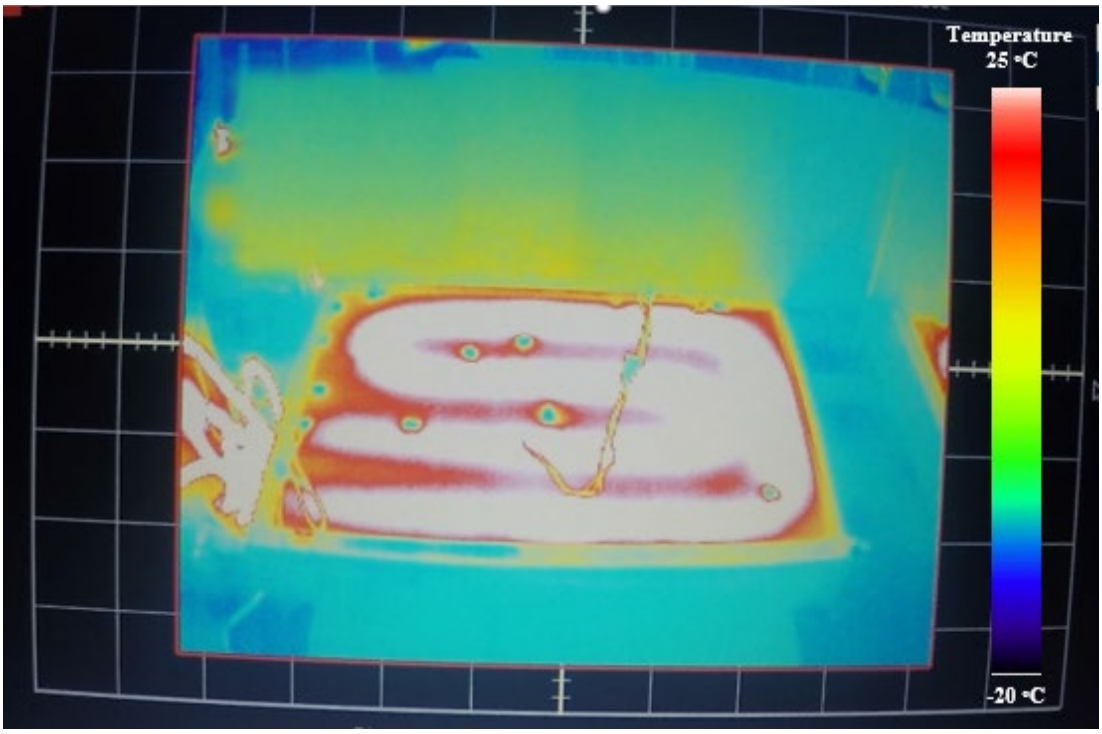

Figure 22. Infrared Thermographic Image of the Hydronic Heated Slab in Operation

4.6 SUMMARY OF KEY FINDINGS FOR HHPS REQUIREMENTS

This section identifies the materials, design, construction, and operational requirements for an HHPS. An experimental prototype hydronic heated slab was designed and constructed to demonstrate the feasibility of using a hydronic slab for melting ice and snow at the ISU PCC laboratory. The major conclusions drawn from this study are summarized below:

- The hydronic heated slab can be used as an alternative technology for melting ice and snow such a system should be implemented over the ECON HPS if the project site has a geothermal source to reduce the operational cost.

- The developed design flow can be utilized to optimize the system parameters as well as to provide construction technique options such as precast concrete, two-lift paving, and concrete overlay in the construction of HHPS. The performance of a hydronic heated slab using PCC over HMA is a better option due to its high thermal conductivity.

- Serpentine or slinky pipe patterns are commonly used for pipe circuit layouts. Industrial software can be used to create circuit design layout and to calculate the design energy for each specific location. The calculation of industrial software was based on ASHRAE methods.

5. THE 3D VISUALIZATION OF ADVANCED CONSTRUCTION TECHNIQUES FOR ECON HPS

5.1 SCOPE AND OBJECTIVES

This section addresses the development of a conceptual design framework for the ECON HPS using PCP, two-lift paving, and concrete overlays. A preliminary schematic of visualization for construction of the ECON HPS using different options was developed.

5.2 DEVELOP ASSESSMENT FRAMEWORK

Conceptual designs for ECON HPS have been developed to provide more detailed understanding of construction and operation schemes of heated pavement system through 3D visualizations. Figure 23 presents in-progress conceptual designs to illustrate the operation schemes of ECON HPS.

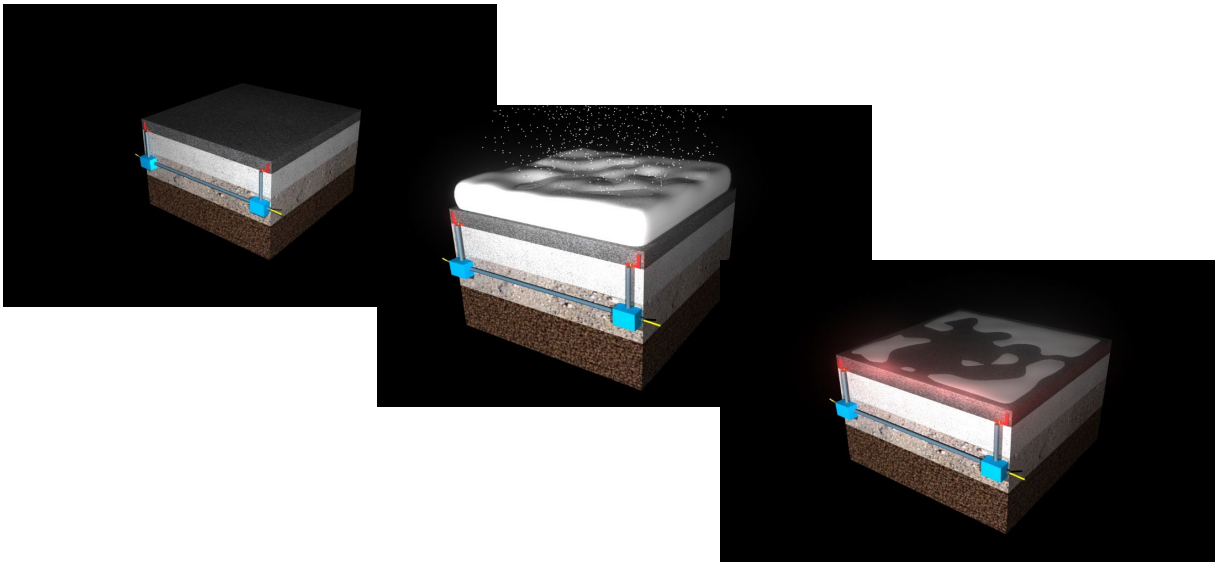

Figure 23. Conceptual Design of ECON HPS During Operation

The overall components of the ECON HPS for large-scale construction are illustrated in Figure 24. These components include the ECON layer, electrodes, polyvinyl chloride (PVC) conduits, temperature sensors, power supply, and control box. ECON is placed as a thin concrete overlay to reduce construction cost and to heat the ECON surface for melting ice and snow. The construction of the ECON layer should be isolated from embedded pavement light and cabling (FAA, 2011). During the vibration of ECON layer, care should be taken to avoid damaging the electrical components, such as electrodes, the temperature sensor wire, etc., embedded in the ECON layer. To automatically activate and deactivate the ECON system, temperature sensors should be installed in the ECON layer and a predetermined set temperatures for turning the system ‘on’ and ‘off’ should be defined (ASHRAE, 2015). The ECON HPS may also be operated with an external thermostat and/or snow detector as alternative options if the temperature sensor somehow fails due to wear and tear resulting from long-term operation. The ECON HPS can be deactivated when the ambient temperature rises above 2 °C to 5 °C (ASHRAE, 2015).

A laboratory test was conducted to identify the best material for electrodes to keep corrosion under control while applying electrical power through electrodes. Galvanized steel was placed in a bucket filled with saltwater to expedite the test while applying electrical power. The galvanized steel is manufactured by coating the steel with a layer of zinc to protect it from corrosion. However, the corrosion protection layer (i.e., zinc) was initially stripped and peeled off during the application of electrical power after approximately 24 hours. As a result, 316L (low carbon) stainless steel was selected as electrode material because of its superior corrosion resistance. The detailed properties for 316L are covered under the American Society for Testing and Materials (ASTM) A 240 and ASTM A 666 specifications.

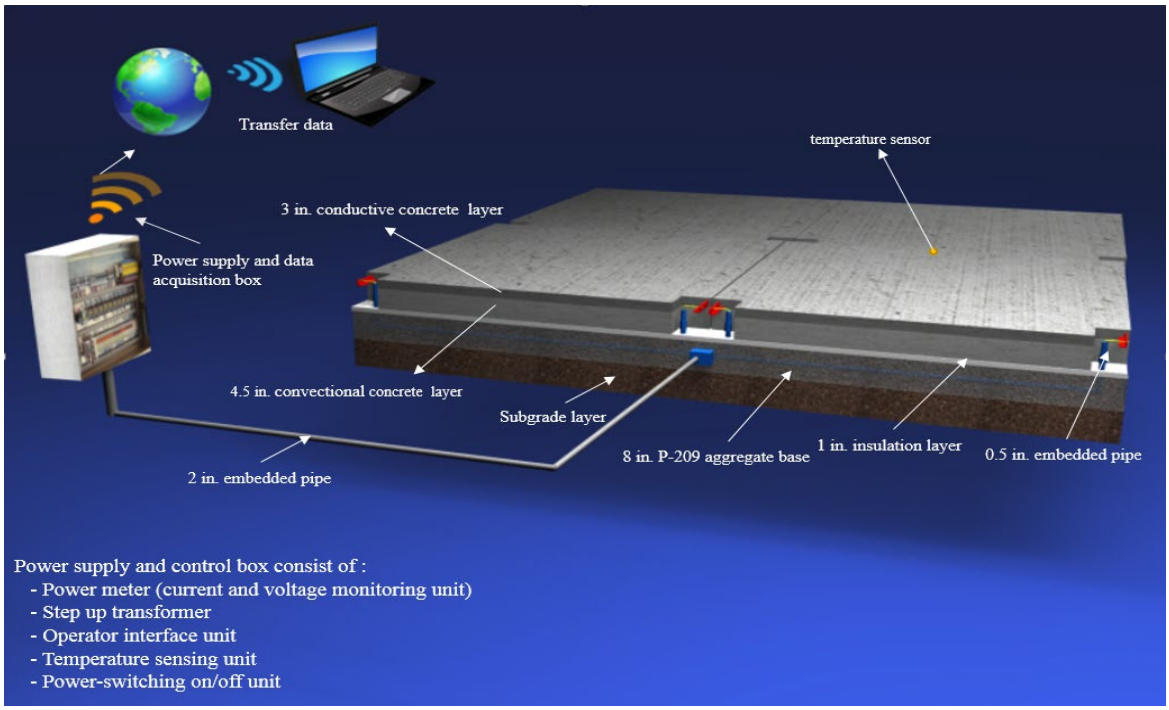

Figure 24. A 3D Visualization of ECON HPS

The power supply and control box consist of a power meter, a step-up/step-down transformer, a power-switching unit, and operator interface units. The power meter records/monitors electric current and voltage values. The step-up/step-down transformer unit allows increasing and decreasing the power and/or the voltage as needed. The power-switching unit can automatically deactivate and activate the ECON system based on the temperature sensor readings. The ECON HPS can be monitored through an operator interface unit that can display data such as temperature readings and electrical current and voltage readings. The operator interface unit can be implemented with a wireless remote-control system to allow for effective remote operation and control of the ECON HPS operation.

Operation of the ECON HPS must not interfere with aircraft navigational systems (NAVAID) or communication equipment nor cause any electromagnetic interference (EMI). The ECON-heated pavement system should be protected by ground fault protection devices (FAA, 2011).

5.3 CONCEPTUAL DESIGN AND CONSTRUCTION CONSIDERATIONS FOR ECON HPS USING PCP

The conceptual designs for ECON HPS for large-scale construction projects were developed through 3D visualization schematics to provide a tangible understanding of its construction and operational schemes.

Figure 25 shows a schematic of construction details of ECON HPS utilizing a precast concrete technique. PCP has demonstrated decent high-performance for bridges, pavements, buildings, and airfield pavement construction. PCP can provide high strength, low permeability, and fewer cracks. These features result from preparing the panels off-site where quality control can be achieved during precast fabrication of panels. The incentive to use precast concrete in pavement construction applications has increased since it has been demonstrated to be a rapid construction technique compared to cast-in-place methods that require long curing time to attain enough strength to be opened for traffic (Bly et al., 2013; Merritt et al., 2004; Priddy, Bly, & Flintsch, 2013).

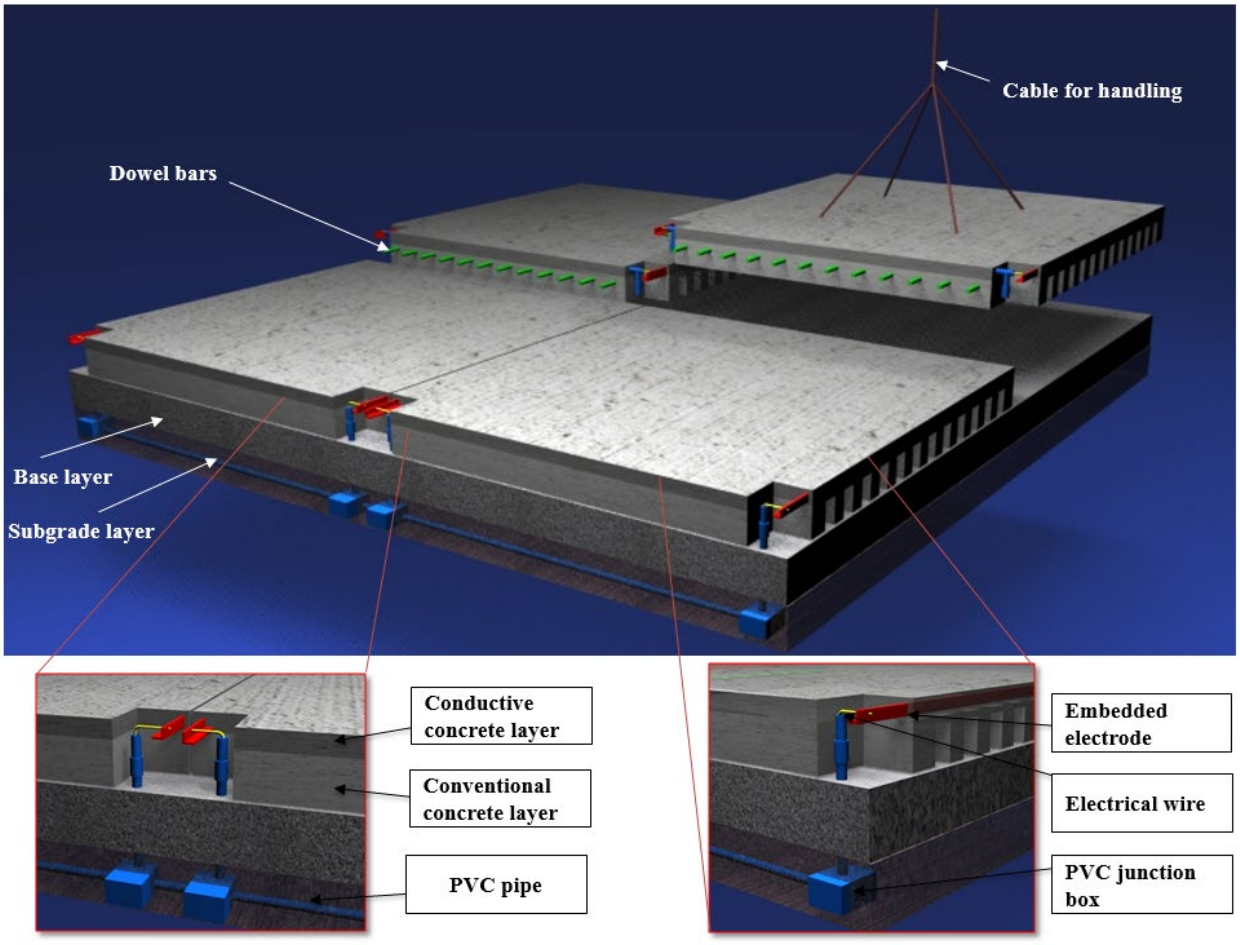

Figure 25. The 3D Visualization Schematics for ECON HPS Construction Using PCP

The construction sequence of the ECON HPS using PCP involves four major steps: fabrication, preparation, placement, and installation.

5.3.1 Step 1: Fabricate ECON Slab Off-Site

ECON slab can be fabricated through off-site construction, as shown in Figure 26(a) and (b). The total thickness of the ECON slab can be divided into two layers where the top is the ECON layer, and the bottom is the conventional concrete layer. Conventional concrete can be placed after positioning dowel bars and making slots for providing load transfer to adjacent slabs. Electrodes should be anchored to the bottom layer using a nylon anchor rod. The precast ECON slabs can be cured and tested before transferring them into a construction site. Each ECON slab contains two electrodes located in the edges to provide electrical connectivity. The electrode numbers and spacing can be determined and designed based on the required energy density for each specific project site to provide sufficient heat generation to prevent snow and ice accumulation. Finally, the ECON layer can be placed after anchoring and securing the electrodes while the bottom layer is wet to enhance the bond between the two layers. The ECON layer is generally 2–4 in. thick to reduce the construction cost of the ECON slab and to heat the top ECON surface.

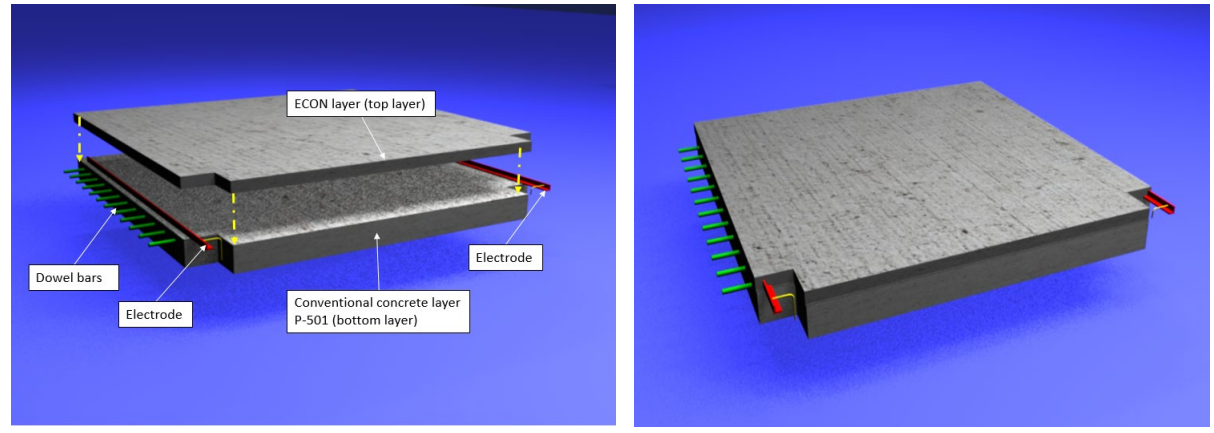

(a) (b)

Figure 26. A 3D Visualization of ECON-Heated Slab Fabrication Using PCP

5.3.2 Step 2: Prepare the Base Layer and Install PVC Conduits

The subgrade and base layers are prepared and compacted to meet the required density, and PVC conduits and a junction box are installed to accommodate the electrical wires for the electrodes system (see Figure 27). The PVC conduits can be installed after preparing the base layer. Trenching should be made for installation of PVC conduits whose positions should align with electrodes so that electrical wires can be connected to the electrodes to provide electrical energy. An alternative option for installing the PVC is to place the PVC at the bottom of the base layer along with setting on top of the subgrade layer. This option is used for in-pavement lighting conduit.

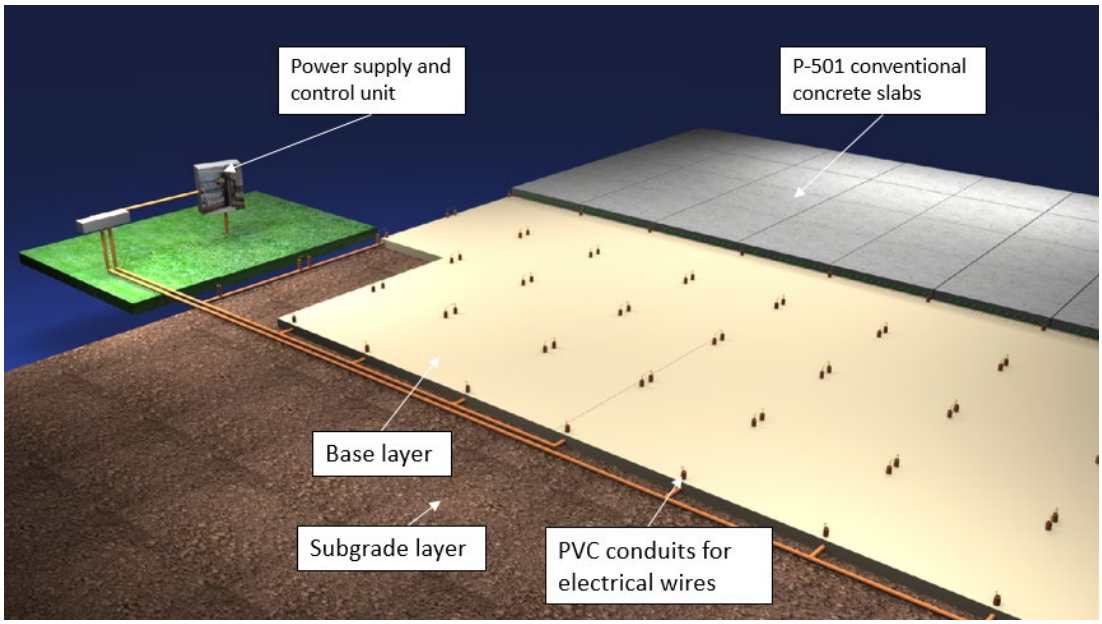

Figure 27. Preparing the Base Layer and Installing PVC Conduits and Junction Box

5.3.3 Step 3: Place the ECON Slabs

The precast ECON slabs are transferred into the construction site and placed on the prepared base layers (see Figure 28(a)). The ECON slab has dowel bars and slots like a traditional precast panel to transfer mechanical loads. The ECON slab includes two electrodes embedded in ECON layer to allow electrical wires to be connected after placing the ECON slab. The exposed electrodes at the edges (see Figure 28(b)) of the ECON slabs should be placed above the PVC conduits so that electrical connections can be made. In this case, the electrical wires will not cross the joints and cause damage to the system of electrical wires.

5.3.4 Step 4: Install Power Supply

The power supply and control unit system are installed in this step. The power supply system can be specified based on the designed energy density that can sufficiently heat the ECON surface to prevent ice and snow accumulation. The ECON system can be operated under either 120V or 240V based on the designed electrodes spacing and the properties of the ECON materials, such as electrical resistivity values. Electrical wires should be connected to the electrode system and tested before filling the voids of the exposed electrodes (see Figure 28(c)). The voids can be filled with conductive patching concrete. The dowel slots of the ECON slab may be filled with grout as in a traditional precast panel to fill the voids of the dowel slots. The grout can be pumped through a dowel grout port and a bedding grout port (Chang, Chen, & Lee, 2004).

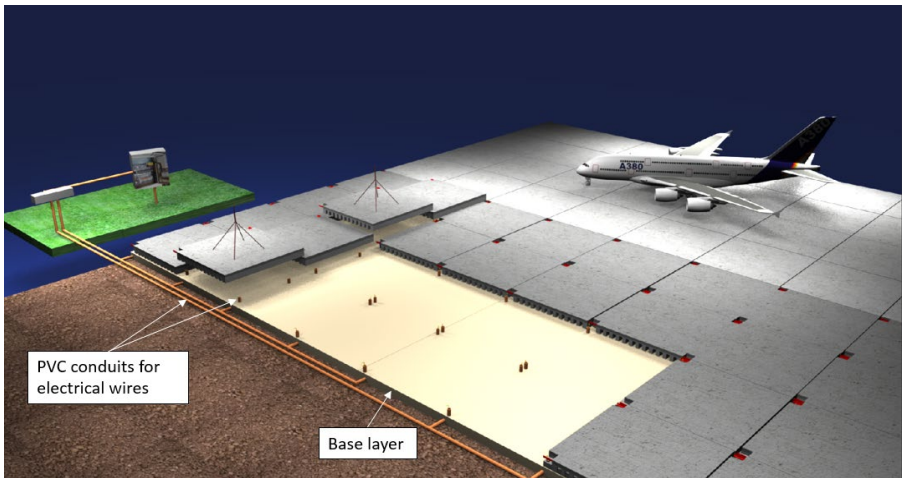

(a)

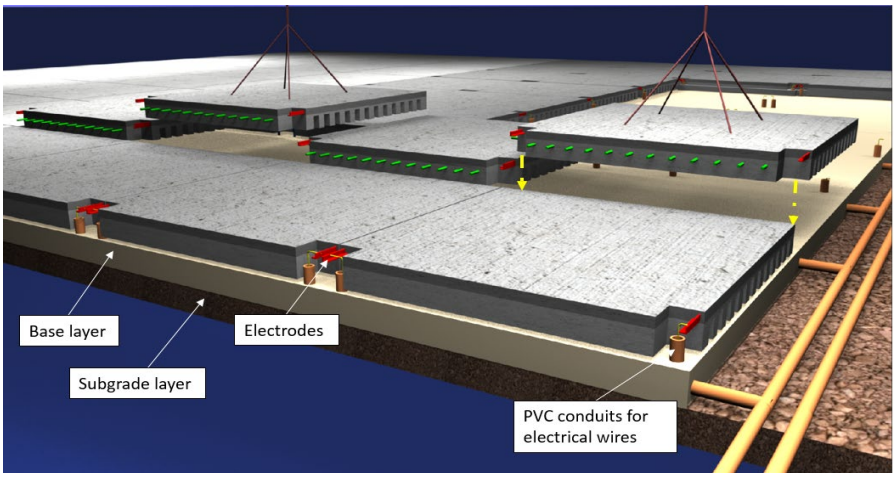

(b)

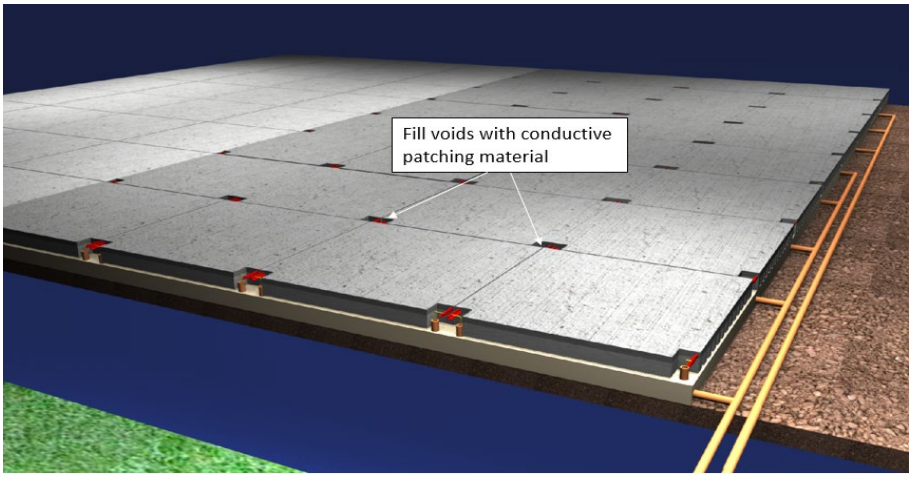

(c)

Figure 28. Construction Sequence of ECON Using PCP: (a) Place ECON Slab, (b) Connect Electrical Wires to the Electrode Systems, and (c) Fill Voids with Conductive Patching Materials

5.4 CONCEPTUAL DESIGN AND CONSTRUCTION CONSIDERATIONS OF ECON HPS USING TWO-LIFT PAVING

The construction sequence of the ECON HPS using two-lift paving involves the following four major steps: (1) preparing the base layer and installing dowel baskets, (2) placing the P-501 layer, (3) placing the electrode system, and (4) placing the ECON layer.

5.4.1 Step 1: Prepare the Base Layer and Install Dowel Baskets

In this step, the base layer is prepared and compacted; the dowel baskets are installed; and PVC conduits are installed to accommodate electrical wires of the electrode system (Figure 29(a) and (b). The PVC conduits should be placed at the bottom of the base layer as well as setting on top of the subgrade layer to protect the PVC conduits from damaging or displacement during the placement of the PCC base layer.

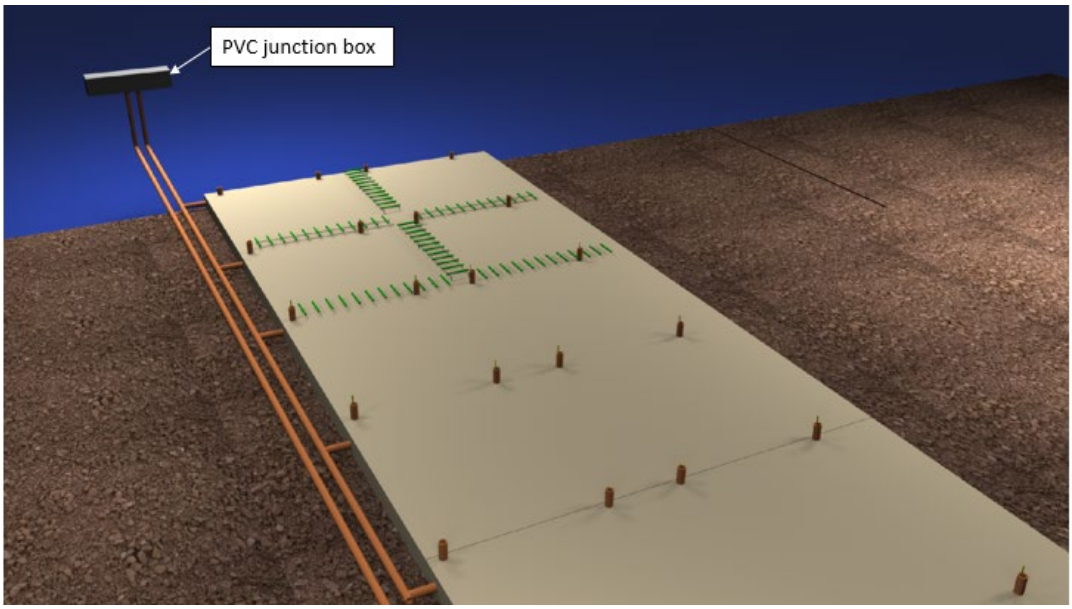

(a)

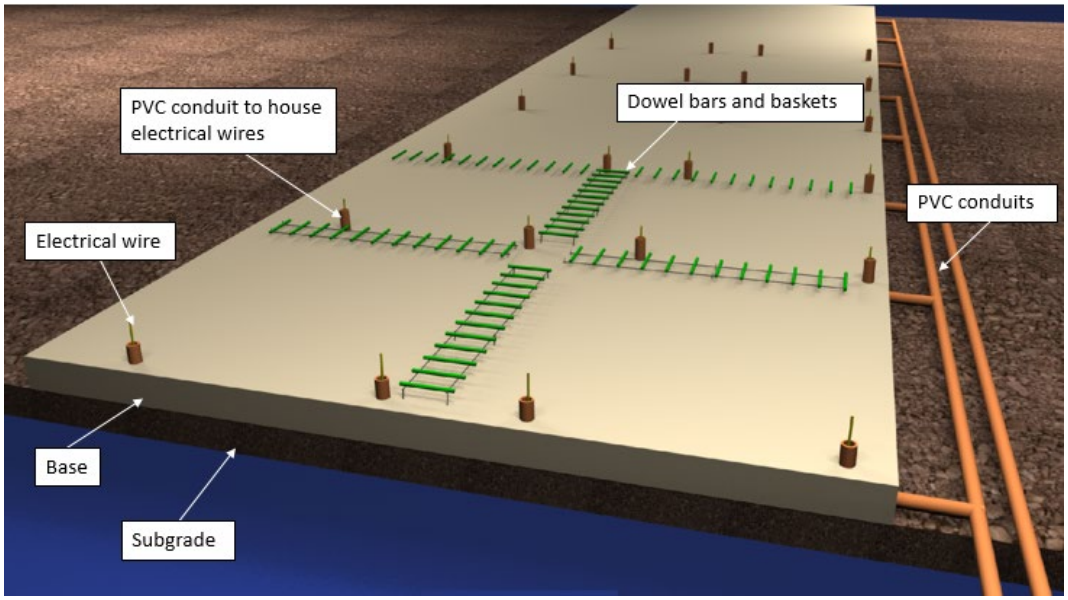

(b)

Figure 29. Construction of ECON Using Two-lift Paving: (a) Prepare Surface, Install Dowel Baskets, and Place PVC Conduits and (b) Zoomed Image Showing Base and Subgrade Layers with PVC Conduits

5.4.2 Step 2: Place P-501 Layer

In this step, the conventional concrete layer (bottom layer) P-501 is placed using a slipform paver (see Figure 30(a) and (b)). Extra attention needs to be taken during concrete paving to protect the PVC conduits embedded in the base layer. The PVC conduits should not interfere with the slipform

paver's vibrators, pan, or auger. The location and spacing of PVC conduits should not interfere with the vibrators so as not to cause damage to the PVC conduits.

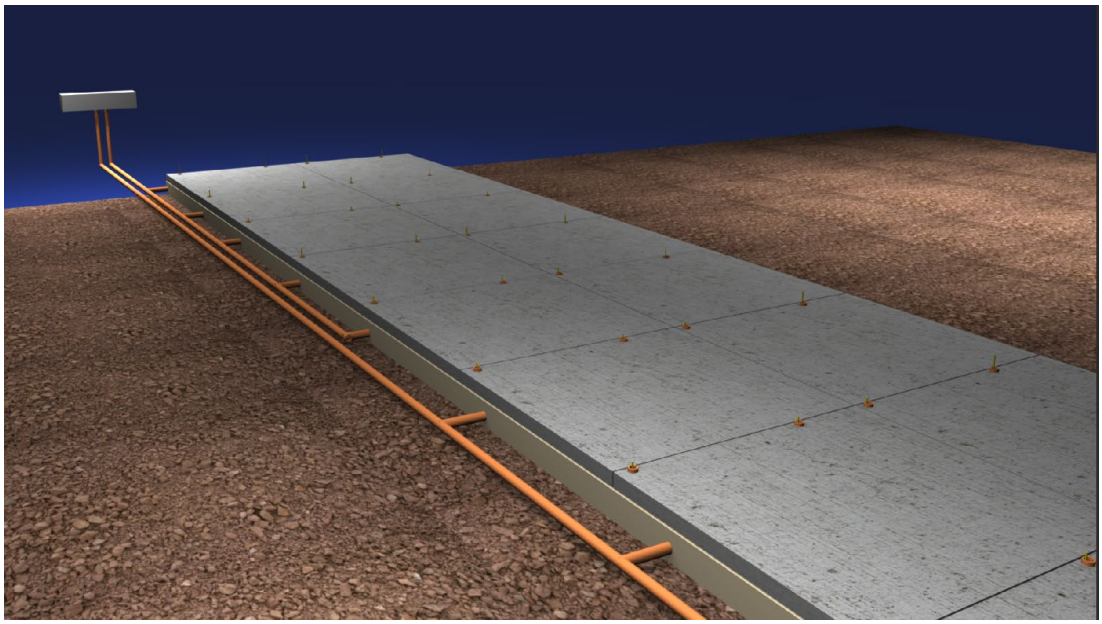

(a)

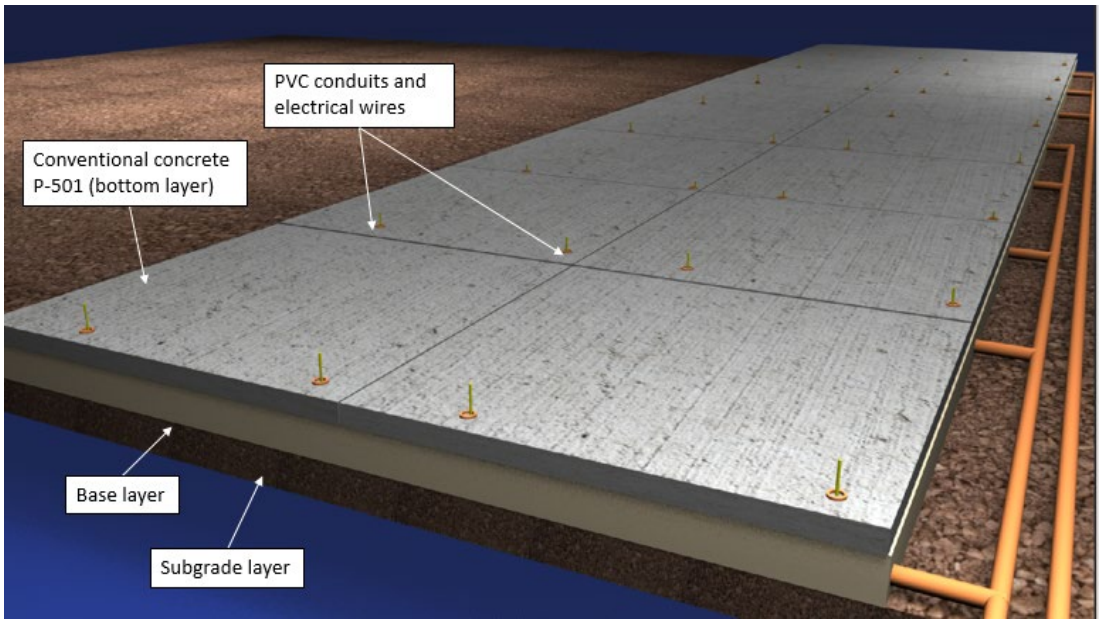

(b)

Figure 30. Construction of ECON Using Two-lift Paving: (a) Placing Conventional Concrete P-501 Layer (Bottom Layer) Using Slipform Paver and (b) a Zoomed Image of the ECON

5.4.3 Step 3: Place Electrode System

After paving the P-501 PCC, electrodes should be placed and fixed using nylon rods as well as making electrical wire connections for the electrode system (see Figure 31(a) and (b)). The challenge of placing the electrodes is that the time required for installing and fixing the electrodes on the bottom lift and connecting the electrodes to the electrical wire will delay the paving of the second layer (ECON layer). These issues may pose challenges for a wet-on-wet process in two-lift concrete paving. Therefore, it is recommended that this option only consider a two-lift paving method that is based on the first lift being cured 24 hours prior to placing the next lift. This will require "wet" curing. No wax-based cure compound can be used as it will act as a bond breaker between lifts of concrete. Joints need to be cut in the slab to prevent shrinkage cracking. The top layer needs to be cut in precisely the same location as the bottom layer to the full depth of the top layer.

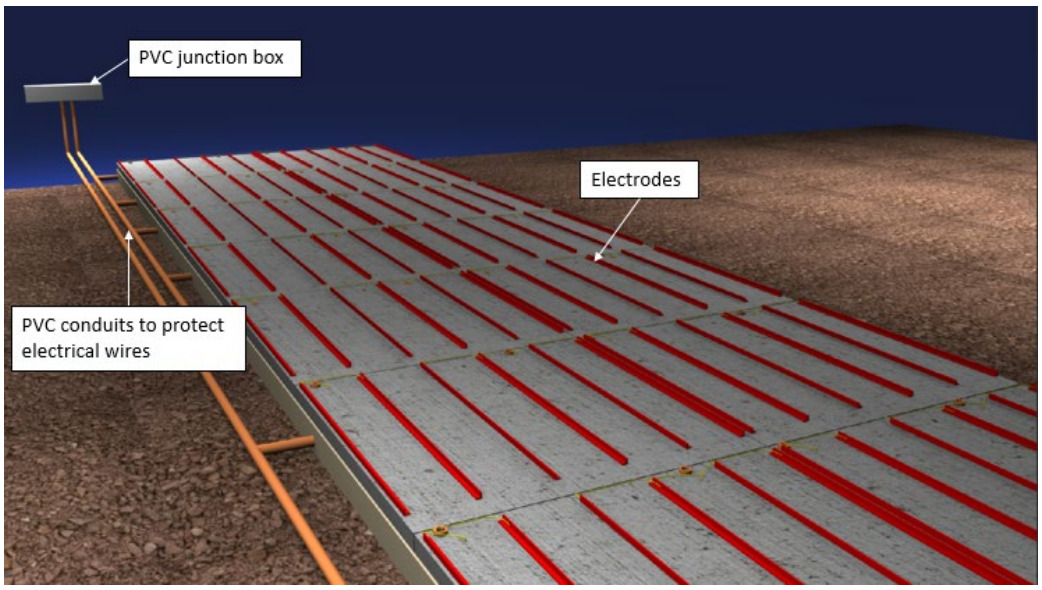

(a)

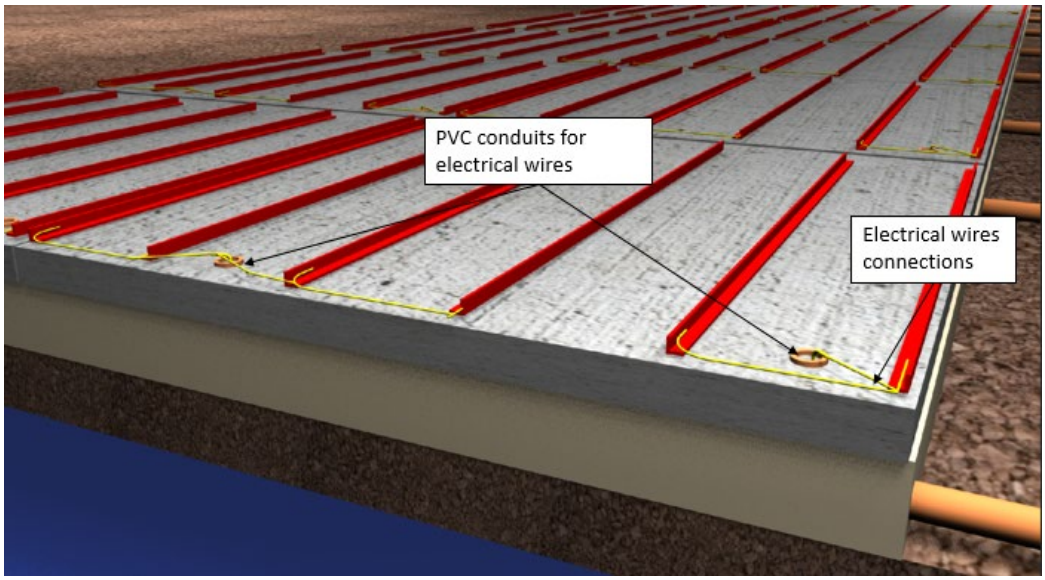

(b)

Figure 31. Construction of ECON Using Two-lift Paving: (a) Placing and Connecting Electrical Wire to the Electrode System and (b) a Zoomed Image of the Electrodes

5.4.4 Step 4: Place ECON Layer

The ECON layer, typically 2–4 in. thick, can be placed as the top layer with the second paver forming the final pavement profile of the ECON HPS (see Figure 32). Prior to placing the ECON layer, electrodes should be cleaned using an air-blower, brooms, and a pressure washer to ensure sufficient bonding between electrodes and the ECON layer. The electrodes should not cause slipform paving clearance problems and should not interfere with the vibrators, auger, or pan. Electrodes should be located within 2 in. of the ECON surface to provide clearance for slipform paving (see Figure 33(a) and (b)). The vibrators are generally positioned no more than 4 in. below the finished pavement surface (Kohn et al., 2003). The vibrator spacing should be different from the electrode spacing to prevent damage or interference with the electrodes.

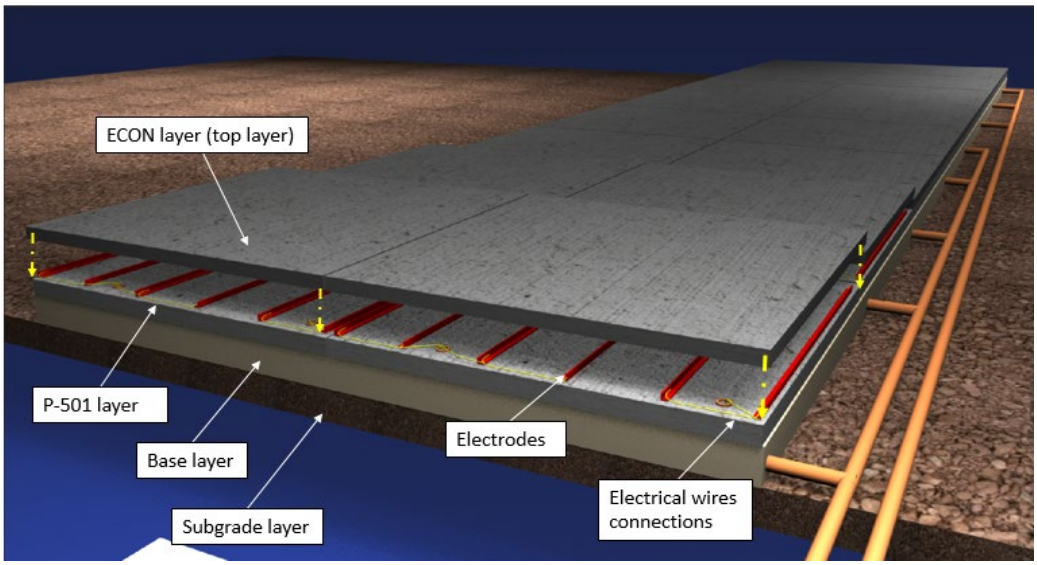

Figure 32. Placement of the ECON Layer (Top Layer)

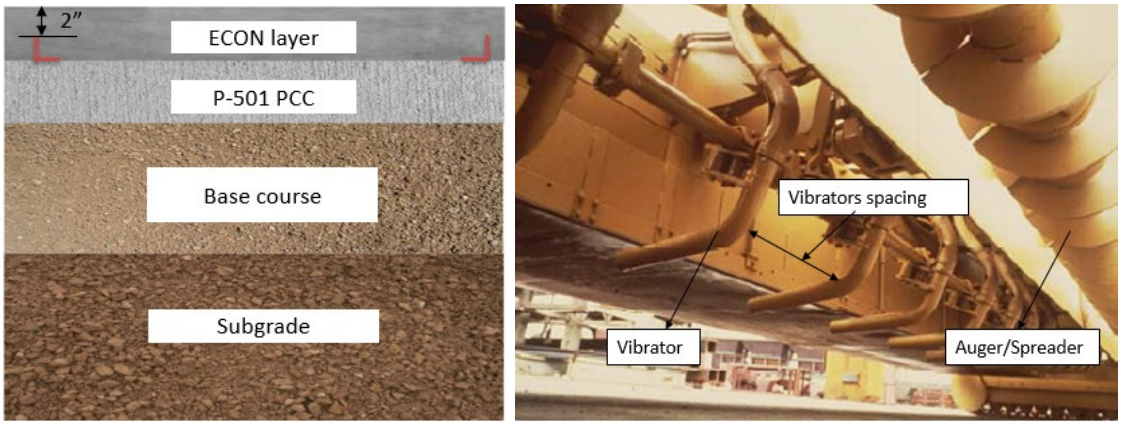

(a) (b)

Figure 33. Paving Considerations: (a) ECON Cross Section and (b) Slipform Paver

Figure 34 shows the sequence of construction steps of the ECON HPS using two-lift paving technology. Electrical wires are connected to the power supply and the control unit to provide electrical energy to the ECON HPS and to remotely turn the ECON HPS on/off. The ECON HPS can be turned on/off automatically based on set temperatures. The PVC junction box houses electrical wires and distributes the electrical wires to the power supply.

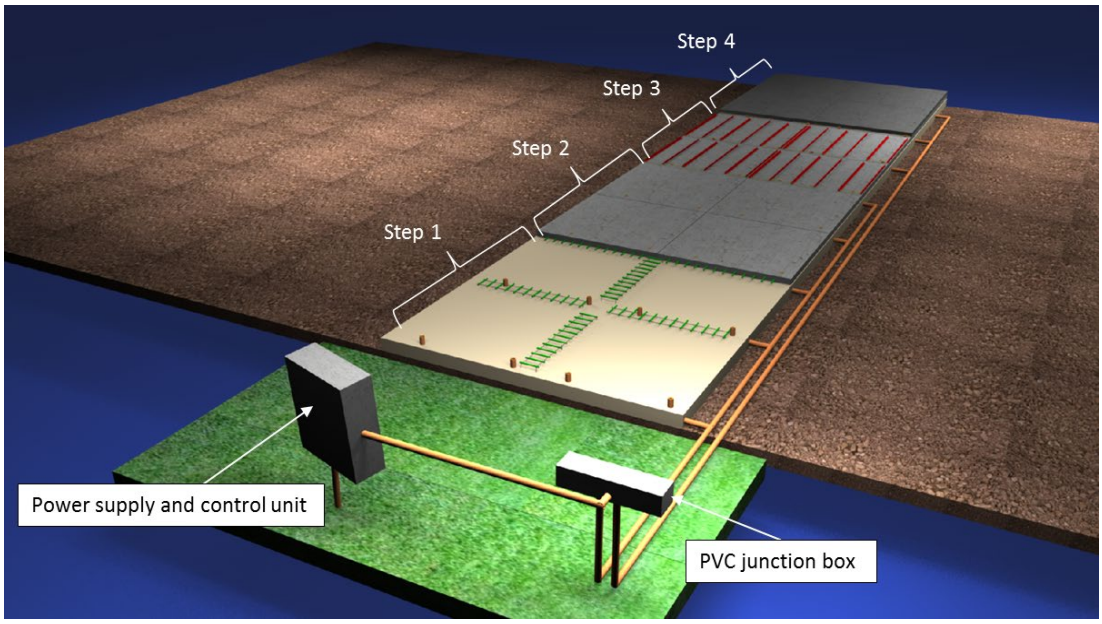

Figure 34. Construction Sequence of ECON HPS Using Two-lift Paving

5.5 CONCEPTUAL DESIGN AND CONSTRUCTION CONSIDERATIONS OF ECON HPS USING CONCRETE OVERLAYS

The concrete overlay system is classified into a bonded resurfacing family and an unbonded resurfacing family. The construction sequence of the ECON HPS using either concrete overlay system may be similar to one another, except that a separate interlay should be placed on the existing concrete pavement for an unbonded concrete overlay to mitigate the reflective cracking potential.

The construction sequence of the ECON HPS using concrete overlay involves the following three major steps: (1) prepare existing pavement and place electrodes, (2) connect electrical wires for electrodes systems, and (3) place ECON layer.

5.5.1 Step 1: Prepare Existing Pavements and Place Electrodes System

Electrodes are placed and secured on the existing concrete; electrical wire connections can be made later (see Figure 35). Perforated stainless steel 316L is recommended for electrodes because of its high corrosion resistance. The existing surface may require resurfacing repairs to meet the required elevation. Threaded nylon rods and nuts can be used to fix the electrodes on the conventional concrete surface to prevent their movement during pouring of the ECON layer, as shown in Figure 35(a) and (b). Nylon materials are used to prevent corrosion and electrical current leakage to the ground as well as to prevent interaction with the electrical field. The electrodes can be anchored on the existing pavement using a drilling machine to drill holes to fix the electrodes (see Figure 35(c and d)).

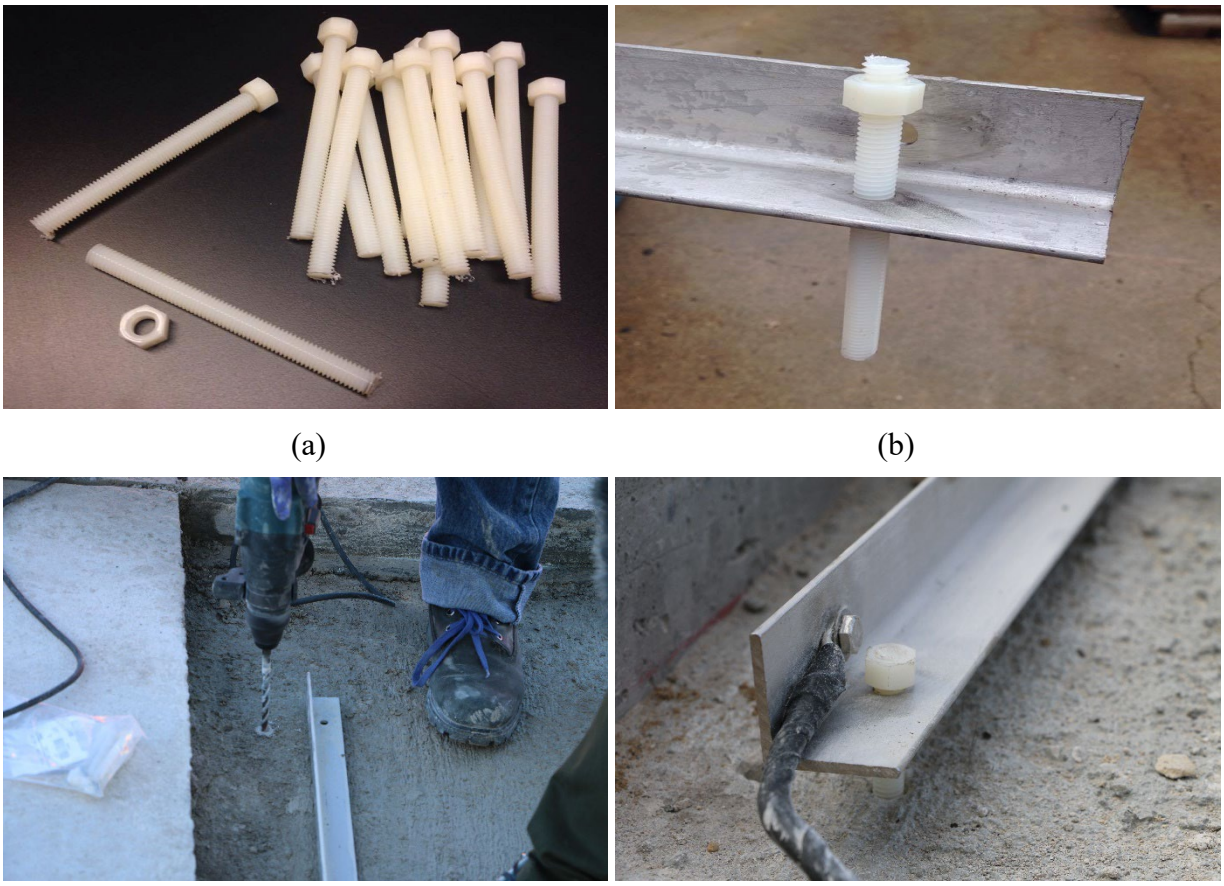

(a) (b)

(c) (d)

Figure 35. Fixing Electrodes on Existing Pavement: (a) Nylon Rods and Nuts, (b) Electrode with Nylon Rod, (c) Drill Hole to Fix Electrode, and (d) Placement of Electrode

Figure 36 shows the layout of the electrode installation on an existing pavement. Electrodes should be placed in each individual slab so that they will not cross the pavement's joints. Installing the electrodes at the designed spacing ensures the performance of the ECON HPS and the required energy density. A minimum of a 2-in. clearance above the top of the electrodes is recommended to prevent any cracking along the electrodes.

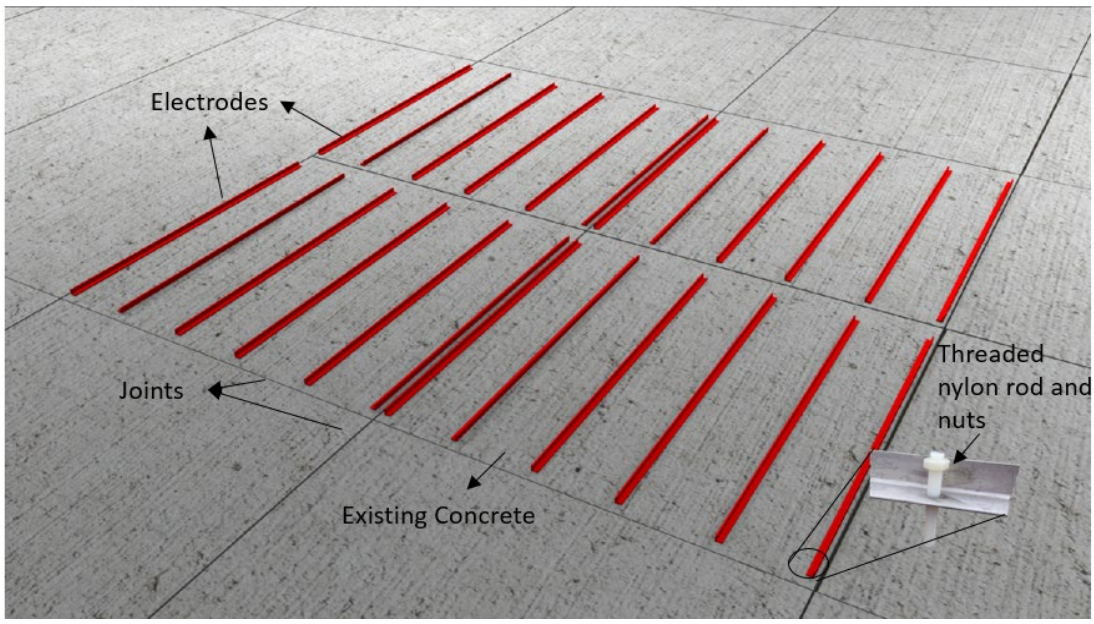

Figure 36. Electrodes Installation on Existing Pavement

To accelerate the installation of the electrodes on the existing pavement, electrodes for one slab can be assembled (see Figure 37) and then placed and secured using nylon threaded rods and nuts. Fiberglass rebar is intended to support and assemble the electrodes so that all electrodes can be placed simultaneously and then secured. Fiberglass rebar can be placed across premade holes in the electrodes to assemble and support the electrodes together. Electrodes with fiberglass rebar may be preassembled and shipped to the project site to expedite construction procedures.

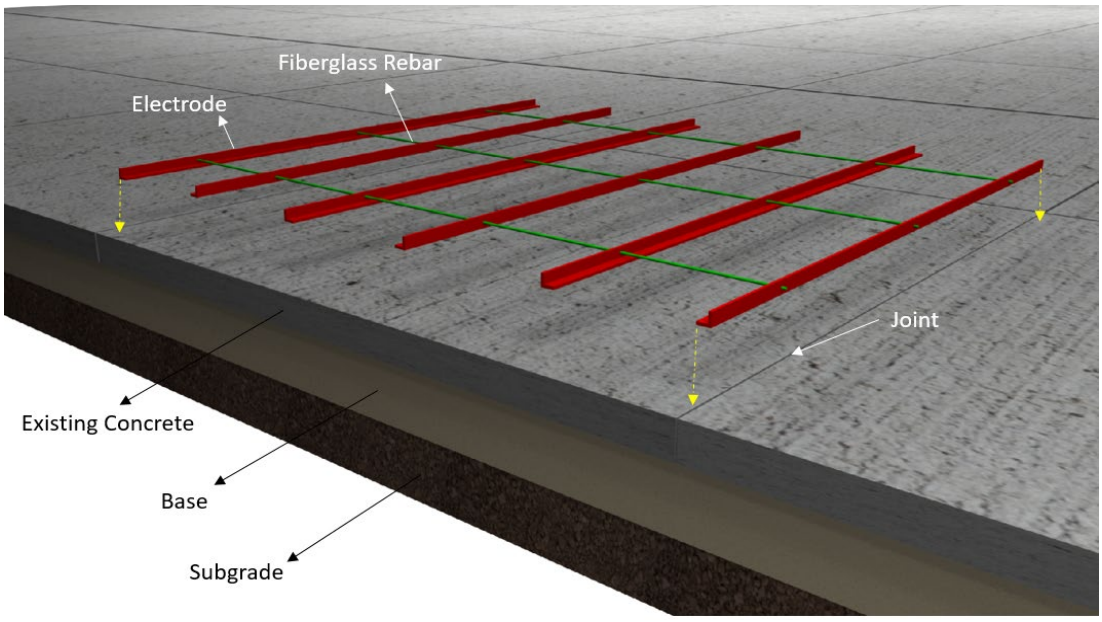

Figure 37. Electrodes Assembly Installation on Existing Pavement

5.5.2 Step 2: Connect Electrical Wires for Electrodes Systems

Electrical wires may be placed on the existing concrete surface and/or by making a trench in which to place the electrical wires (see Figure 38). Electrical wires should pass under the joints to protect them (see Figure 39) from damage because concrete will expand or contract at the saw-cut joints of the ECON layer.

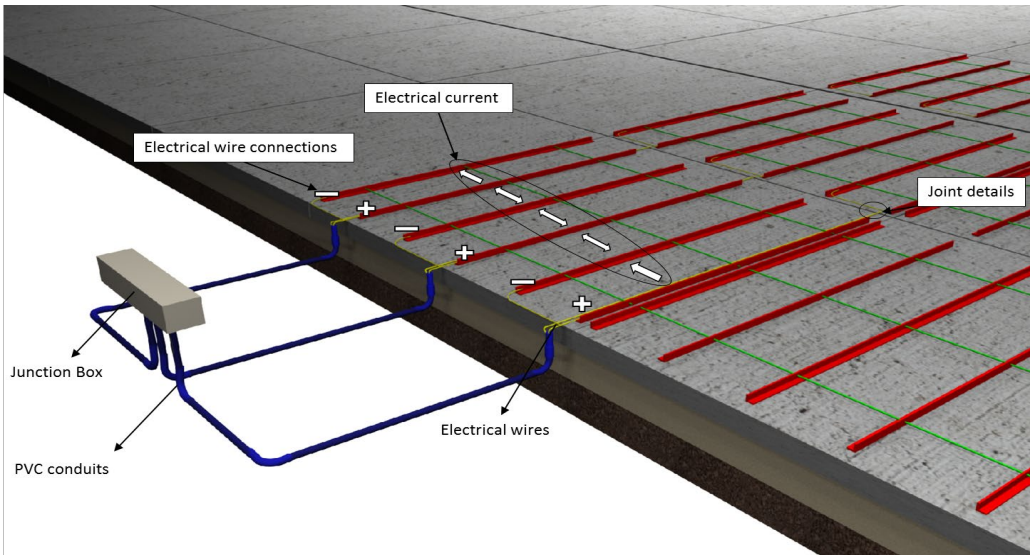

Figure 38. Electrical Wires Connection for Electrodes System

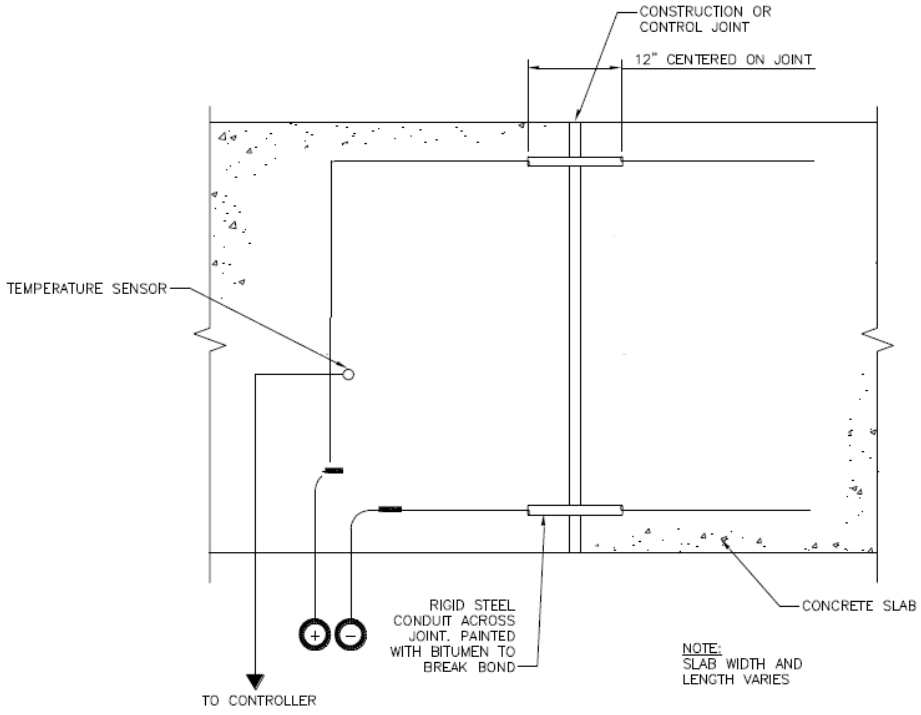

Figure 39. Electrical Wires Details at Joints (FAA, 2011)

5.5.3 Step 3: Place ECON Layer

The ECON layer can be placed after placing and securing the electrodes and connecting the electrical wires of the electrodes. Concrete overlays are constructed using conventional equipment and procedures (Harrington et al., 2014). Figure 40 shows the recommended placement of concrete overlay for large areas such as parking (Harrington & Riley, 2012) and can be similarly applied for airfield concrete pavement. These types of placements are known as block placement (see Figure 40(a)) and strip placement (see Figure 40(b)). Block placement may be used for large areas to expedite the paving procedure and to reduce the formwork. Laser screeds are one option for block placement. This method has been used as common practice for parking lots and could be an ideal implementation in airfield pavements, which have large areas. Strip placement is a highly productive paving method compared to block placement. A slipform paver can be used for the strip placement with a predesigned width of the strip.

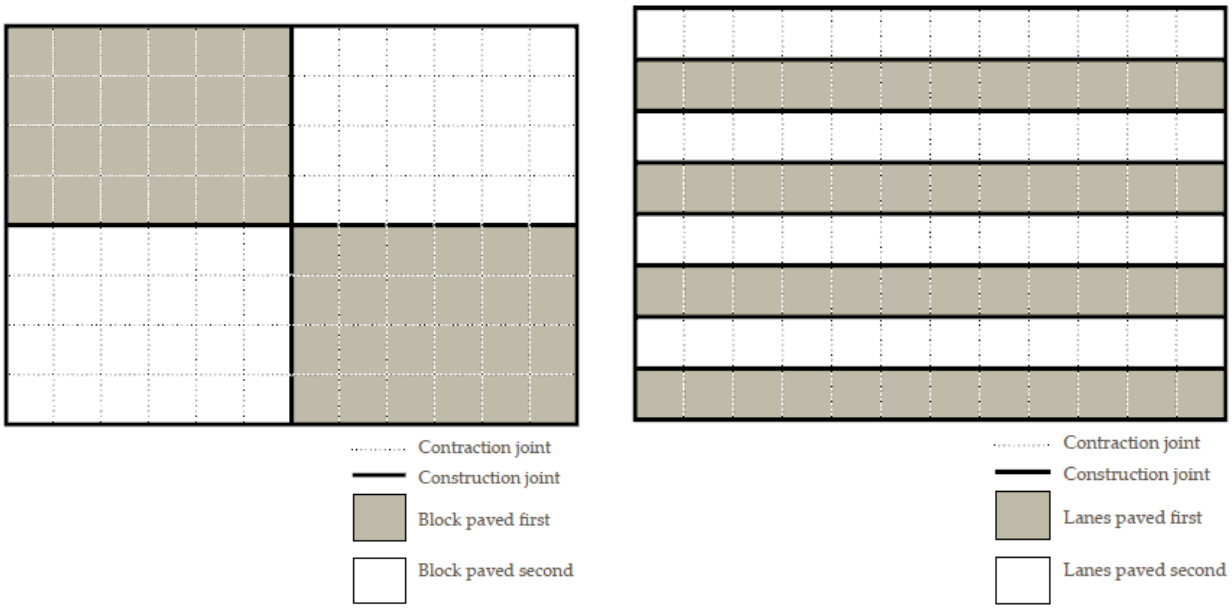

(a) Block placement (b) Strip placement

Figure 40. Placement of the ECON Layer: (a) Block Placement and (b) Strip Placement (Harrington & Riley, 2012)

5.5.3.1 Options for ECON Overlay Placements

There are many ways of paving that could be used to place the ECON overlay as follows (Kohn et al., 2003; Harrington & Riley, 2012):

1. Lightweight finishing machines
2. Laser screed
3. Slipform paving

5.5.3.1.1 Lightweight Finishing Machines

Truss screed or roller screed are used in lightweight finishing machines (Kohn et al., 2003). These types of machines are normally used for thin concrete pavement, and they require a stationary metal form. Roller screeds are recommended with a concrete mixture with higher slump and are used for small, medium, or large projects at paving width ranging from 10 to 24 ft (see Figure 41(a, b, and c)). Vibratory truss screeds (see Figure 41d) are commonly used on placements as wide as 60 ft (Harrington & Riley, 2012). The benefit of truss screeds is their capability to screed larger areas in a single pass.

(a) (b)

(c) (d)

Figure 41. Placement Types: (a) Spinning Tube Screed, (b) Triple-roller Tube Paver, (c) Roller Screed, and (d) Vibratory Truss Screed (Harrington & Riley, 2012)

5.5.3.1.2 Laser Screed

Laser screed is an efficient method for the construction of large block pavement placement (Harrington & Riley, 2012). Using the technology of laser control, a laser screed is used to both consolidate and strike off the concrete and can provide an accurate grade level. The concrete can be placed by using pump or conveyors or directly from a concrete truck (see Figure 42(a) and (b)).

(a) (b)

Figure 42. Laser Screed Applications via (a) Concrete Pump Truck and (b) Laser Screed

5.5.3.1.3 Slipform Pavers

A slipform paver is recommended for high production rates, and the grade level can be adjusted using a string line or a global positioning system (GPS) (Harrington & Riley, 2012). When using a slipform paver, as shown in Figure 43, there is no need to use a fixed form; however, such a paver can be used in side-form application by stretching the paver width beyond the forms (Kohn et al., 2003). The concrete mixture should meet the requirements of the operation of the slipform paver, such as low-slump concrete. A slipform paver can be stretched up to 50 ft (15 m), depending on the machine type. A slipform paver is recommended for airfield pavement 8 in. (200 mm) thick or more (Kohn et al., 2003).

Figure 43. Slipform Paver (Photo Courtesy of Gomaco)

5.5.3.2 Consideration Before Placing the ECON Layer

1. Electrodes should be located 2 in. below the ECON surface to provide clearance for slipform paving (see Figure 33(a)).
    a. Electrodes should not interfere with the vibrators and auger (see Figure 33(b)).
2. Electrodes should be cleaned using an air-blower, brooms, and a pressure washer prior to placing the ECON layer to ensure sufficient bond between electrodes and the ECON layer.
3. Care should be taken to ensure that the elevation of the electrodes is equal.
4. Electrodes should be placed and fixed to prevent any movement of electrodes while placing the ECON layer.
5. The electrode system should be tested for the electrical connection to ensure that the power supply is properly providing power to the ECON HPS.
6. Visual inspection is recommended for the electrical connection with the electrode system.

An ECON layer may be placed as either a bonded or an unbonded layer depending on the existing pavement condition. The main difference between unbonded and bonded overlays is that in an unbonded overlay, an HMA layer or Geotextile fiber is placed on the existing layer to break the bond between two layers. Figure 44 shows the ECON HPS as a bonded concrete installation that includes electrodes, electrical connections, PVC conduits, and a junction box. The ECON HPS should be placed after placing the electrode system using a paving machine determined to be appropriate to the project location, size, shape, etc.

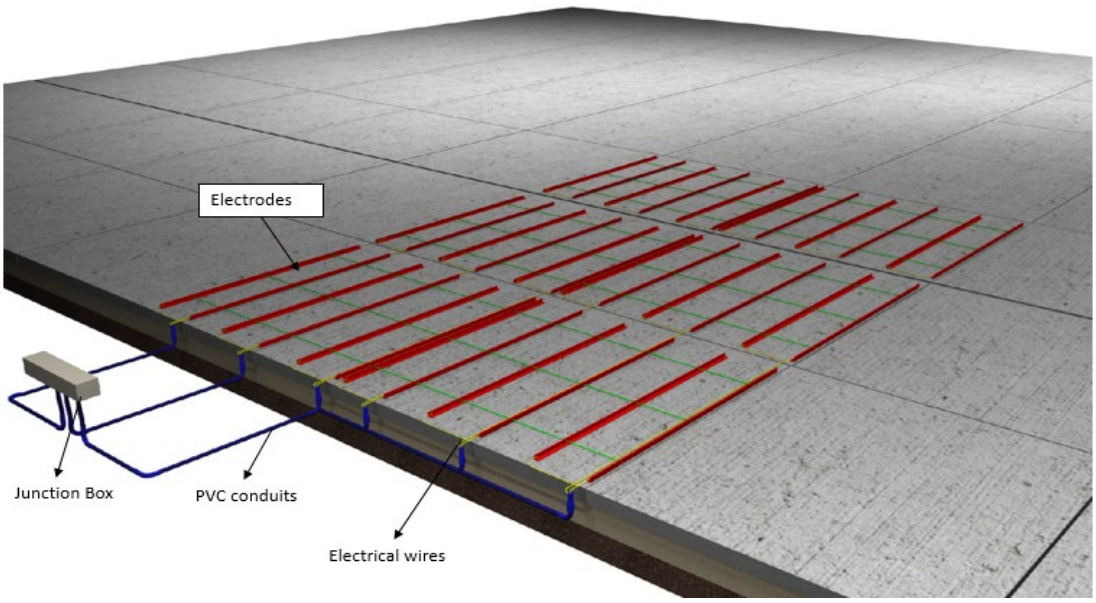

Figure 44. Electrode Placement and Electrical Wire Connections for a Bonded System

Figure 45 shows the cross section of the ECON slab using a bonded overlay. The bonded concrete overlays (top layer) are generally 2–5 in. thick (Harrington et al., 2014). The recommended joint spacing of bonded concrete overlay to reduce curling and warping stresses is in the range of 3–8 ft (Harrington et al., 2014). The ECON layer (top layer) is recommended to be in the range of 2–4 in. thick, close to the thickness of a bonded overlay. The electrode number and spacing can be designed according to the required energy density to meet the heating performance and should be capable of maintaining the temperature of the ECON surface above the freezing point. The electrodes are installed and fixed on a prepared surface. The ECON layer (top layer) can be placed on any existing surface such as concrete, asphalt, or composite.

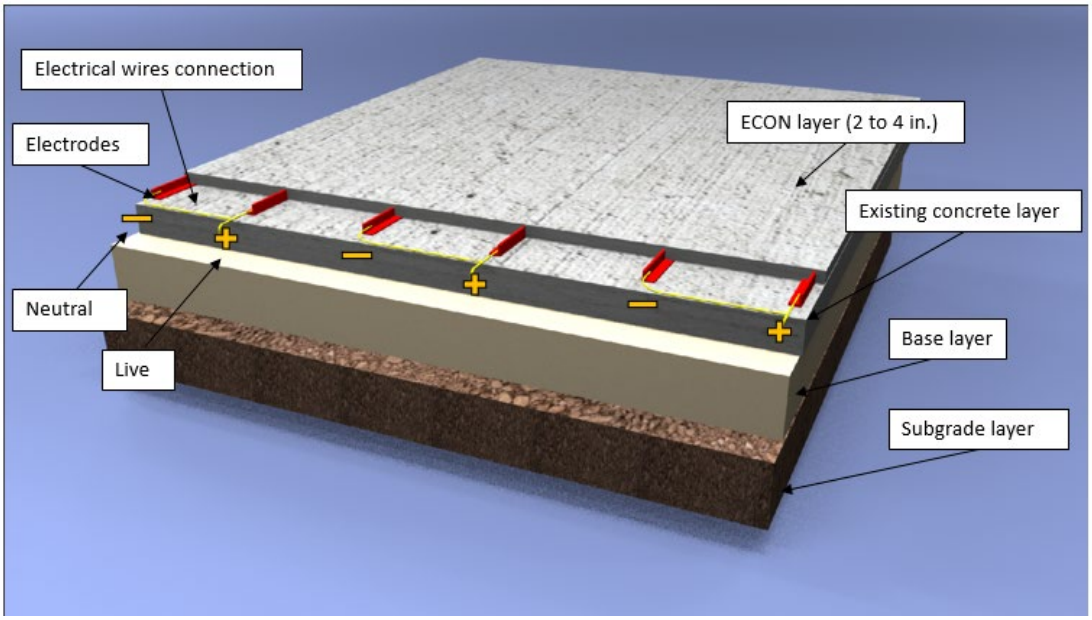

Figure 45. A Cross Section of ECON HPS

Figure 46 shows the separator layer placed before installing the electrode system. The electrode spacing can be designed based on the design energy density to achieve the required heat generation. PVC conduits are used to accommodate and protect the electrical wires. A PVC junction box is placed and installed to connect to the PVC conduit and allow the electrical wires to be connected to the power supply. An ECON HPS using unbonded overlay techniques could provide better performance due to the use of the separator layer in which the ECON layer (top layer) can be freely moved without the bottom layer.

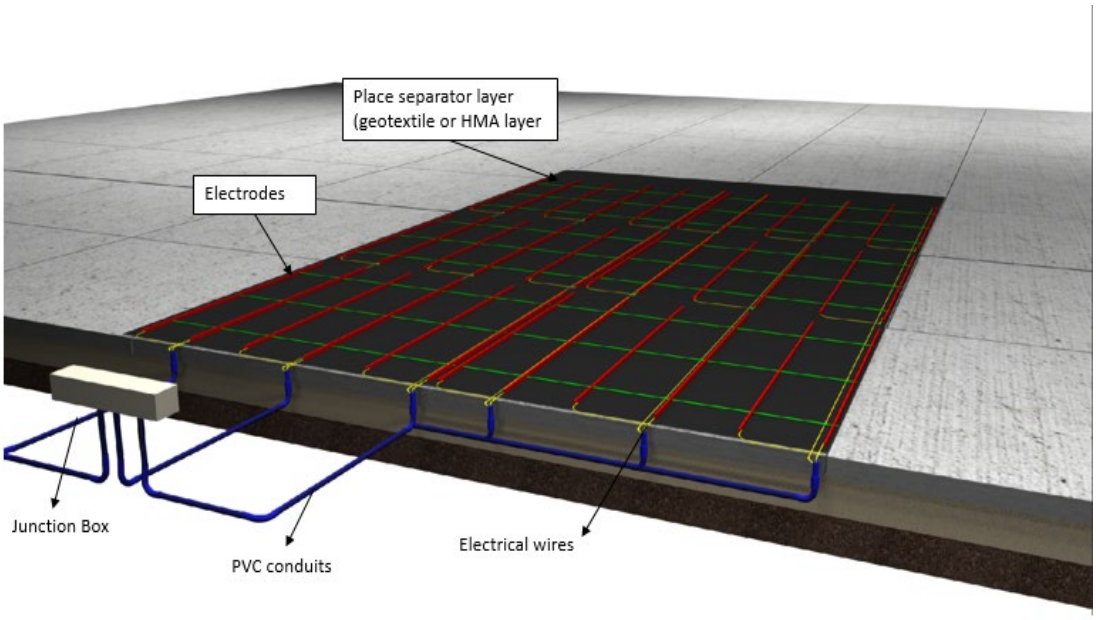

Figure 46. Electrodes Placement, Electrical Wires Connection for Electrodes, and Separator Layer for Unbonded System

Figure 47 shows the cross section of the ECON slab utilizing unbonded overlay techniques. Unbonded concrete overlays are generally 4–11 in. thick (Harrington et al., 2014). If the unbonded overly thickness is greater than 4 in., the top layer may be divided into two layers; the top layer is the ECON layer and the bottom layer is regular concrete, as shown in Figure 47. The ECON layer (top layer) is generally 2–4 in. thick. The separator layer is placed on the existing layer, and then the regular concrete can be poured. After pouring the regular concrete, the electrode system should be anchored, and the ECON layer is placed afterward. The joint spacing of an unbonded concrete overlay is typically recommended to be in the range of 6–15 ft, depending on the thickness of the overlay (Harrington et al., 2014). As a rule of thumb, the joint spacing should be 2 times the thickness of the unbonded overlays. Dowel bars to transfer the load across the joints are required when the thickness of the unbonded layer is larger than 7 in. If the pavement thickness is less than 7 in. thick, conventional dowels may cause clearance problems for a slipform paver (Harrington et al., 2014). Alternative dowels, such as plate dowels that provide extra clearance for the paver, can be used for a thinner unbonded layer of 5-in. thickness or less; plate dowels, however, are a newly developed technology whose performance is not yet well understood. Fibers can also be used to hold cracks and joints together (Harrington et al., 2014).

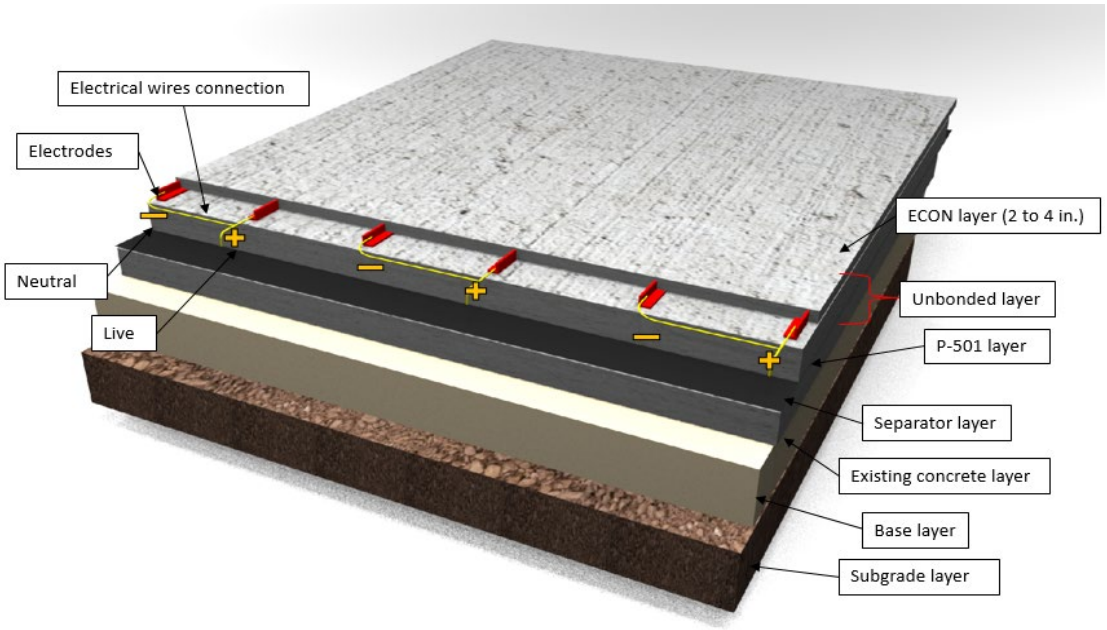

Figure 47. Using an ECON Layer as Unbonded Concrete Overlay

5.5.4 Step 4: Install Power Supply and Control System

For this step, the power supply and the control system are installed. Both should be placed near the PVC junction box where electrical wires and wires for sensors systems can go through the junction box and then connect to the power supply and control system (see Figure 48). The control system consists of data acquisition for collecting temperature sensors, a laptop, and operator interface units. The control system is designed to turn the system on/off either manually or automatically based on programing for given temperature values. The power supply consists of contactors, circuit breakers, and electrical sensors. The contactors can receive a signal remotely to turn the system on or off based on temperature sensors. The circuit breaker is designed to monitor the electrical current usage and prevent the system from drawing more than the designed value of electrical current. The circuit breaker will turn the system off if the electrical current values exceed the designed values.

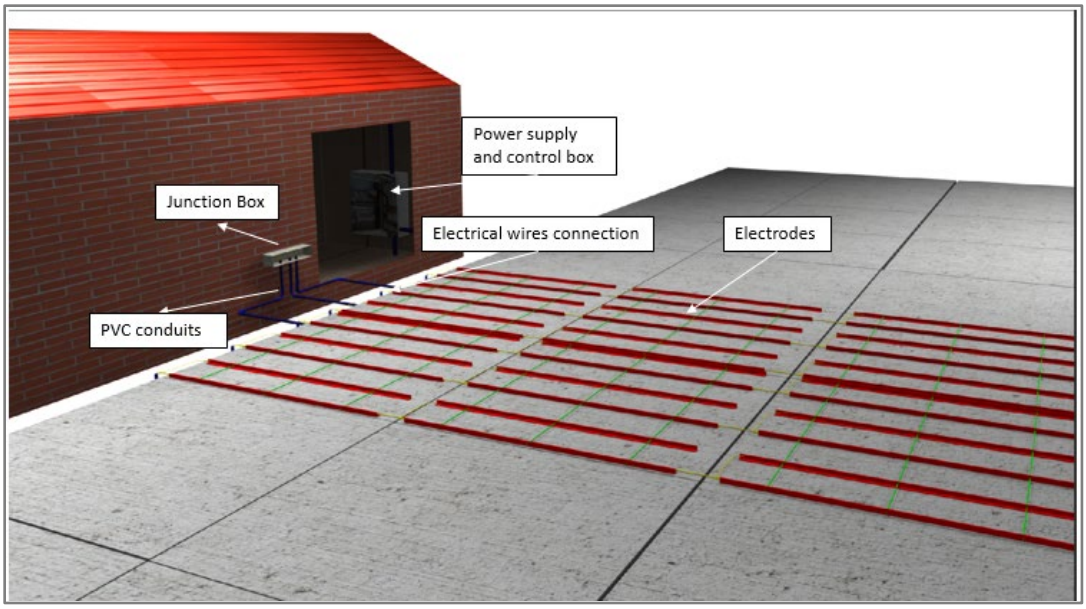

Figure 48. Power Supply and Control Systems for ECON HPS Using Concrete Overlay Technology

5.6 THE 3D VISUALIZATION OF ADVANCED CONSTRUCTION TECHNIQUES FOR ECON HPS: SUMMARY, FINDINGS, AND RECOMMENDATIONS

The conceptual design and construction procedures of the ECON system using PCP, two-lift paving, and concrete overlay techniques have been identified. The major conclusions drawn from this study are summarized below:

- Construction considerations and 3D visualization workflows for ECON HPS using advanced construction techniques were developed to develop more robust construction scheme, well-performing heated airport pavements, and good construction practices. 3D visualization for HPS ensures that the pavement system will perform as desired (uniform heat destitution in installed areas, effective ice and snow melting, leak-proof systems with advanced pavement joint details, etc.)

- ECON using PCP was developed to provide design and construction guidance for large-scale heated airport pavements. Detailed design, such as joint interfaces between ECON panels and materials selection, was provided to ensure good construction practices while using PCP. Another benefit of ECON using PCP is that it can be implemented for new pavements or existing pavements, expediting the construction procedures, reducing labor, reducing delays prior to opening to traffic, and minimal weather restrictions.

- ECON layer (top layer) using the concrete overlays approach can be placed as a thin layer. This approach is considered cost-effective because it is placed on the existing pavement (bottom layer) without the need for reconstruction. The ECON system installation as an unbonded overlay is recommended due to bonding issues, and because it can move freely without the restriction of the bottom layer. Different concrete paving methods, such as laser

screeds or slipform pavers, may be used depending on the project size, location, and construction time.

- ECON using two-lift paving can be used for new construction, and slipform can expedite the construction process for large-scale construction in comparison to conventional methods.

- Electrodes can be assembled and installed in a set of electrodes for each slab to expedite the construction procedure for any option of advance construction techniques.

6. THE 3D VISUALIZATION OF ADVANCED CONSTRUCTION TECHNIQUES FOR HYDRONIC HEATED PAVEMENT SYSTEMS

6.1 SCOPE AND OBJECTIVES

This section focuses on the development of a conceptual design framework for hydronic heated pavement using PCP, two-lift paving, and concrete overlays. The scope of this work was to provide guidance to design and construct hydronic heated pavement utilizing 3D visualization with various options.

6.2 DEVELOP ASSESSMENT FRAMEWORK

Conceptual designs for HHPSs have been developed through 3D visualizations to provide more detailed understanding in construction and operational schemes of HPSs. Figure 49 presents a 3D visualization that illustrates the general operational scheme of HPSs.

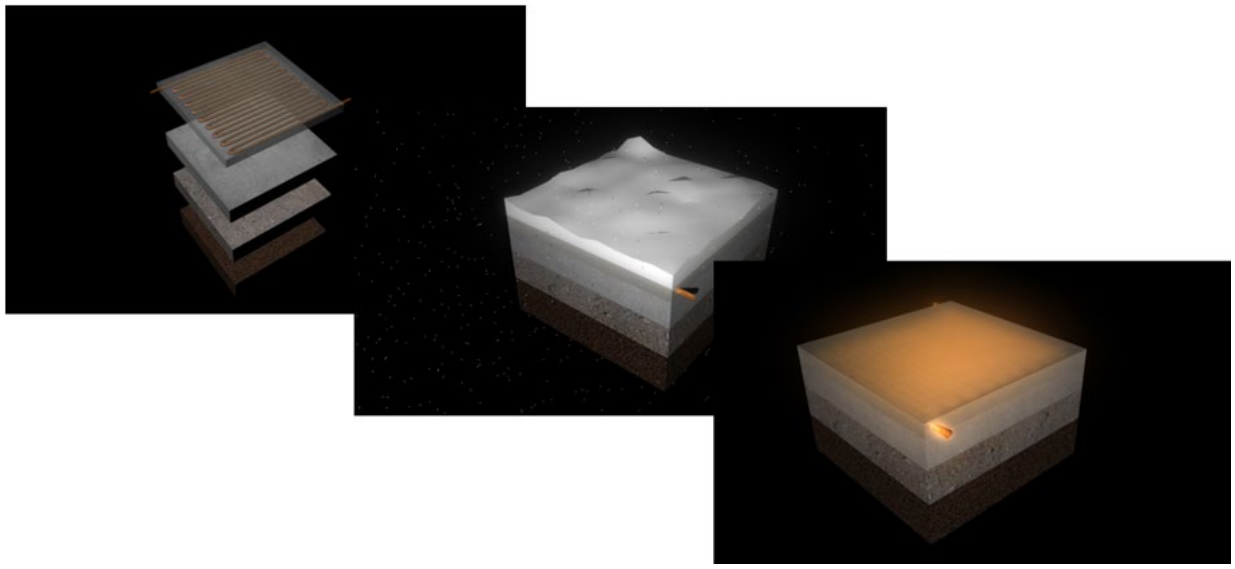

Figure 49. Conceptual Design of an HHPS

6.3 CONCEPTUAL DESIGN AND CONSTRUCTION CONSIDERATIONS FOR HHPS USING PCP

Figure 50 presents the 3D visualization for HHPS fabrication using PCP with pipes that can be placed inside each panel before placement and connected to each other after placement. The benefit of using PCP is to accelerate the construction process in comparison to other techniques. The construction sequence of the HHPS using PCP involves the following three major steps: (1) fabrication of the hydronic heated slab, (2) base layer preparation and slab placement, and (3) pipe connection to the power source.

6.3.1 Step1: Fabricate Hydronic Heated Slab Off-Site

A hydronic heated slab can be fabricated through off-site construction using PCP (see Figure 50) with formwork designed to facilitate the pipes, wire mesh, dowel bars, and slots (see Figure 50(a) and (b)). The formwork has open areas so that the inlet and outlet pipes can be connected to other hydronic slabs. The pipe is placed on top of wire mesh to elevate the pipe near the surface and hold it there when pouring the concrete. A minimum of 50 mm of concrete cover over the top of the pipe is typically required (ASHRAE, 2015). The pipe pattern can be designed based on a specific job site to provide heat sufficient for melting ice and snow. After securing the pipe, concrete is poured into the formwork and then is screed and cured before transferring those into a construction site (see Figure 50(c) and (d)).

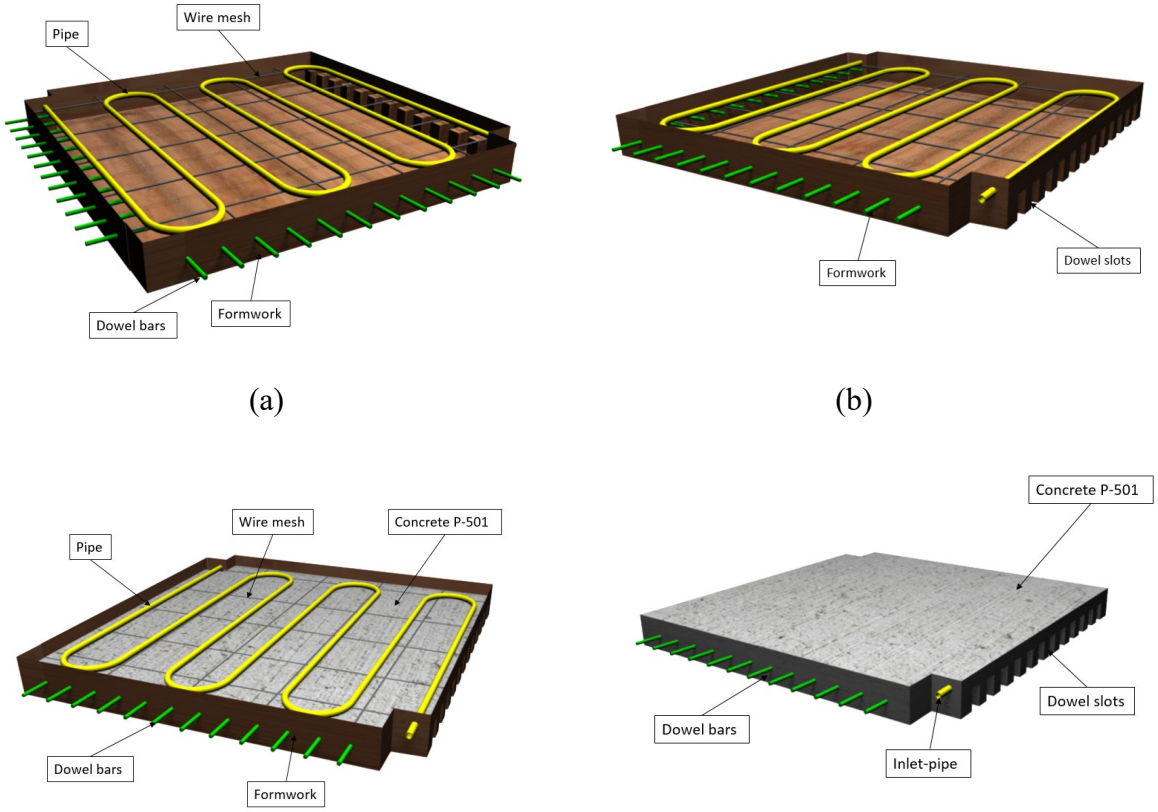

Figure 50. A 3D Visualization of Hydronic Heated Slab Fabrication Using PCP

6.3.2 Step2: Prepare the Base Layer and Place Hydronic Heated Slabs

In this step, the subgrade and base layers are prepared and compacted to satisfy the required density and to identify the location of manifolds to define pipe circuit length and pattern. The pipe pattern and spacing can be altered based on the project site, geometry, size, required energy, and locations. The hydronic heated slab can be transported and placed into the project site. The hydronic heated slab has dowel bars and slots to provide load transfer like a traditional PCP. The pipes can be connected to each panel after placing the hydronic slabs, and the voids of the dowel slots are filled to ensure the desired panel elevation is achieved. Figure 51(a) and (b) shows the pipe pattern and connection between hydronic heated slabs.

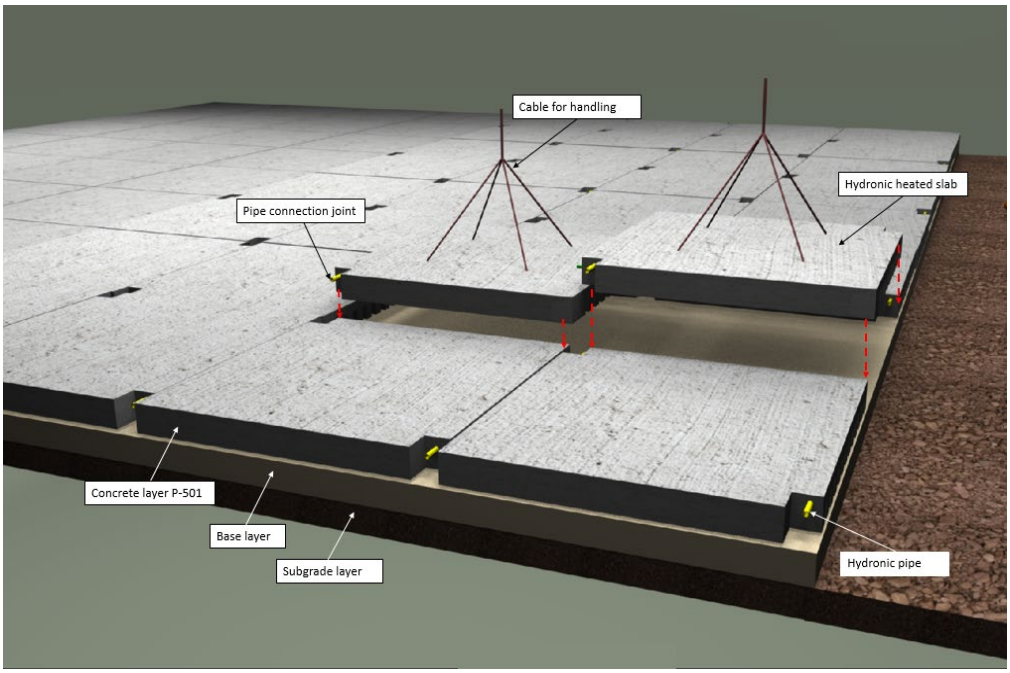

(a)

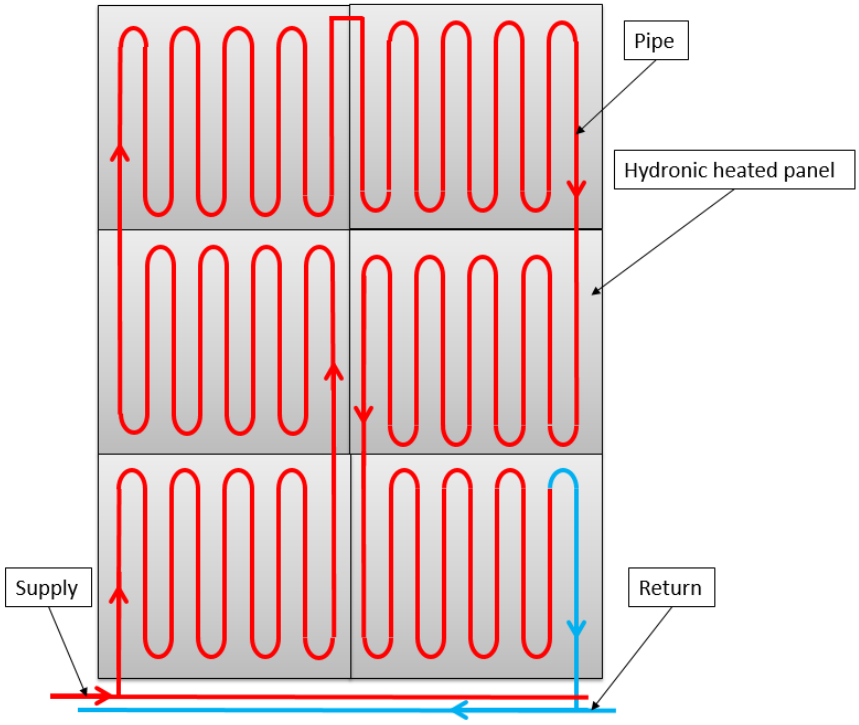

(b)

Figure 51. Hydronic Heated Slabs Assembly

6.3.3 Step3: Connect Pipes to Heat Source

After identifying and connecting the manifold to the pipes, the manifold should be connected to the heat source. Fluid can then circulate in the embedded pipe where the heat source heats the cold fluid (see Figure 52). A variety of heat sources, such as boilers, geothermal wells, or natural gas heaters, can be used depending on their availability of the project site. For example, a geothermal source that includes a heat pump can obtain a sufficient level of heat to melt ice and snow (Ceylon, Kimm Gopalakrishnan, 2014). A hydronic heated system can be operated automatically using a control system to turn the system on/off based on a set temperature value that can be measured using temperature sensors embedded in concrete. To provide satisfactory operation the hydronic heated system should be warmed up before snow and ice accumulates on the surface (ASHRAE, 2015).

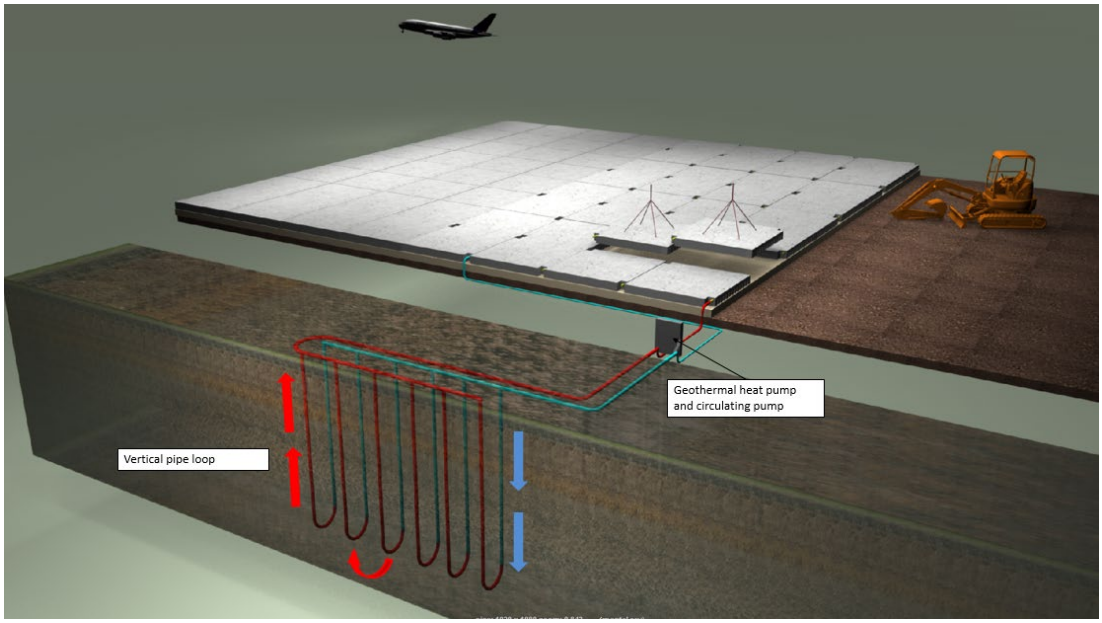

Figure 52. Sample HHPS with Geothermal Wells as Heat Source

6.4 CONCEPTUAL DESIGN AND CONSTRUCTION CONSIDERATIONS OF HHPS USING TWO-LIFT PAVING

The construction sequence of the HHPS using two-lift paving involves the following three major steps: (1) preparing the base layer and install the dowel baskets, (2) placing pipes, and (3) placing the P-501 layer.

6.4.1 Step 1: Prepare the Base Layer and Install Dowel Baskets and Wire Meshes

This step involves preparing and compacting the base layer, then installing dowel baskets and wiring mesh to raise the pipes near the surface (see Figure 53(a) and (b)). Wire mesh is placed on plastic chairs; then, pipes can be placed on the prepared wire mesh and tied to prevent movement when pouring the concrete. Pipes should be placed a minimum of 50 cm below the concrete surface to warm up the surface and prevent ice and snow accumulation (ASHRAE, 2015).

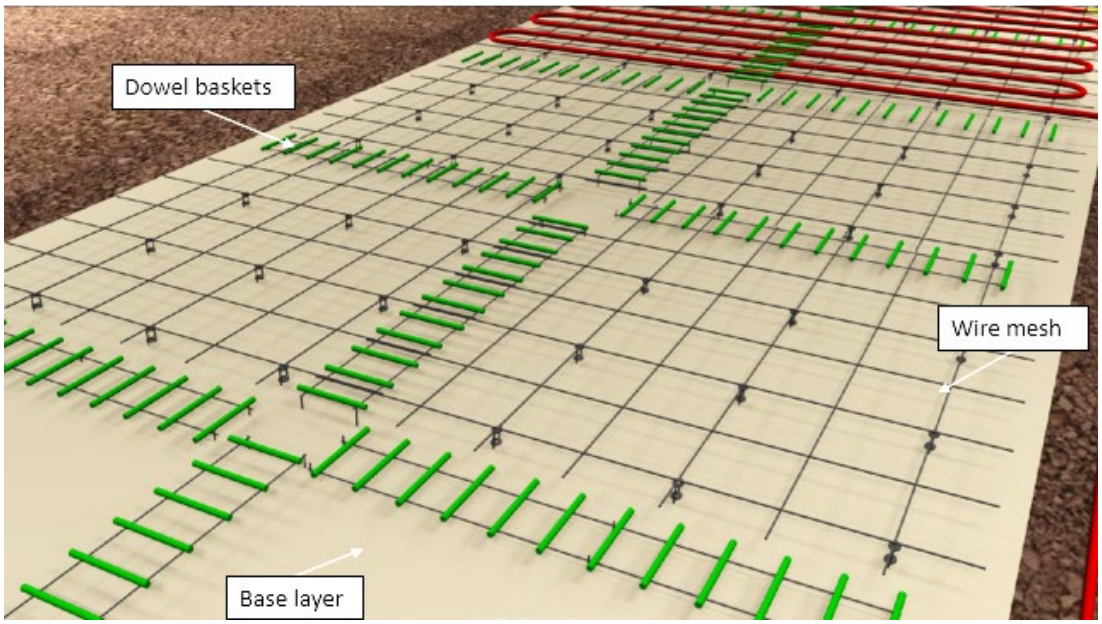

(a)

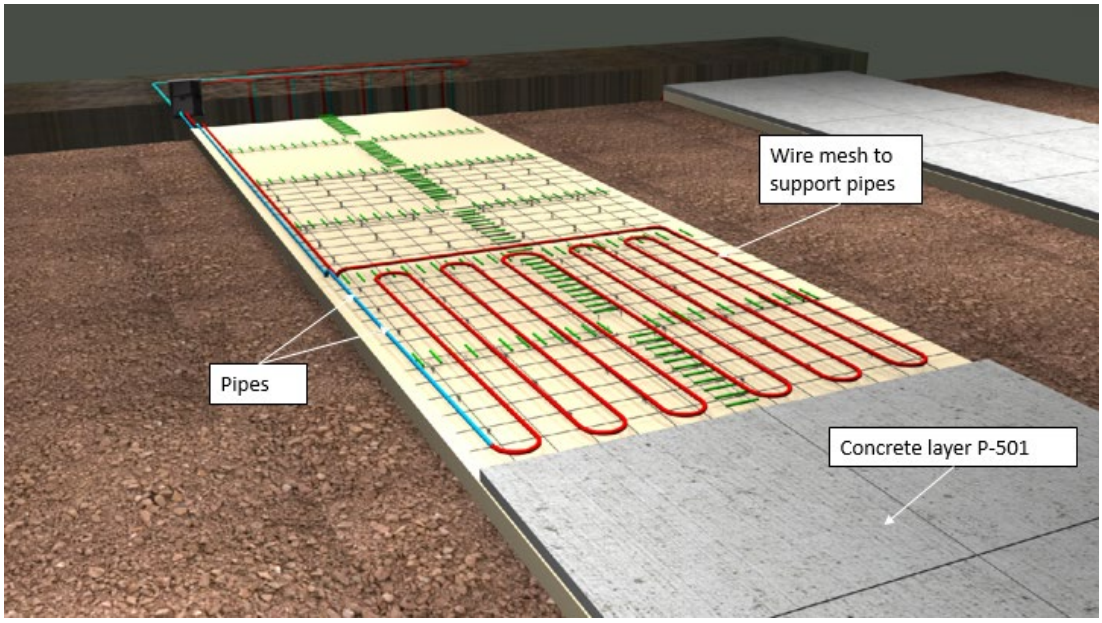

(b)

Figure 53. View of the HHPS Using Two-lift Paving

6.4.2 Step 2: Place Pipes on Wires Mesh

For this step, first the pipe pattern and spacing and the location of the manifold are defined. The pipe pattern and spacing are determined based on the required energy density that is effective in melting ice and snow for the specific project site. The pipe should not interfere with the saw-cut at the joints to prevent damages to the pipes. The recommended joint options that protect the pipes

once cross the joints are presented in Figure 54 (FAA, 2011; ASHRAE, 2015). The pipes should be examined using air testing to identify any cracks or leakages before placing the concrete.

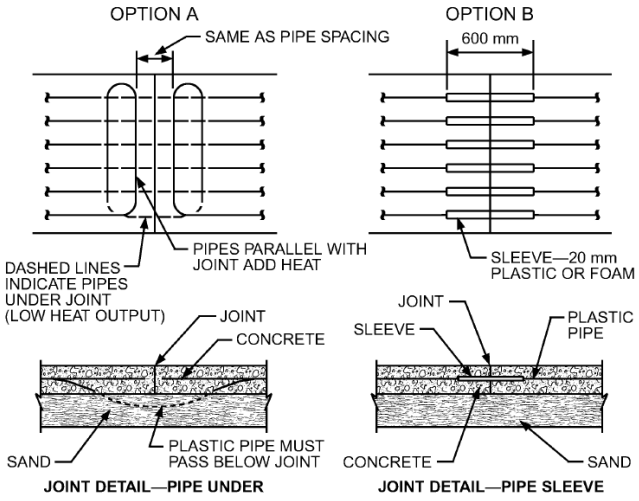

Figure 54. Pipe Details for Concrete Construction of HHPS Using Two-lift Paving (ASHRAE, 2015)

6.4.3 Step 3: Place P-501 Layer

In this step, the concrete layer is placed, and the pipes are connected to a heat source. Concrete can be placed after ensuring the pipes will not cause a slipform paving clearance problem. Pipes should be located 5 cm below the concrete surface to provide clearance for slipform paving's vibrators and auger (see Figure 55). The fluid circulated in the closed-loop pipe can be heated using geothermal energy, as shown in Figure 56. A geothermal energy system at an installation cost of 1.6 million was installed at the greater Binghamton airport to heat an area of 260 m^2 (Zeigler, 2013). While installation of geothermal energy is expensive, the operational cost of using geothermal energy is considered cost-effective.

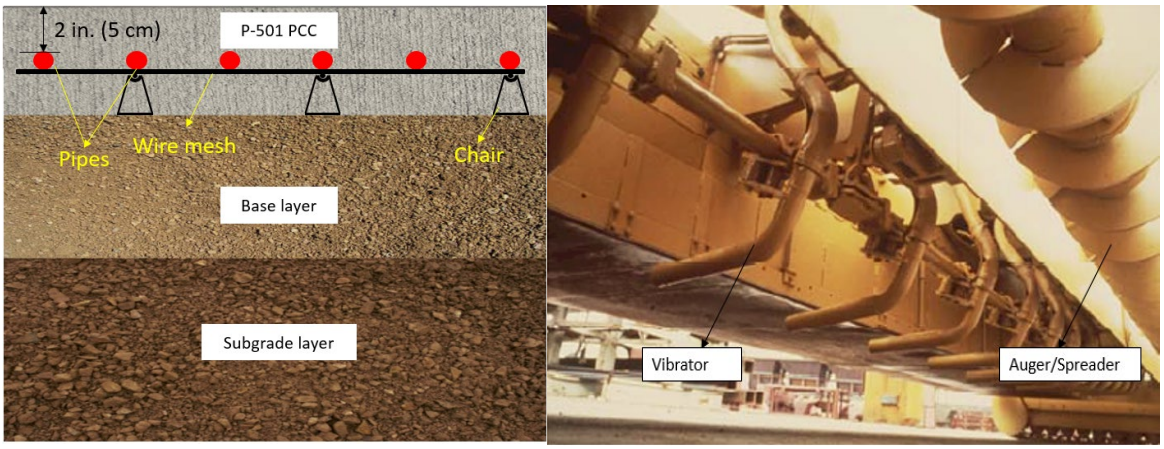

(a) (b)

Figure 55. Paving Considerations: (a) Cross Section of HHPS and (b) Slipform Paver

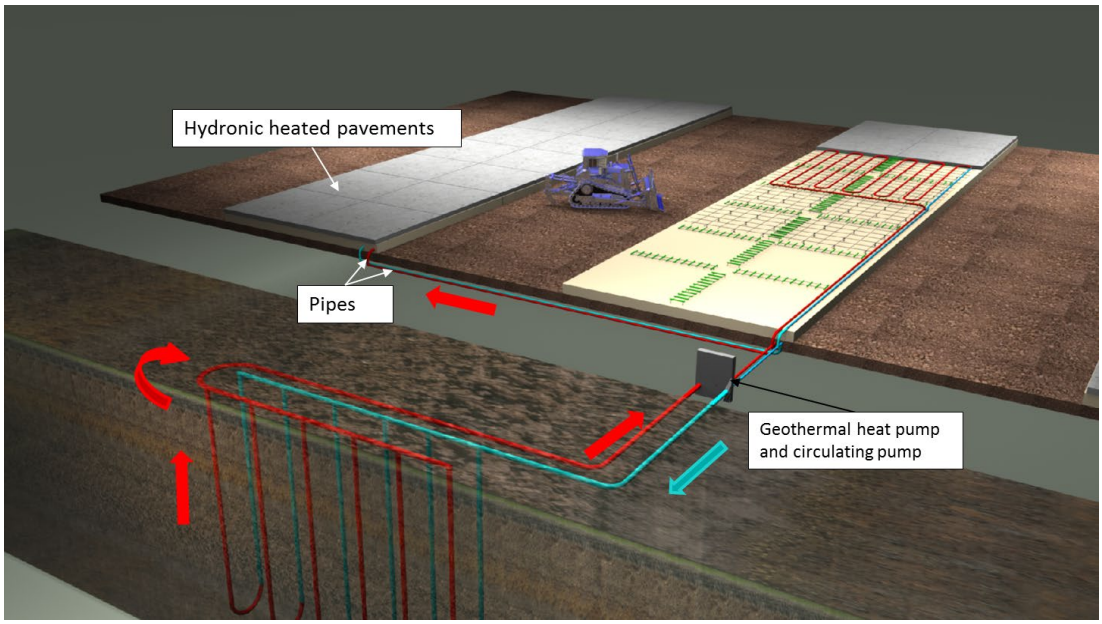

Figure 56. Geothermal Wells as Heat Source for HHPS Using Two-lift Paving

6.5 CONCEPTUAL DESIGN AND CONSTRUCTION CONSIDERATIONS FOR HHPS USING CONCRETE OVERLAY

The construction sequence of the HHPS using concrete overlay involves the following two major steps: (1) preparing existing pavement and placing pipes and (2) placing the P-501 layer.

6.5.1 Step 1: Prepare Existing Pavements and Place Pipes

In this step, the existing pavement is prepared, pipes are placed on the existing pavement, and manifold locations are identified. The preparation for existing pavement depends on existing pavement conditions. The existing surface may be milled to meet the required elevation if necessary. Pipes are installed on existing pavement and anchored either using clips or tied to wire mesh to prevent their movement when pouring concrete (see Figure 57). Choice of pipe pattern and spacing, size, and lengths are based on the required energy density for the specific project location. Pipes should not interfere with the saw-cut at the joints to prevent damages to the pipes. The recommended joint options to pass the pipes trough the joints are shown in Figure 54(b) (ASHRAE, 2015). The required number of manifolds is dependent on the project size and total length of pipe. Insulation layers, such as XPS boards, can be placed on the existing pavement before placing pipes to reduce the heat loss. The pipes should be air-tested to look for any cracks or leakages before placing concrete.

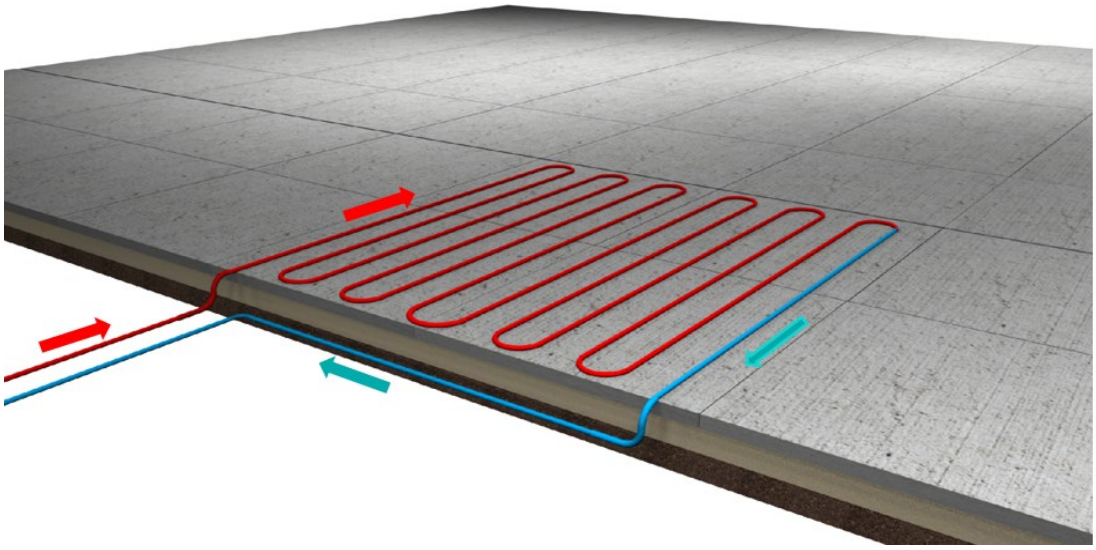

Figure 57. View of HHPS Constructed Using Concrete Overlay

6.5.2 Step 2: Place P-501 Layer

In step 2, the concrete layer is placed, and pipes are connected to the heat source. Concrete can be placed after ensuring the pipes will not cause slipform paving clearance problems. Pipes should be located at least 5 cm below the concrete surface to provide clearance for slipform paver vibrators and auger (see Figure 55). After identifying and connecting the manifolds to the pipes, the manifold should be connected to the heat source. The fluid circulated in closed-loop pipes can be heated using geothermal energy, as shown in Figure 58. The HHPS can be operated automatically using the control system to turn the system on/off based on a set temperature value and embedded temperature sensors in the concrete. To provide satisfactory operation the hydronic heated system should be warmed up before snow and ice have accumulated on surface (ASHRAE, 2015).

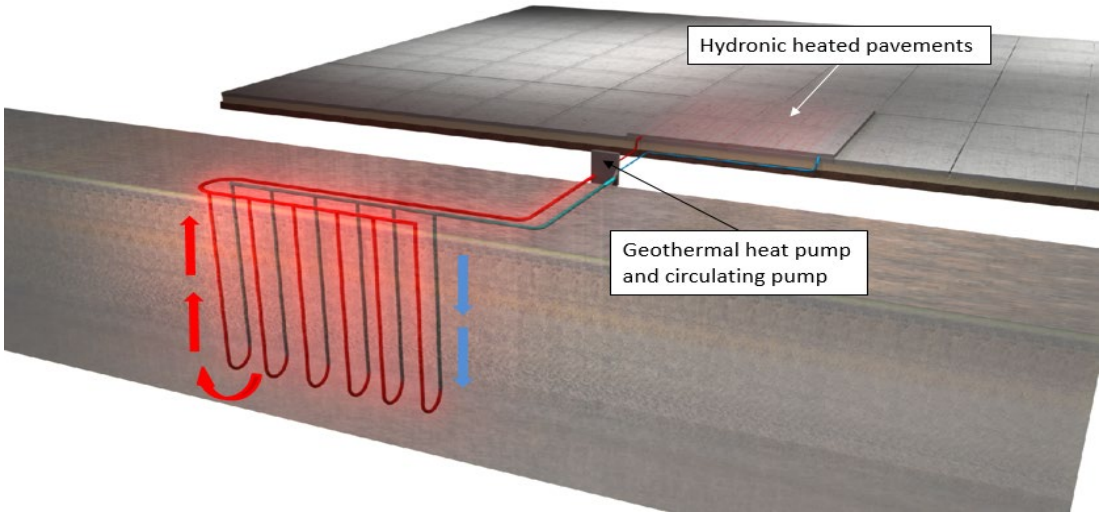

Figure 58. Geothermal Wells as Heat Source for HHPS Using Concrete Overlays

HHPS can be installed using either bonded or unbonded concrete overlay techniques. Figure 59 shows cross sections of an HHPS using bonded and unbonded concrete overlays. In HHPS using bonded concrete overlay techniques, pipes are installed and anchored using wire ties on prepared existing surface (see Figure 59(a)). In HHPS using unbonded concrete overlay techniques, pipes are placed and anchored on separator layers if the thickness of the top layer is not sufficient enough for anchoring (see Figure 59(b)).

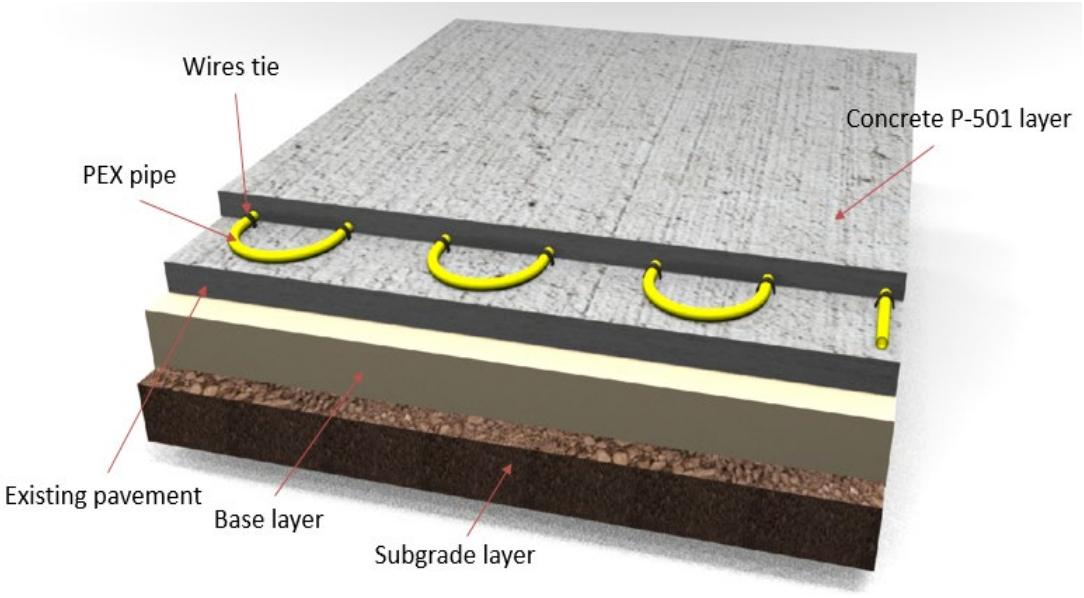

(a)

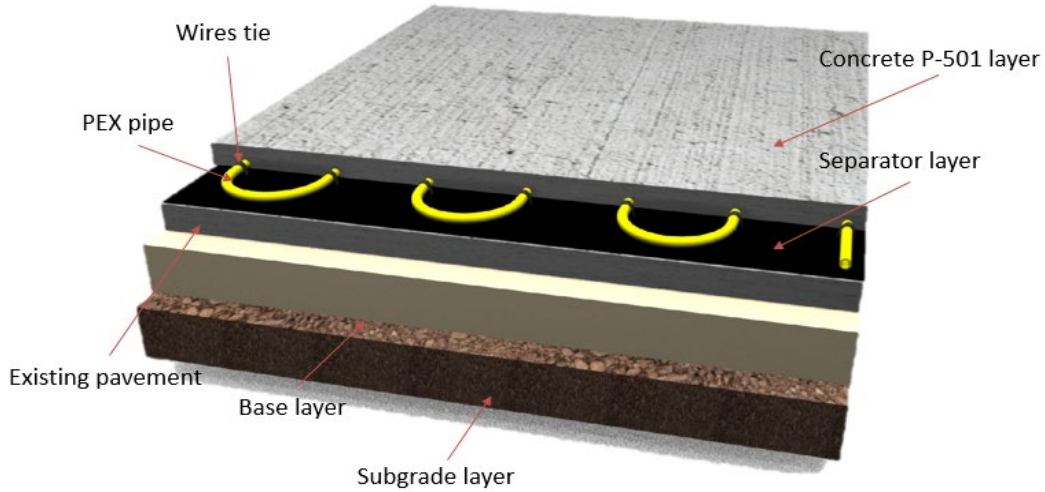

(b)

Figure 59. Hydronic Heated Cross Section (a) Using Bonded Concrete Overlay and (b) Using Unbonded Concrete Overlay

6.6 A 3D VISUALIZATION OF ADVANCED CONSTRUCTION TECHNIQUES FOR HHPS CONSTRUCTION: SUMMARY, FINDINGS, AND RECOMMENDATIONS

The design and construction of the HHPS utilizing concrete overlay, two-lift paving, and PCP was identified and the major conclusions drawn from this study are summarized below:

- HHPS using PCP was developed to provide design and construction guidance for large-scale heated airport pavements. Design details such as joint interface between hydronic heated slabs and material selections were provided to ensure good construction practices when using PCP. Another benefit of using PCP is that HHPS using PCP can be implemented for either new pavement or existing pavement to expedite construction procedures, reduce labor costs, reduce delay prior to opening to traffic, and in minimal weather restrictions.

- HHPS using the concrete overlay approach is considered to be cost-effective because pipes can be placed on existing pavement without having to remove or reconstruct it.

- HHPS using two-lift paving can be used for new construction, and slipform paving has the potential to expedite the construction process for large-scale construction compared to conventional methods.

7. FEASIBILITY STUDY ON DEVELOPMENT OF 3D FINITE ELEMENT MODEL FOR ECON HPS

7.1 SCOPE AND OBJECTIVES

This section focuses on the development of a 3D finite element (FE) modeling approach as an alternative method for evaluating ECON HPS time-dependent heating performance to achieve design optimization in a timely manner. The 3D FE model for ECON slab was developed by examining the decoupling of thermal-electrical analysis (Joule heating) (Sridharan et al., 2011) using COMSOL Multiphysics® software (COMSOL, 2012) and validated by comparison with experimental test results. By employing the developed 3D FE modeling approach, the sensitivity of ECON HPS design variables to heat generation and distribution performance was identified. This could be useful for providing guidance when performing design optimization.

7.2 THEORETICAL CONSIDERATIONS

The ECON HPS operates by applying voltage through embedded electrodes in a conductive concrete layer. Because the conductive concrete acts as a resistor, it generates heat energy through Joule heating that can be numerically evaluated using coupled electrical field and heat transfer equations.

A transient heat conduction model was employed to predict variation of the temperature as a function of time and position within an ECON slab. The 3D mathematical model for transient heat conduction in solids (Cengel, 2003) is given by equation (3):

$$\rho C_p \frac{\partial T}{\partial t} - \nabla \cdot (k \nabla T) = Q \tag{3}$$

where, ρ is the density in (kg/m^3), C_p is the heat capacity in (J/(kg.K)), T is the temperature in (°C), t is time in (s), ∇ is the Laplace operator, k is the thermal conductivity in (W/(m·K)), and Q is the rate of heat generation in (W/m^3).

The required electrical current in the ECON layer is generated by applying an electrical potential to electrodes embedded within the ECON layer. The 3D mathematical model for the electric field in a solid (Tungjitkusolmun et al., 2000) is:

$$\boldsymbol{E} = -\nabla V \tag{4}$$

where, V is the electrical potential in (V) and ∇ is the gradient operator.

Joule heating corresponds to the rate of electrical energy dissipated by electrical current flowing through a conductor and is correlated with the amount of electrical energy converted into heat (Ogasawara, 2010), as described in equation (5):

$$\mathrm{Q} = \boldsymbol{J} \cdot \boldsymbol{E} = (\sigma \cdot \boldsymbol{E}) \cdot \boldsymbol{E} \tag{5}$$

where, J is the electrical current density in (A/m^2), σ is the electrical conductivity in (S/m), and E is the electrical field in (V/m). The value of the electrical conductivity is σ, and it is dependent on the material temperature.

7.3 DEVELOPMENT OF 3D FE MODEL FOR ECON SLAB

A description of a FE model and subsequent analysis of the heat generation and distribution in an ECON slab using decoupling thermal-electrical interfaces in COMSOL is presented in the following sections.

7.3.1 Description of ECON Slab and Geometry Modeling

A prototype ECON slab (122 cm long × 86 cm wide × 10 cm thick) was constructed in Ames, Iowa (Abdualla et al., 2016) for experimental investigations. The 10-cm-thick layer consisted of a 5-cm ECON top layer and a 5-cm conventional concrete bottom layer. Two perforated galvanized steel angles, connected to an AC power supply to enable generation of heat, were embedded in the ECON layer. Temperature sensors were installed in both concrete layers. Insulation layers of 2.5-cm-thick XPS foam with an R-value of 1.32 C·m^2/W were placed at the edges and bottom of the slab to reduce heat loss. The ECON slab was tested in a controlled laboratory testing environment, and temperature was recorded for a total time duration of 150 minutes.

COMSOL Multiphysics (release 5.1) software was used to develop a 3D FE model of the ECON slab. The FE model illustrated in Figure 60 was developed to numerically simulate the heat generation response and distribution under the application of electric potential from an AC power supply. The dimensions of the modeled ECON slab were the same as the prototype tested at ISU, 122 cm long × 86 cm wide × 10 cm thick. The electrodes, also modeled in the 3D FE model (see Figure 60) were considered as boundaries for electric potential values used to generate current flow through the ECON layer.

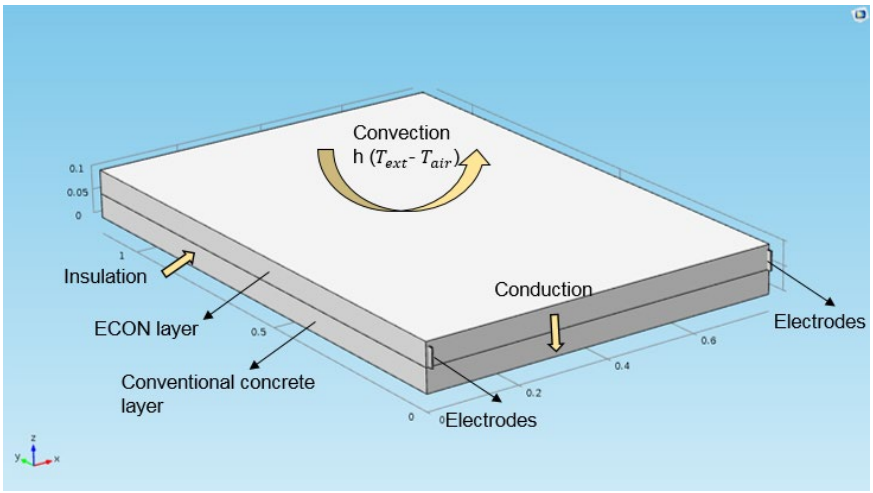

Figure 60. The 3D FE Model of ISU ECON Slab and Boundary Conditions

7.3.2 Assumptions and Boundary Conditions

Since multiphysics interfaces, e.g., thermal-electrical coupling, were used to analyze the modeled ECON slab, boundary conditions (see Figure 60) were assigned for each interface to simulate ECON slab heat generation and distribution as a function of time. The ECON slab, composed of conventional concrete and ECON, was treated as homogenous and isotropic. While the various heat transfer mechanisms that could possibly affect thermal performance include conduction, convection, and short- and long-wave radiation, in the 3D FE analysis only conduction and convection were considered. The effect of radiation heat flux was neglected since the temperature difference during snowfall between the ECON surface temperature and the ambient temperature was considered negligible (ASHRAE, 2015; Zhao et al., 2011).

To describe the transient heat transfer physics, a boundary condition was set up using the energy balance at a solid surface (Cengel, 2003) where the convection heat flux equals the conduction heat flux at the ECON slab surface (equation 6).

$$\boldsymbol{n} \cdot (k\nabla T) = h_c(T_{sur} - T_{air}) \tag{6}$$

where $\boldsymbol{n}$ is the normal vector to the surface, k is the thermal conductivity, T_{sur} is the pavement surface temperature in (°C), T_{air} is the ambient temperature in (°C), and h_c is the heat transfer coefficient in (W/m^2·°C).

The convection heat transfer coefficient, h_c, was calculated based on a ASHRAE handbook (2015) by assuming an average wind speed of 16 km/h that existed during the experimental test. The pavement surface temperature was -1 °C at the beginning of the experimental tests conducted on the ISU ECON slab, and the ambient temperature was also -1 °C, so this value was introduced into the COMSOL environment as an initial value. It was assumed that the edges and bottom of the ECON slab were insulated since insulation boards had been placed at these locations.

The electrical ground and electrical potential boundaries were selected as 0 V and 80 V, respectively, at each electrode, representing the power supply voltages assigned to the ECON slab

during the experimental test to create heat generation in the electrically conductive concrete layer. Electrodes were embedded in the electrically conductive layer, and their material properties were defined in the COMSOL environment to represent the actual electrode material and the galvanized steel used in constructing the ECON slab.

7.3.3 Description of Material Modeling

The slab modeled in this study was composed of ECON and conventional concrete. The electrical resistivity of ECON is very small compared to conventional concrete, which has resistivity values higher than 1,000 kΩ·cm (Gopalakrishnan et al., 2015a). An ECON HPS with lower resistivity (i.e., higher conductivity) can reduce energy demands needed to melt snow and ice and improve cost-effectiveness.

There is an inverse relationship that follows the Arrhenius equation between the electrical resistivity and temperature (Cengel, 2003). The electrical resistivity can be calculated using the first- and second-Ohm's law (Wu, Huang, Chi, & Weng, (2013) as follows:

$$R = \frac{V}{I}, \rho = \frac{R \times A}{L} \tag{7}$$

where, ρ is electrical resistivity (i.e., reciprocal of electrical conductivity), R is the electrical resistance, A is the cross-sectional area parallel to the electrodes, L is the electrode spacing, V is voltage, and I is electrical current.

The material properties used in the FE model were obtained from experimental laboratory tests conducted in this study, from the COMSOL library, and from a previous study (Tuan, 2004b). The material property inputs include electrical resistivity, density, heat capacity, and thermal conductivity for conventional concrete, electrodes, and ECON (see Table 8). The material properties for conventional concrete and galvanized steel electrodes were obtained from the COMSOL material library. An experimental test was executed to identify the electrical resistivity values of the ECON under various temperature conditions. Figure 61 shows that the electrical resistivity value decreases as the temperature increases. However, the electrical resistivity values of ECON only slightly differed in the range -1 °C to 15 °C, the heated pavement operational ranges for melting snow and ice. Based on these experimental test results, a constant electrical resistivity value of 70 Ω·cm for ECON was used at -1 °C ambient temperature as a constant value in the FE model.

Table 8. Material Properties Used in FE Simulations

Material	Density (kg/m^3)	Thermal Conductivity (W/m·K)	Heat Capacity (J/kg·K)	Electrical Resistivity (Ω·cm)
Conventional concrete	2300	1.4	880	5.4×10^5
Steel AISI 4340 (electrodes)	7850	44	475	1.7×10^{-9}
ECON	2500	4.2	480	70

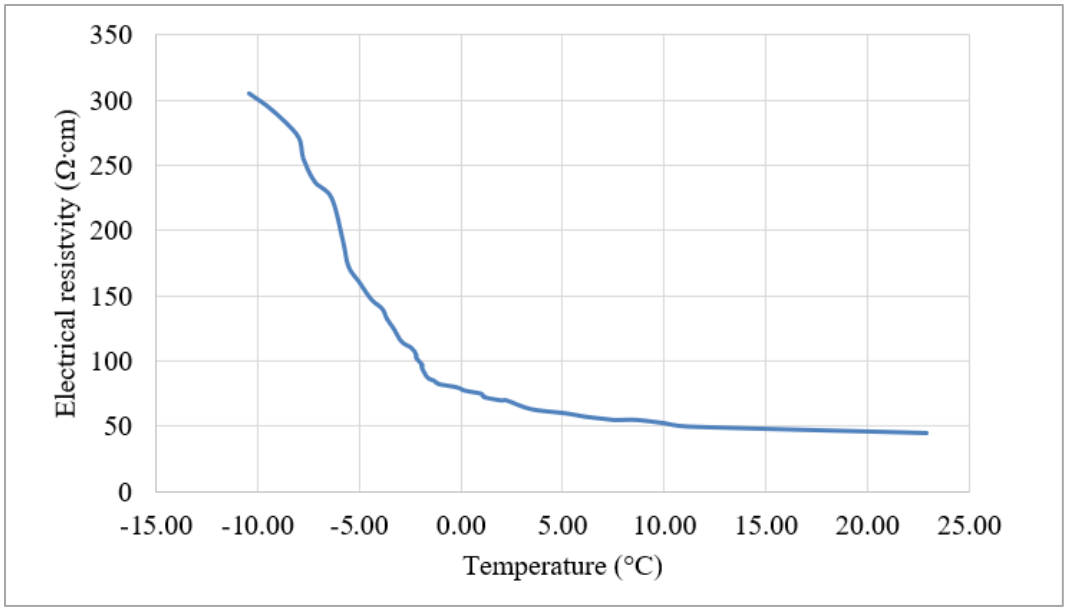

Figure 61. Electrical Resistivity and Temperature Changes for ECON

7.3.4 Description of Mesh Generation

After defining the geometric features and other required variables including boundary conditions and material properties, the element type and FE mesh were defined. A tetrahedral element type was used to discretize the ECON slab into smaller elements, as shown in Figure 62a. The tetrahedral element has four points and six edges with two degrees of freedom with respect to temperature and electrical potential. The convergence of the FE model was evaluated using different mesh sizes with the number of linear and quadratic tetrahedral elements ranging from 15,125 to 201,253, with the results tending to match the experimental results better as mesh size decreased. Since the FE results differed very little when the number of elements was greater than 60,000, quadratic tetrahedral elements at this mesh size were selected and used for the 3D FE model.

The electrical potential was applied through the electrodes, and the temperature at each node was calculated. The embedded electrodes and their surrounding areas were more finely meshed (see Figure 62(a) and (b)) to more precisely model the interaction between the electrodes and the surrounding areas.

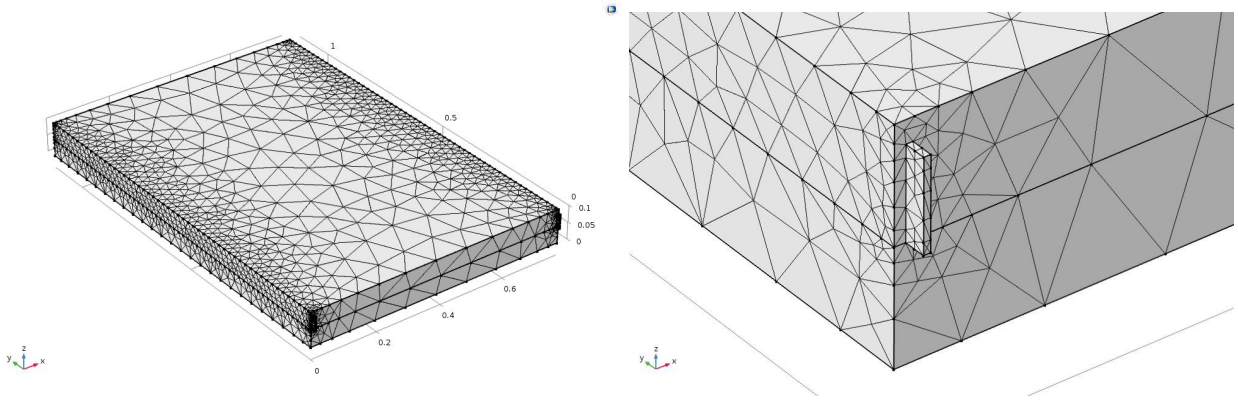

(a) (b)

Figure 62. The ECON Mesh Distribution: (a) 3D Mesh of ECON Slab and (b) Zoomed-in View of the Meshed Construction Region Around the Electrode and the ECON Slab

7.4 RESULTS AND DISCUSSIONS

An FE analysis of joule heating was conducted using an electrical potential of 80 V to power the ECON layer. The temperature distribution of the ECON slab was numerically calculated over the interval from 0 to 150 minutes at time divisions of 8 minutes. Temperature values on the 3D FE modeled ECON slab surface are presented in Figure 63(a) at 8 minutes, Figure 63(c) at 100 minutes, and Figure 63(e) at 150 minutes. The heat initially tended to accumulate in the central part of the ECON surface and then was distributed across the entire surface area. The highest temperature predicted by the FE analysis was observed in the middle area of the ECON surface and the temperature near the electrodes was about 2 °C to 5 °C less than that at the middle area. This could be attributed to the electrodes radiating electrical energy that got converted into heat (energy); the middle areas thus heated first and became hotter.

Temperature distributions inside the 3D FE modeled ECON slab are presented in Figure 63(b) at 8 minutes, Figure 63(d) at 100 minutes, and Figure 63(f) at 150 minutes. Because of the low electrical resistivity (i.e., high electrical conductivity) of the ECON layer, heat was initially induced in the ECON layer due to its lower resistivity, then transferred through conduction into the adjacent conventional concrete layer. This behavior could be explained as follows: the electrical energy passing into the ECON layer is converted into heat through resistive losses and the heat is then transferred to the other layer through thermal conduction by the collision of the molecular particles (Cengel, 2003).

The temperature at the center of the 3D FE modeled ECON slab surface was 2.2 °C at 8 minutes (see Figure 63(a)). The temperatures in the middle depths of the ECON and conventional layers were about 2.4 °C and -0.5 °C, respectively, at 8 minutes (see Figure 63(b)).

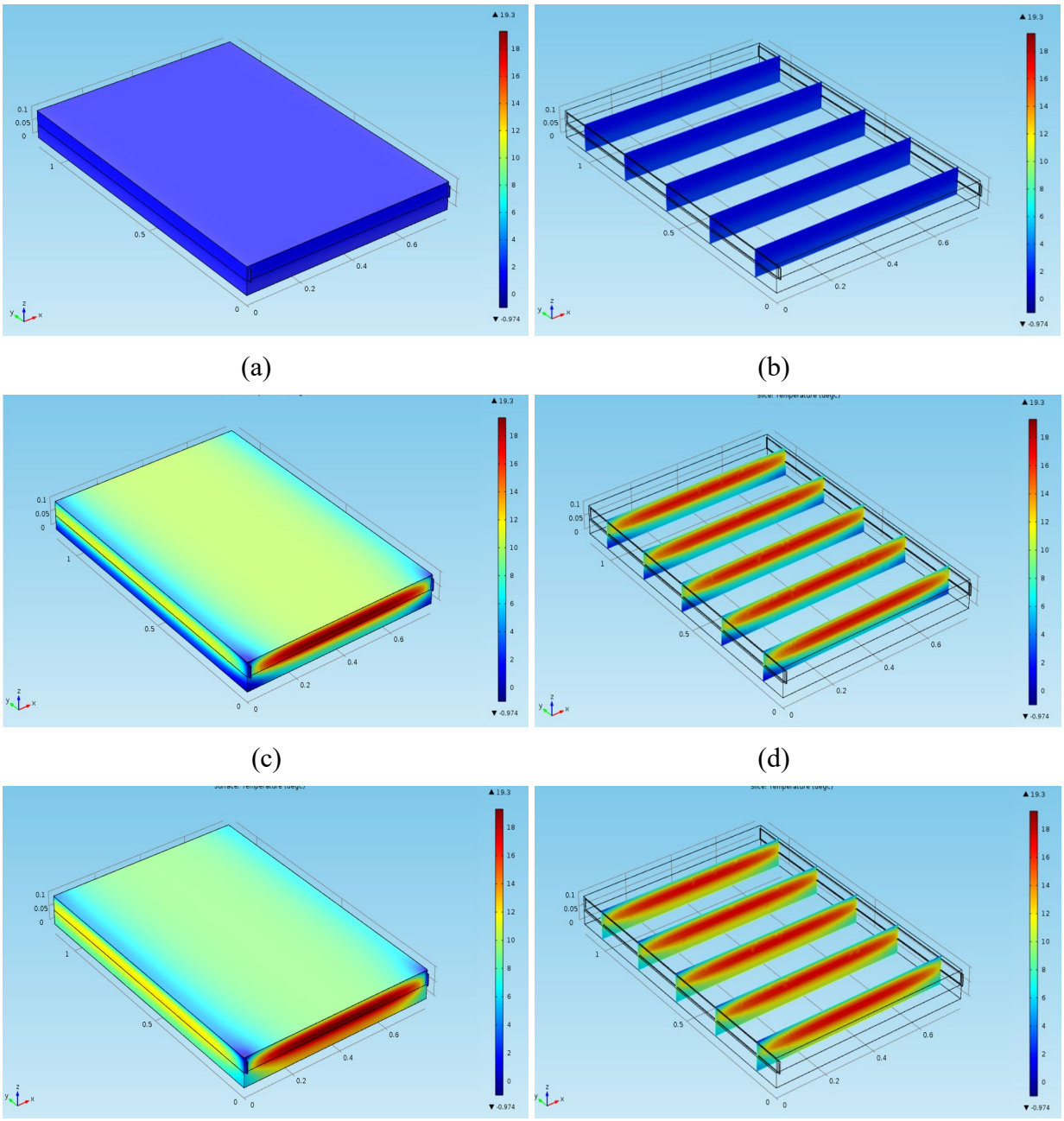

(a) (b)

(c) (d)

(e) (f)

Figure 63 Changes in Surface and Inside Temperatures vs Time in the 3D FE Modeled ECON Slab: (a) the Surface at 8 Minutes, (b) the Inside at 8 Minutes, (c) the Surface at 100 Minutes, (d) the Inside at 100 Minutes, (e) the Surface at 150 Minutes, and (f) the Inside at 150 Minutes

The temperature at the center of the ECON slab surface was 13.4 °C at 100 minutes (see Figure 63), and the temperature at the middle depth of the ECON layer was 15.3 °C at 100 minutes (see Figure 63(d)). The reason for this difference was that the ECON slab surface was exposed to the environment and the convection heat transfer was considered at the top surface of the ECON slab.

The temperatures at the middle depth of the ECON and the conventional layers were about 16.4 °C and 17.4 °C, respectively, at 150 minutes (see Figure 63(e) and Figure 63(f)), showing that the temperatures inside the two layers were close to one another at 150 minutes. This result indicates that thermal stresses are not an issue due to the small temperature differences between the ECON and the conventional layers. The temperature inside the conventional concrete increased with time due to its thermal mass that absorbed and stored heat as well as the effect of the insulation layer that prevents heat loss.

The temperature changes at the center of the ECON slab during its operation were measured (see Figure 64(a)) and compared to those obtained from the 3D FE model. As shown in Figure 64(b), this comparison acknowledged the validity of the results obtained from the FE analysis. The FE model tended to slightly overestimate the predicted temperature compared to the experimental data. This difference could be because only convection effects were considered in the FE model, not those due to other sources of heat loss, such as radiation.

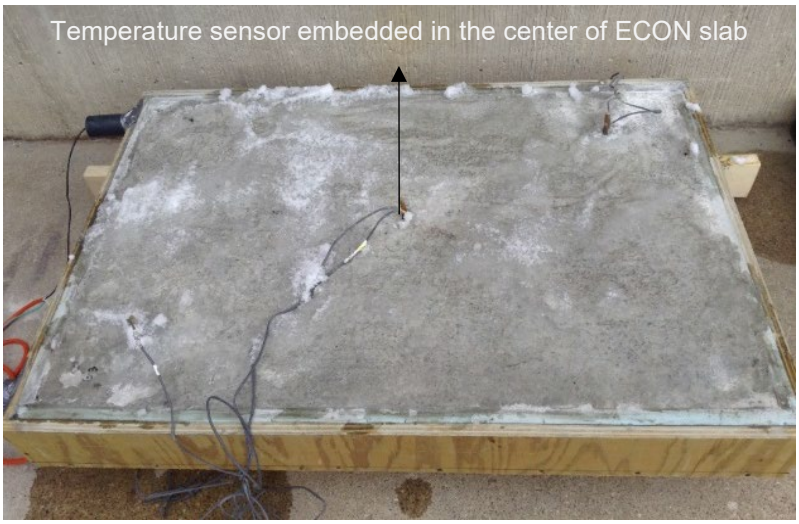

(a)

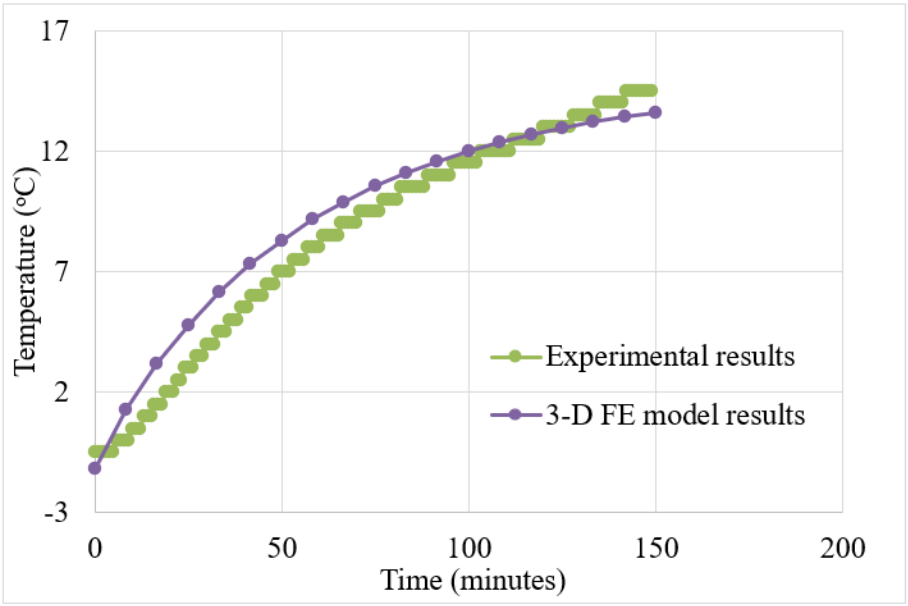

(b)

Figure 64. The 3D FE Model Validation: (a) ECON Slab with Embedded Temperature Sensor and (b) Comparison of Temperature Changes Between Experimental Measurements and FE Simulation Results (R^2= 0.80)

7.5 SENSITIVITY ANALYSIS OF THE DEVELOPED 3D FE MODEL

The design variables for ECON HPS include ECON electrical resistivity, electrode spacing, voltage, and ambient temperature. To evaluate the effect of these design variables on the heating performance of ECON HPS, sensitivity of these variables to temperature changes at the center surface of slab was identified using the developed ECON 3D FE model.

The dimensions of the ECON slab, 4.6 m long × 4.6 m wide × 19 cm thick, were selected to represent an actual slab that might be used in large-scale airport pavement. The thickness of the model is made up of two layers: a 7.6-cm ECON top layer and an 11.4-cm bottom layer of conventional concrete. Table 9 lists the base case values for each variable of the ECON layer. In the one-at-a-time (OAT) sensitivity analysis, the value for one variable was changed while the other variables were kept constant. The material properties of conventional concrete used as base case values (i.e., constant values) in the sensitivity analysis were obtained from Table 1.

Table 9. Base Case Variables and Values of the ECON Layer for Sensitivity Analysis

Variables	Values
Electrode spacing	1.5 m
Electrical resistivity	50 Ω·cm
Voltage	220 V
Width of ECON slab	4.6 m
Ambient temperature	-10 ºC

7.5.1 Effect of Electrical Resistivity on Heating Performance

To better understand the effect of electrical resistivity, temperature changes as a function of time were investigated by alternating the electrical resistivity between 50 Ω·cm and 300 Ω·cm. Figure 65 shows that when the electrical resistivity value of ECON layer was varied while fixing the other variables the temperature considerably increased within the 150 minutes time interval investigated. When the electrical resistivity value was 50 Ω·cm, the surface temperature increased from -10 °C to an above-freezing point (i.e., about 1 °C to 2 °C) in about 10 minutes. When the electrical resistivity values were 100 Ω·cm and 200 Ω·cm, the surface temperature increased from -10 °C to an above-freezing point in about 25 minutes and more than 66 minutes, respectively. However, an electrical resistivity of 300 Ω·cm was not sufficient to increase surface temperature to an above-freezing point within the 150 minutes-interval investigated.

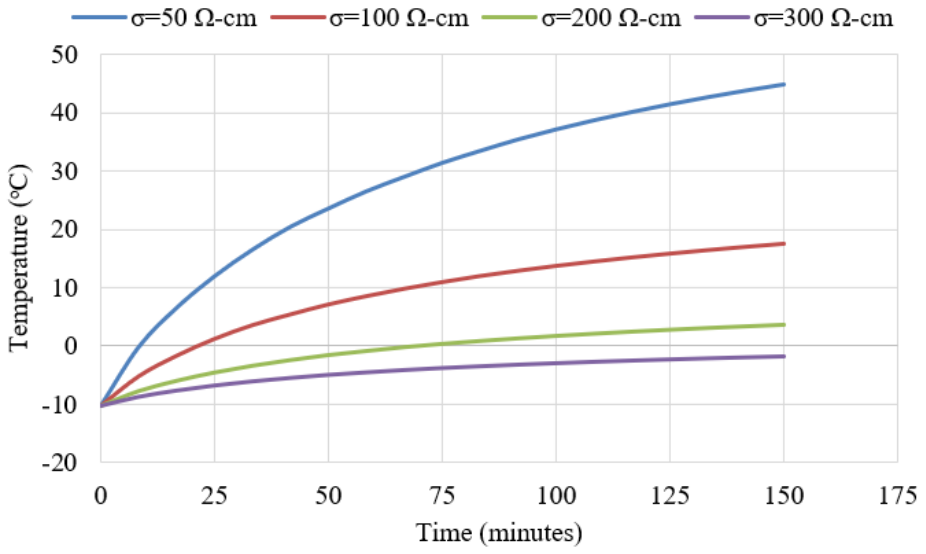

Figure 65. Changes in ECON Temperature Time for Different Electrical Resistivity Values

7.5.2 Effect of Electrode Spacing on Heating Performance

The design of electrode spacing is one of the challenging tasks in achieving an efficient ECON system. To investigate the effect of electrode spacing on ECON slab heating performance, changes in ECON temperature with time were investigated by choosing three electrode-spacing design options: 1.5 m for four-electrode installation, 2.3 m for three-electrode installation, and 4.6 m for two-electrode installation in a fixed ECON slab dimension (i.e., 4.6 m long × 4.6 m wide).

As the electrode spacing increases, the time to achieve temperature above freezing point on ECON surface dramatically increases (see Figure 66). When 1.5-m and 2.3-m electrode-spacing design options were selected, the surface temperature increased from -10 °C to an above-freezing point within 30 minutes; this would be expected to prevent snow and ice accumulation for an operating ECON pavement system. However, the 4.6-m electrode-spacing design option could not increase surface temperature to an above-freezing point within the 150-minutes interval.

The obtained results are in agreement with Ohm's law, i.e., the relation between electrical resistance and electrode spacing, as electrode spacing increases, the resistance increases. From these findings, it is recommended that the electrode spacing in ECON slab should be optimized by taking into consideration all factors, such as electrical resistivity, ambient temperature, power supply, etc., for a large-scale project, since building and testing a large-scale ECON slab is not an efficient way to design electrode spacing. In such a case, the 3D FE model is considered a useful and powerful tool.

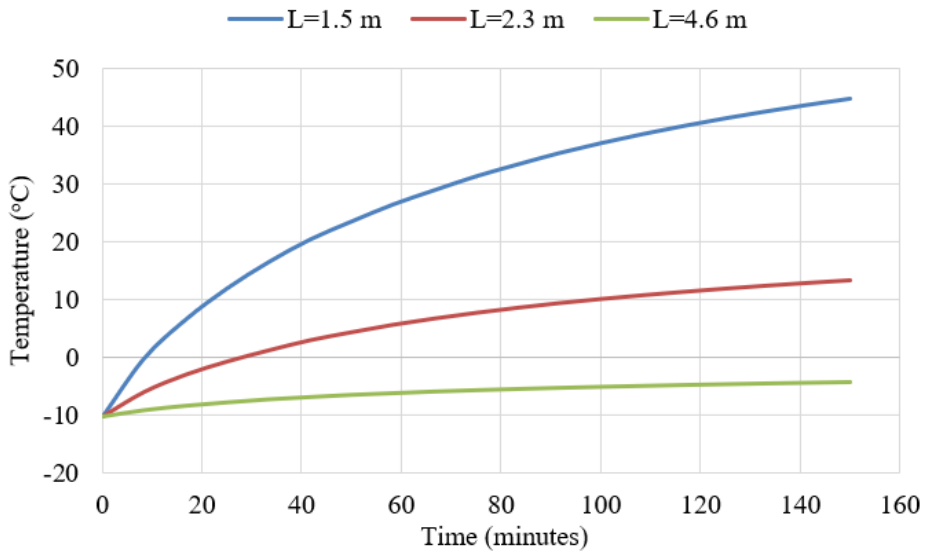

Figure 66. Changes in ECON Temperature with Time for Different Electrode Spacing Values

7.5.3 Effect of Voltage on Heating Performance

Voltage and power density are important parameters to be determined in maintaining low-cost operation of the ECON system. Figure 67 shows how ECON slab temperature changes with time for voltage values ranging from 60 V to 220 V. When the applied voltage increased from 120 V to

220 V, the time to reach a temperature above the freezing point decreased from 42 minutes to 9 minutes. These results are in agreement with the experimental results reported in a previous study wherein a set of voltage values were applied during the experiment test and a noticeable increase in the temperature was observed (Wu, Huang, Chi, & Weng, 2013). However, voltage values of 60 V and 80 V were not sufficient to increase the surface temperature above the freezing point within the 150-minutes interval.

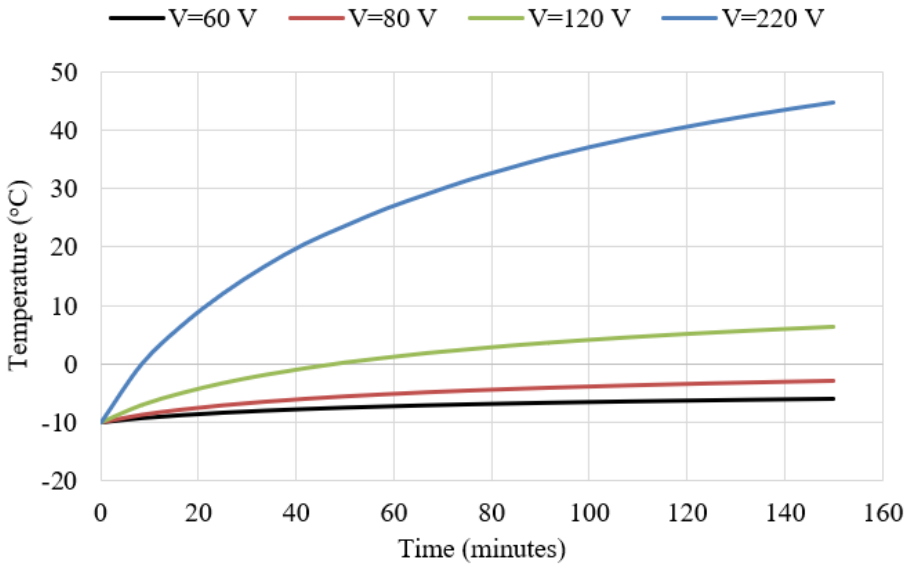

Figure 67. Changes in ECON Temperature with Time for Different Voltage Values

7.5.4 Effect of Ambient Temperature on Heating Performance

An ambient temperature has been used to determine the required energy for HPS operation using the steady-state energy balance equations that do not consider time-dependent heating performance. The effect of ambient temperature on ECON slab heating performance was investigated by alternating three ambient temperature values (-5 °C, -15 °C, -25 °C) to represent temperature conditions over a wide range of geographical locations in the United States where ECON might be used.

Figure 68 displays the changes in ECON slab temperature with time for different ambient temperature conditions. The times required to increase the temperature from -5 °C, -15 °C, and -25 °C to an above-freezing point were about 5, 16, and 32 minutes, respectively. The results indicate that the ECON HPS could be employed in most geographical locations within the United States by developing surface temperatures above the freezing point almost immediately after its operation.

Based on temperature sensor or weather forecast data, the ECON system should be turned on about 30 minutes before the expected time of snowfall in some geographical locations (or seasonal times) with ambient temperatures below -25 °C. In such cases, snow and ice will melt more quickly when they hit the ECON HPS surface, which can reduce snow and ice accumulations and consequently reduce electrical power demands to allow a system to run more efficiently.

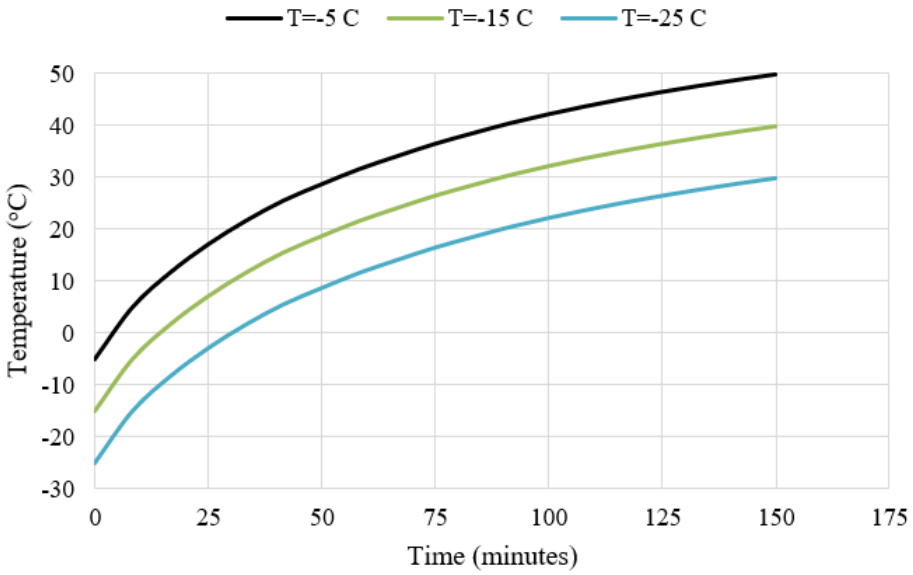

Figure 68. Changes in ECON Temperature with Time for Different Ambient Temperatures

7.6 A 3D FE MODEL: SUMMARY, CONCLUSIONS, AND RECOMMENDATIONS

The primary goal of this section was to examine the development of a 3D FE model for evaluating the effects of various design parameters on time-dependent ECON heating performance for ECON HPS design optimization. A 3D FE model was developed based on an ECON slab (122 cm long × 86 cm wide × 10 cm thick) built at ISU. To validate the 3D FE model, changes in ECON temperature from the 3D FE model simulations were compared with the temperature change measurements obtained from the center of ISU ECON slab during its operation. Using the developed 3D FE modeling approach, a sensitivity analysis was conducted on various design variables with respect to ECON heat generation and distribution performance. For the sensitivity analysis, realistic, large-scale airport pavement ECON slab dimensions (4.6 m long × 4.6 m wide × 19 cm thick) were used. The major conclusions of this study are as follows:

- The developed 3D FE model for ECON can predict heat generation and distribution changes over operational time. It can be used as a cost-effective evaluation tool for examining the effects of various design parameters on the time-dependent heating performance of ECON HPS design optimization.

- Given the assumed boundary conditions, the model shows that during the ECON operation the temperature initially is highest at the central area of ECON surface and then becomes distributed across the entire slab.

- The temperature inside the conventional concrete layer increases with time because the insulation layer and the slab boundaries reduce heat losses. This temperature comes closer to the temperature inside the ECON layer within an hour after beginning ECON operation. These results indicate that thermal stresses between surfaces are not an issue because there were minor temperature differences between the ECON and conventional layers.

- The ECON electrical resistivity is one of the most influential parameters governing the heating performance. As the electrical resistivity value increases, the time to achieve temperatures above the freezing point on ECON surface increases. The 3D FE model results indicate that electrical resistivity ranges of about 50 Ω·cm to 200 Ω·cm can provide sufficient heat for realistic ECON slab (4.6 m long × 4.6 m wide × 19 cm thick) dimensions typically found for large-scale airport pavement slabs.

- As the electrode spacing increases, the time to achieve the temperature above freezing point on ECON surface dramatically increases. Based on the 3D FE model results, it is recommended to design electrode spacing such that more than two electrodes could be accommodated in an ECON slab to ensure that the ECON surface temperature will be above freezing.

- The voltage values and the ambient temperature can also affect the time to achieve an above-freezing point temperature on an ECON surface. As voltage values increase, the ECON surface temperature reaches above-freezing point temperature more quickly.

- Thirty minutes or less are required to increase slab temperature from ambient temperature ranges (-5 °C, -15 °C, -25 °C) to above-freezing temperatures. Considering that the ambient temperature ranges selected for the study are representative of temperature conditions in a wide range of geographical locations in the United States, ECON HPS could be employed in most geographical locations in the United States and be able to achieve above-freezing point temperatures in these locations.

8. CONCLUSIONS

HPSs are viable alternatives to the traditional snow-removal method which utilize chemicals and mechanical instruments like snowplows. In this study, advanced construction techniques to best automate and accelerate the construction of large-scale heated pavements at airports were discussed. Problems like material selection, joint interfaces, new equipment necessary for installation of heating elements, timing and procedures for construction and installation of elements, and location of airport ancillary equipment were addressed. The findings and conclusions drawn from this study can be summarized as follows:

8.1 REVIEW ON ADVANCED CONSTRUCTION TECHNIQUES

8.1.1 Feasibility of Using Precast Concrete Pavement for Heated Pavement Systems

- Heated Pavement Systems (HPSs) using precast concrete pavement (PCP) are a viable option for accelerating construction procedures, reducing labor costs, and minimizing traffic disruptions. In addition, it enhances the heat distribution of the pavement surface since the HPS slabs are fabricated offsite where quality can better be controlled.

- The bedding support materials used under PCP can be modified to behave as an insulation layer by adding admixtures to mitigate heat loss, so HPSs using PCP could provide better performance and reduce the operational cost of HPS.

- HPSs using PCP have potential to be installed in small areas such as gates to prevent snow and ice accumulation in a short time to minimize flight delays or cancellations.

- Another benefit of using PCP is that it can be implemented either for new pavements or existing pavements.

- HPSs using PCP can be tested in term of heat generation and performance before transporting and placing it at the project site.

8.1.2 Feasibility of Using of Two-lift Paving for HPS

- HPSs using two-lift paving has potential to expedite the construction work of HPSs for new construction through the use of slipform pavers. The mixture of the bottom lift could be used to mitigate the heat loss by using lightweight aggregates in the mixture.

- HPSs using two-lift paving is a good approach for constructing a large-scale project such as a runway. It provides better production rates in comparison to cast-in-place methods.

- The top lift of two-lift paving can be used for an electrically conductive concrete (ECON) layer as well as using an additional slipform paver, concrete plant, and spreader for paving the ECON layer.

8.1.3 Feasibility of Using of Concrete Overlays for HPSs

- HPSs using concrete overlays have the benefit of facilitating the HPS's components such as electrodes or pipes easily in comparison to other construction techniques. In addition, it is suitable for construction on existing pavements.

- HPSs using concrete overlays can be constructed rapidly and combined with other advanced construction techniques.

8.2 SYSTEM REQUIREMENTS FOR ECON HPS

- The prototype ECON slab developed in this study provided the lowest energy consumption and the lowest energy cost among all the electrically HPSs developed and reported in the literature so far (Zuofu, Zhuoqiu, & Jianjum, 2007; Yang, Yang, Song, & Singla, 2012; Tuan & Yehia, 2002). Such excellent operational performance is because the newly developed ECON materials provide higher conductivity (about 50 Ω-cm of electrical resistivity), which result in uniform heating on the entire surface to melt snow and ice quickly.

- The two-layer approach used in the design and construction of the prototype ECON slab places a thin ECON layer (top layer) on a conventional concrete layer (bottom layer). This approach is cost effective in terms of material cost, energy consumption, and operational cost savings. It can be implemented for large-scale ECON HPSs using precast concrete techniques, concrete overlays, and two-lift paving.

- The design parameters to be determined for large-scale ECON HPSs include slab dimensions, distance between electrodes, electrical resistance, and voltage. The design flow developed in this study can be used to determine these parameters for given design criteria.

- Key construction materials required for high-performing ECON HPS are low-resistivity (i.e., high conductivity) ECON materials, electrodes well-bonded with ECON, and cost-effective thermal insulation.

- Use of alternating current (AC) to heat ECON can provide more spread-out heat distribution by enabling the electrons take different paths into conductive materials inside ECON than direct current (DC) that takes only one path.

8.3 SYSTEM REQUIREMENTS FOR HYDRONIC HEATED PAVEMENT SYSTEM

- An HHPS can be used as an alternative technology to melt ice and snow. An HHPS should be chosen over ECON HPS if the project site has a geothermal source that would reduce operational costs.

- The developed design flow can be used to optimize system parameters as well as to provide options of advanced construction techniques such as PCP, two-lift paving, and concrete overlay. The performance of a HHPS using Portland cement concrete (PCC) over hot-mix asphalt (HMA) is a better option because of its high thermal conductivity.

- Industrial software can be used to create circuit design layouts and to calculate the design energy for specific locations. The calculation using industrial software was based on ASHRAE methods. Serpentine or slinky pipe patterns are commonly used for pipe circuit layout.

8.4 THE 3D VISUALIZATION OF ADVANCED CONSTRUCTION TECHNIQUES FOR ECON HPS

- Three-dimensional (3D) visualization ensures that HPSs will perform as desired (uniform heat destitution in installed areas, effective ice and snow melting, leak-proof systems with advanced pavement joint details, etc.).

- Construction considerations and 3D visualization workflows for ECON HPS were developed using different construction techniques to develop more robust construction schemes, high-performing heated airport pavements, and good construction practices.

- Design details, such as joint interfaces and material selection, were provided to ensure that good construction practices using advanced construction techniques were followed.

- The ECON layer (top layer) using the concrete overlays approach can be placed as a thin layer. This approach is considered cost-effective because ECON layer (top layer) is placed on the existing pavement (bottom layer) without reconstructing existing pavement.

- The ECON system installation as an unbonded overlay is recommended due to bonding issues. It allows the ECON layer (top layer) to move freely without the restriction of the bottom layer. Different concrete paving such as laser screed or a slipform paver may be used depending on the project size, location, and construction time.

- ECON using two-lift paving can be used for new construction; slipform paving provides more feasibility of expediting the construction process for large-scale construction when compared to cast-in-place methods.

- Electrodes can be assembled and installed as a set for each slab to expedite the construction procedure for any of the optional advanced construction techniques.

8.5 THE 3D VISUALIZATION OF ADVANCED CONSTRUCTION TECHNIQUES FOR HHPS

- 3D visualization ensures that the HHPS will perform as desired (uniform heat destitution in installed areas, effective ice and snow melting, leak-proof systems with advanced pavement joint details, etc.).

- Design details, such as joint interface between hydronic heated slabs and material selection, were provided to ensure use of good construction practices while using PCP. Another benefit of using PCP is that HHPS using PCP can be implemented for both new pavements or existing pavements to expedite construction procedures, reduce labor costs, reduce delay prior to opening to traffic, and exhibit minimal weather restrictions.

- HHPS using the concrete overlay approach is considered cost-effective because pipes can be placed on existing pavement without reconstructing the existing pavement.

- HHPS using two-lift paving can be used for new construction, and slipform paving offers greater feasibility of expediting the construction process for large-scale construction compared to conventional methods.

8.6 FEASIBILITY STUDY ON DEVELOPMENT OF 3D FINITE ELEMENT MODEL FOR ECON HPS

- The developed 3D finite element (FE) model for ECON can rationally predict heat generation and distribution changes over its operational life.

- 3D FE can be utilized as a cost-effective evaluation tool for examining the effects of various design parameters on the time-dependent heating performance through ECON HPS design optimization.

- Given the assumed boundary conditions, the 3D FE model shows that, during the ECON operation, the temperature is initially highest at the central area of ECON surface and then becomes more evenly distributed across the entire slab.

- The temperature inside the conventional concrete layer increases with time both because it has thermal mass as well as an insulation layer that reduces heat losses. This temperature becomes nearer to the temperature inside the ECON layer within an hour after beginning the ECON operation. These results indicate that thermal stresses between surfaces will not be an issue because there was very small temperature difference between the ECON and conventional layers.

- ECON electrical resistivity is one of the most influential parameters governing the heating performance. As the electrical resistivity value increases, the time to achieve temperature above the freezing point on ECON surface increases. The 3D FE model results indicate that electrical resistivity ranges of about 50 Ω·cm to 200 can provide sufficient heat for realistic ECON slab dimensions (4.6 m long × 4.6 m wide × 19 cm thick) representing real, large-scale airport pavement slabs.

- As the electrode spacing increases, the time to achieve temperatures above the freezing point on ECON surface dramatically increases. Based on the 3D FE model results, it is recommended to design electrode spacing such that more than two electrodes could be accommodated in an ECON slab to ensure that the ECON surface temperature would be above freezing.

- The voltage values and the ambient temperature can also affect the time to achieve above-freezing point temperature on ECON surface. As voltage values increase, the ECON surface temperature reaches above-freezing point temperature more quickly.

8.7 BENEFITS OF ADVANCED CONSTRUCTION TECHNIQUES FOR HPS.

Advance construction techniques application in HPS could offer several potential benefits over traditional conventional concrete paving (cast-in-place). The potential benefits that can be attributed to HPS are summarized below.

- A systematic collection of advanced construction techniques and practices for large-scale heated airport pavement construction projects was developed that can be easily used in construction projects, regardless of airport size or project scope.

- HPS using two-lift paving is considered a sustainable approach that enables the use of locally available or recycled materials while the top layer is optimized for long life and functionality and reduces construction material costs.

- Economic ECON HPS for new construction can be achieved by using two-lift paving where the ECON layer is constructed as a thin top layer for large-scale construction.

- The benefits of HPS using PCP for large-scale heated airport pavement includes reduced traffic disruptions, acceleration of the construction process, and significant reduction in labor and time (including curing time) consumed on-site.

- HPS using concrete overlays can be constructed on existing pavement and considered to be a cost-effective maintenance and rehabilitation solution for a wide range of

combinations of existing pavement types, conditions, desired service life, and anticipated traffic loading.

8.8 USING 3D VISUALIZATION OF ECON HEATED PAVEMENTS FOR AIRPORT RUNWAY

The overarching goal of this study is to keep airports open, safe, and accessible as well as to prevent personnel from slipping and falling, or to prevent any aircraft from skidding off runways. ECON can help provide a safe environment and fewer delays. To meet these goals, HPS could be implemented on all airport pavement surfaces, including runways and aprons. The growth of these technologies and their applicability for large-scale heated airport pavement will reduce initial costs and improve the overall quality of heated airport pavements management by enabling more effective maintenance and repair methods. Figure 69 presents a 3D artist rendition and visualization illustrating the general operation scheme for implementing full-scale HPS at airport.

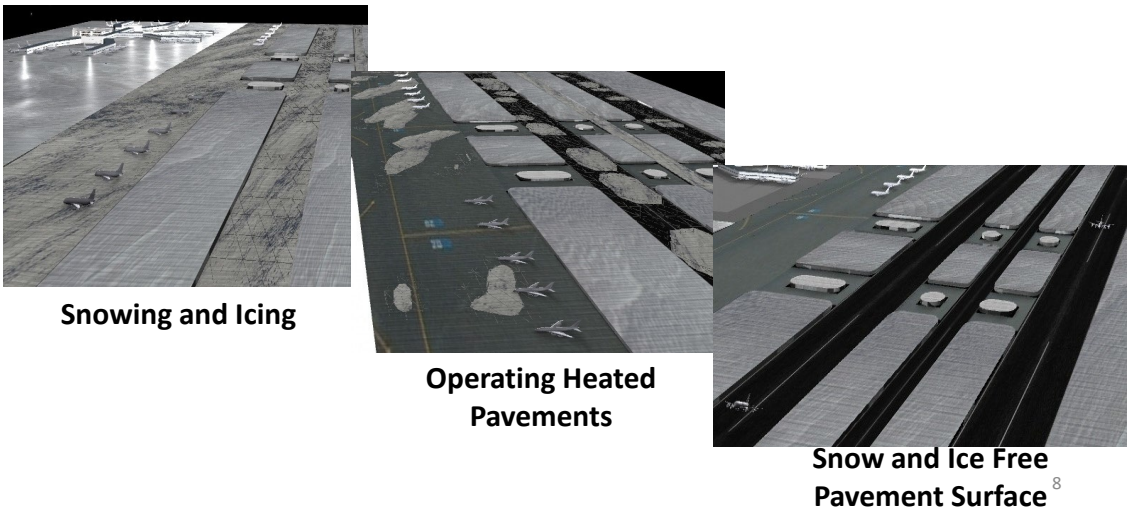

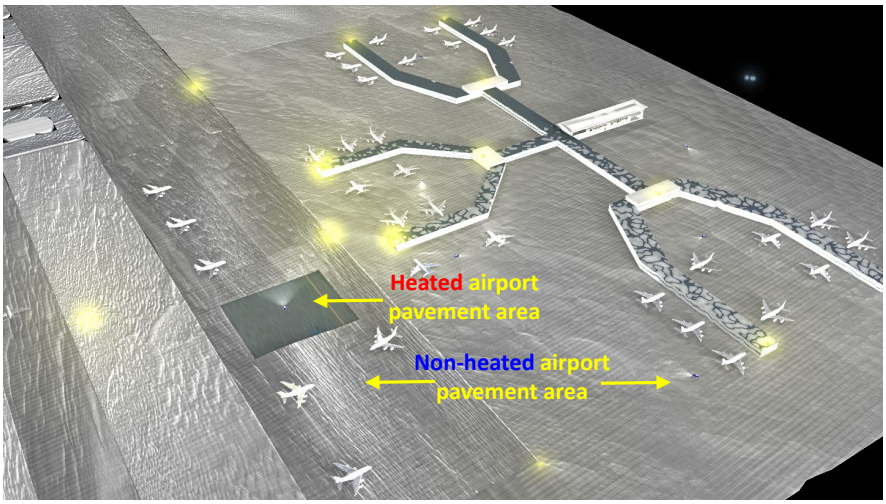

Figure 69. Visualization of Airport HPS Operations

9. RECOMMENDATIONS AND FUTURE RESEARCH DIRECTIONS

Implementing the advanced construction techniques described in this report will automate and accelerate construction of large-scale heated airport pavements to prevent ice and snow accumulation on paved surfaces. Based on the findings of this research, the following recommendations are proposed for future improvements and implementation of heated pavements:

- The findings of this study can be used to design and construct full-scale implementations of HPS to further study using two-lift paving through field demonstration in actual airport environments. It would be beneficial to develop a mix design for the bottom lift to mitigate heat loss during the operation of HPS.

- A comprehensive study should be performed to investigate the effect of implementing ECON HPS as either bonded or unbonded overlays to identify which type is more efficient in term of heat loss, bonding issues, and operational cost.

- Practical implementation issues that should be identified and addressed with respect to full-scale implementation of heated concrete pavements. Currently, there are few full-scale heated concrete pavement sites or test beds around the globe, and most have focused on geothermal energy-sourced hydronic heated pavements.

- A comprehensive study should be performed to investigate the effect and the performance of implementing advanced construction techniques for large-scale heated airport pavement in terms of heat loss, thermal and mechanical stresses, and curling and warping effects to identify which techniques would be considered more efficient and reliable

- Safety issues related to ECON HPS during operation should be investigated, especially where voltage is applied through the embedded electrodes and the effect of ECON with respect to electromagnetic interference (EMI) with aircraft navigation aid (NAVAID) systems or communication equipment at airports.

10. REFERENCES

Abdualla, H., Ceylan, H., Kim, S., Gopalakrishnan, K., Taylor, P. C., & Turkan, Y. (2016). System requirements for electrically conductive concrete heated pavements. *Transportation Research Record: Journal of the Transportation Research Board*, *2569*(1), 70-79. https://doi.org/10.3141%2F2569-08

American Association of State Highway and Transportation Officials (AASHTO). (1993). *AASHTO Guide for Design of Pavement Structures*. American Association of State Highway and Transportation Officials, Washington, D.C. https://habib00ugm.files.wordpress.com/2010/05/aashto1993.pdf

American Concrete Institute (ACI) Committee 325. (2006). *Concrete overlays for pavement rehabilitation* (ACI 325.13R-06). American Concrete Institute Publication.

American Concrete Pavement Association (ACPA). (1998). *Whitetopping-State of the Practice.* American Concrete Pavement Association Publication EB210P, Skokie, IL

American Concrete Pavement Association (ACPA). *Strength converter*. http://apps.acpa.org/applibrary/StrengthConverter/ Accessed October 25, 2015.

American Society of Heating, Refrigeration and Air-Conditioning Engineer (ASHRAE). (2015). Snow melting and freeze protection (TC 6.5, Radiant heating and cooling). In *ASHRAE Handbook—HVAC Applications* (pp. 51.1-51.20). American Society of Heating, Refrigeration and Air-Conditioning Engineer, Inc.

Bly, P. G., Priddy, L. P., Jackson, C. J., and Mason, Q. S. (2013, June). *Evaluation of precast panels for airfield pavement repair. Phase 1: System optimization and test section construction* (Report No. ERDC/GSL TR-13-24). U.S. Army Corps of Engineers Research and Development Center. https://apps.dtic.mil/dtic/tr/fulltext/u2/a582186.pdf

Cable J. (2004, September). *Reassessing two-lift paving, Tech transfer summary*. (FHWA Cooperative Agreement DTFH61-01- 00042 Project 8). National Concrete Pavement Technology Center. Reassessing Two-Lift Paving (iastate.edu)

Cable, J. K., & Frentress, D. P. (2004). *Two-lift Portland cement concrete pavements to meet public needs* (Report No. DTF61-01-X-00042 [Project 8]). Center for Transportation Research and Education. Two Lift DatabaseFINAL.xls (iastate.edu)

Cengel, Y.A. (2003). *Heat and mass transfer: A practical approach* (2nd ed.) McGraw-Hill.

Ceylan, H. (2015, May 27-28). *Project 01: Heated airport pavements* [Slide presentation]. FAA Partnership to Enhance General Aviation Safety, Accessibility, and Sustainability (PEGASAS) Center of Excellence (COE) 3rd Annual Meeting, Purdue University, West Lafayette, IN.

Ceylan, H., Kim, S., & Gopalakrishnan, K. (2014, September 23-26). *Heated transportation infrastructure system: Existing and emerging technologies*. The 12th International Symposium on Concrete Roads, Prague, Czech Republic. https://dr.lib.iastate.edu/server/api/core/bitstreams/a429d49c-5c01-48ba-b335-bb8542101340/content

Chang, L., Chen, Y., & Lee, S. (2004). *Using precast concrete panels for pavement construction in Indiana* (Report No. FHWA/IN/JTRP-2003/26). Indiana Department of Transportation, Indianapolis, IN. Using Precast Concrete Panels for Pavement Construction in Indiana (purdue.edu)

Chen, W., & Gao, P. (2012, October 18-22). Performance of electrically conductive concrete with layered stainless steel fibers. In *Proceedings of Second International Conference on Sustainable Construction Materials: Design, Performance, and Application*, American Society of Civil Engineers (ASCE), pp. 164-172. https://doi.org/10.1061/9780784412671.0014

COMSOL. (2012). *COMSOL Multiphysics® user's guide* (pp. 707-755). Stockholm, Sweden. The COMSOL Multiphysics User's Guide (ethz.ch)

Delatte, N. J. (2014). *Concrete pavement design, construction, and performance*. CRC Press.

Gopalakrishnan, K., Ceylan, H., Kim, S., Yang, S., & Abdualla, H. (2015a). Electrically conductive mortar characterization for self-heating airfield concrete pavement mix design. *International Journal of Pavement Research and Technology*, *8*(5), 315-324. https://doi.org/10.6135/ijprt.org.tw/2015.8(5).315

Gopalakrishnan, K., Ceylan, H., Kim, S., Yang, S., & Abdualla, H. (2015b). Self-heating electrically conductive concrete for pavement deicing: A revisit. In *Transportation Research Board 94th Annual Meeting Compendium of Papers,* No. 15-4764.

Federal Aviation Administration (FAA). (2011, March 29). *Airside use of heated pavement systems* (Advisory Circular (AC) 150/5370-17). https://www.faa.gov/documentLibrary/media/Advisory_Circular/150_5370_17.pdf

FAA. (2016, November 10). *Airport pavement design and evaluation* (Advisory Circular (AC) 150/5320-6F). https://www.faa.gov/documentLibrary/media/Advisory_Circular/150-5320-6F.pdf

Gerhardt, T. (2013). *Two-lift concrete paving workshop*. Texas Department of Transportation. https://static.tti.tamu.edu/conferences/tsc13/presentations/materials-2/fowler.pdf

Harrington, D., Degraaf, D., Riley, R., Rasmussen, R. O., Grove, J., & Mack, J. (2007). *Guide to concrete overlay solutions*. National Concrete Pavement Technology Center, Ames, IA. Guide to Concrete Overlay Solutions (iowa.gov) https://www.concreteparking.org/downloads/guide_concrete_overlays.pdf

Harrington, D., Fick, G., Bordelon, A., Cable, J., DeGraaf, D., Parkes, N., Riley, R., Rodden, R, Roesler, J., & Vandenbossche, J.M. (2014). *Guide to concrete overlays: sustainable solutions for resurfacing and rehabilitating existing pavements (3rd edition)* (ACPA Publication TB021.03P). National Concrete Pavement Technology Center. http://dx.doi.org/10.13140/RG.2.1.3106.4724

Harrington, D.S., Riley, R.C., Allen, J. D., Bordelon, A., Holland, J. & Parkes, N. (2012, October). *Guide to Concrete Overlays of Asphalt Parking Lots*. National Concrete Pavement Technology Center.

Heinrichs, K. W., Liu, M. J., Darter, M. I., Carpenter, S. H., & Ioannides, A. M. (1989). *Rigid pavement analysis and design* (No. FHWA-RD-88-068). United States. Federal Highway Administration

Heymsfield, E., Osweiler, A.B., Selvam, R.P., & Kuss, M. (2013). *Feasibility of anti-icing airfield pavements using conductive concrete and renewable solar energy* (DOT/FAA/TC-13/8). Feasibility of Anti-Icing Airfield Pavements Using Conductive Concrete and Renewable Solar Energy (faa.gov)

Hu, J., Fowler, D., Siddiqui, M. S., & Whitney, D. (2014*). Feasibility study of two-lift concrete paving: Technical report* (FHWA/TX-14/0-6749-1). Texas State University-San Marcos and Center for Transportation Research. Feasibility study of two-lift concrete paving : technical report. (bts.gov)

Joerger, M. D., & Martinez, F. C. (2006). *Electric heating of I-84 in Ladd Canyon, Oregon* (Report No. FHWA-OR-RD-06-17). Oregon Department of Transportation, Salem, OR. Electric heating of I-84 in Ladd Canyon, Oregon. (bts.gov)

Kohler, E., du Plessis, L., Smith, P. J., Harvey, J., & Pyle, T. (2007, November). Precast concrete pavements and results of accelerated traffic load test. In *International Conference on Optimizing Paving Concrete Mixtures and Accelerated Concrete Pavement Construction and Rehabilitation*, pp. 263-281. Atlanta, Georgia.

Kohn, S.D., Tayabji, S., Okamoto, P., Rollings, R., Detwiller, R., Perera, R., Barenberg, E.J., Anderson, J., Torres, M., Barzegar, H., Thompson, M.R, & Naughton, J. (2003). *Best practices for airport Portland cement concrete pavement construction (Rigid airport pavement)* (Report No. IPRF 01-G-002-1/ACPA No. JP007P). American Concrete Pavement Association.

Lewis, W.M. (1999). *Studies of environmental effects of magnesium chloride deicer in Colorado* (Report No. CDOT-DTD-R-99-10). Colorado Department of Transportation. https://codot.gov/programs/research/pdfs/1999/magchlorideenveffects.pdf

Mallick, R.B., & El-Korchi, T. (2013). *Pavement engineering: principles and practice* (2nd ed.). CRC Press.

Merritt, D. K., McCullough, B. F., Burns, N. H., & Rasmussen, R. O. (2004). *Construction of the California precast concrete pavement: Demonstration project* (Report No.FHWA-IF-06-010). Federal Highway Administration, U.S. Department of Transportation, Washington, DC. https://rosap.ntl.bts.gov/view/dot/41141

Minsk, L.D. (1999). *Heated bridge technology—Report on ISTEA Sec. 6005 program* (Report No. FHWA-RD-99-158). Federal Highway Administration. https://www.fhwa.dot.gov/publications/research/infrastructure/bridge/99158/

Ogasawara, T., Hirano, Y., & Yoshimura, A. (2010). Coupled thermal–electrical analysis for carbon fiber/epoxy composites exposed to simulated lightning current. *Composites Part A: Applied Science and Manufacturing*, *41*(8), 973-981. https://doi.org/10.1016/j.compositesa.2010.04.001

Packard, R.G. (1984). *Thickness design for concrete highway and street pavements*. Portland Cement Association (PCA), Skokie, Illinois.

Priddy, L. P., Bly P. G., & Flintsch, G. W. (2013). Review of precast Portland cement concrete panel technologies for use in expedient Portland cement concrete airfield pavement repairs. In *Transportation Research Board 92nd Annual Meeting Compendium of Papers*, No. 13-2956.

Sassani, A., Ceylan, H., Kim, S., & Gopalakrishnan, K. (2015, August 19–20). *Optimization of electrically conductive concrete (ECC) mix design for self-heating pavement systems* [Paper presentation] Present at 2015 Mid-Continent Transportation Research Symposium, Ames, IA.

Spitler, J.D., & Ramamoorthy, M. (2000, August 17-18). *Bridge deck deicing using geothermal heat pumps*. The Fourth International Conference on Heat Pumps in Cold Climates. Aylmer, Quebec, Canada.

Sridharan, S., Zhu, J., Hu, G., and Xuan, X. (2011). Joule heating effects on electroosmotic flow in insulator-based dielectrophoresis. *Electrophoresis, 32*(17), 2274-2281. https://doi.org/10.1002/elps.201100011

Sutter, L., Peterson, K., Julio-Betancourt, G., Hooton, D., Van Dam, T., & Smith, K. (2008). *The deleterious chemical effects of concentrated deicing solutions on Portland cement concrete—Implementation guide* (Report No. SD2002-01-G). South Dakota Department of Transportation Office of Research. The Deleterious Chemical Effects of Concentrated Deicing Solutions on Portland Cement Concrete (iowa.gov)

Tayabji, S., Buch, N., & Kohler, E. (2009, April). Precast concrete pavement for intermittent concrete pavement repair applications. In *National Conference on Preservation, Repair, and Rehabilitation of Concrete Pavements*, pp. 317-334.

Tayabji, S. (2019, November). *Precast concrete pavement technology* (No. FHWA-HIF-19-013). U.S. Department of Transportation, Federal Highway Administration American Association of State Highway and Transportation Officials National Cooperative Highway Research Program. https://www.fhwa.dot.gov/pavement/concrete/pubs/hif19013.pdf

Tayabji, S., Ye, D., & Buch, N. (2013). *SHRP 2 Report S2-R05-RR-1: Precast concrete pavement technology*. Transportation Research Board of the National Academies, Washington, DC. https://dx.doi.org/10.17226/22710

Tian, X., & Hu, H. (2012). Test and study on electrical property of conductive concrete. *Procedia Earth and Planetary Science*, *5*, 83-87. https://doi.org/10.1016/j.proeps.2012.01.014

Torres, H. N., Roesler, J., Rasmussen, R. O., and Harrington, D. (2012). *Guide to concrete overlays using existing methodologies* (Report No. DTFH61-09-H-00011 [Work Plan 13]). National Concrete Pavement Technology Center and Institute for Transpiration.

Tuan, C.Y. (2004a). Electrical resistance heating of conductive concrete containing steel fibers and shavings. *ACI Materials Journal*, *101*(1), 65-71.

Tuan, C.Y. (2004b). *Conductive concrete for bridge deck deicing and anti-icing* (Report No. SPR-PL-1(037) P512). Nebraska Department of Roads. https://dot.nebraska.gov/media/5677/final-report-p512.pdf

Tuan, C.Y. (2008). *Implementation of conductive concrete for deicing (Roca Bridge)* (SPR-PL-1(04) P565). Nebraska Department of Roads. Conductive Concrete for Bridge Deck Deicing and Anti-icing (Enr.Com)

Tuan, C.Y., Nguyen, L., & Chen, B.(2010). *Conductive concrete for heating and electrical safety* (International Publication Number WO2010059169 A1), European Patent Office, Munich, Germany. https://www.google.com/patents/WO2010059169A1?cl=en&dq=Electrically+conductive+concrete&hl=en&sa=X&ei=qSTYU_WqKOvMygO24YDABw&ved=0CCIQ6AEwATgU

Tuan, C.Y., & Yehia, S. A. (2002, May 5-7). *Airfield pavement deicing with conductive concrete overlay* [Paper presentation]. 2002 Federal Aviation Administration Technology Transfer Conference, Atlantic City, NJ. https://digitalcommons.unomaha.edu/cgi/viewcontent.cgi?article=1001&context=civilengfacproc#:~:text=This%20technology%20is%20readily%20available%20for%20airfield%20pavement,become%20the%20most%20cost-effective%20concrete%20pavement%20deicing%20method.

Tungjitkusolmun, S., Woo, E.J., Cao, H., Tsai, J.Z., Vorperian, V.R., & Webster, J.G. (2000). Thermal—electrical finite element modelling for radio frequency cardiac ablation: Effects of changes in myocardial properties. *Medical and Biological Engineering and Computing*, *38*(5), 562-568. https://doi.org/10.1007/bf02345754

Viega. (2005). S-no-Ice Snow® Melting System Installation Manual. http://www.viega.us/xbcr/en-us/Viega_S-no-ice_Snow_Melting_System.pdf. Accessed July 15, 2015.

Wu, T., Huang, R., Chi, M., & Weng, T. (2013). A study on electrical and thermal properties of conductive concrete. *Computers and Concrete*, *12*(3), 337-349. https://doi.org/10.12989/cac.2013.12.3.337

Xi, Y., & Olsgard, P. J.(2000, November) *Effect of de-icing agents (magnesium chloride and sodium chloride) on corrosion of truck components* (Report No. CDOT-DTD-R-2000-10). Colorado Department of Transportation, Denver, CO. truckcomponents.pdf (codot.gov)

Xie, P., & Beaudoin, J. J. (1995, June 11-14). Electrically conductive concrete and its application in deicing. In *Proceedings of the Second CANMET/ACI International Symposium on Advances in Concrete Technology*, pp. 399-418, Las Vegas, NV.

Xie, P., Gu, P., Fun, Y., and Beaudoin, J.J. (1995). *Conductive cement-based compositions* (U.S. Patent No. US5447564 A). U.S. Patent and Trademark Office. https://patentimages.storage.googleapis.com/e9/0e/1a/89ba49d83d86eb/US5447564.pdf .

Yang, Z., Yang, T., Song, G., & Singla, M. (2012). *Experimental study on an electrical deicing technology utilizing carbon fiber tape* (Report No. INE/AUTC 12.26). Alaska University Transportation Center.

Yehia, S.A., & Tuan, C.Y. (1999). Conductive concrete overlay for bridge deck deicing. *ACI Materials Journal*, *96*(3), 382-390.

Yehia, S., Tuan, C. Y., Ferdon, D., & Chen, B. (2000). Conductive concrete overlay for bridge deck deicing: mixture proportioning, optimization, and properties. *American Concrete Institute* (*ACI) Materials Journal*, *97*(2), 172-181.

Zhao, H., Wu, Z., Wang, S., Zheng, J., & Che, G. (2011). Concrete pavement deicing with carbon fiber heating wires. *Cold Regions Science and Technology*, *65*(3), 413-420. https://doi.org/10.1016/j.coldregions.2010.10.010

Zuofu, H., Zhuoqiu, L., & Jianjun, W. (2007). Electrical conductivity of the carbon fiber conductive concrete. *Journal of Wuhan University Technology-Mater. Sci. Ed.*, *22*(2), 346-349.

APPENDIX A—LIST OF WRITTEN PUBLICATIONS AND ORAL PRESENTATIONS

Abdualla, H., Ceylan, H., Kim, S., Gopalakrishnan, K., Mina, M., Taylor, P. C, and Cetin, K. S. (2017). *Development of a Finite Element Model for Electrically Conductive Concrete Heated Pavements*. In Transportation Research Board 96th Annual Meeting (No. 17-05389), Washington, DC, January 8-12, 2017.

Abdualla, H., Ceylan, H., Kim, S., Gopalakrishnan, K., Mina, M., Taylor, P. C, and Cetin, K. S. (2017). *Configuration of Electrodes for Electrically Conductive Concrete Heated Pavement*. ASCE International Conference on Highway Pavements and Airfield Technology, Philadelphia, PA, August 27-30, 2017. https://doi.org/10.1061/9780784480946.001

Abdualla, H., Ceylan, H., Kim, S., Gopalakrishnan, K., Taylor, P.C. and Turkan, Y. (2016). System Requirements for Electrically Conductive Concrete Heated Pavements. *Transportation Research Record: Journal of the Transportation Research Board*, *2569*(1), 70-79. https://doi.org/10.3141%2F2569-08

Sassani, A., Ceylan, H., Kim, S., Gopalakrishnan, K., Arabzadeh, A., and Taylor, P. C. (2017). *Factorial Study on Electrically Conductive Concrete Mix Design for Heated Pavement Systems*. Transportation Research Board 96th Annual Meeting of Transportation Research Board, Transportation Research Board, National Research Council, Washington, DC, January 8-12, 2017. https://dr.lib.iastate.edu/handle/20.500.12876/13676

Sassani, A., Ceylan, H., Kim, S., Gopalakrishnan, K., Taylor, P. C., and Arabzadeh, A. (2016). *Electrically Conductive Concrete (ECON) for Application in Airport Heated Pavement Systems*. Student poster competition presentation in the 11th International Conference on Concrete Pavements (ICCP11), San Antonio, Texas, August 28-31, 2016.

Ceylan, H. (2016). *FAA PEGASAS COE Project 1: Heated Airport Pavements*. The FAA PEGASAS COE 4th Annual Meeting, Iowa State University, Ames, Indiana, June 7-9, 2016.

Sassani, A., Ceylan, H., Kim, S., Gopalakrishnan, K., and Taylor, P. C. (2016). *Optimization of Electrically Conductive Concrete (ECON) for Heated Pavement Systems*. Poster presentation at the FAA PEGASAS COE 4th Annual Meeting, Iowa State University, Ames, Iowa, June 7-9, 2016.

Gopalakrishnan, K., Ceylan, H., Kim, S., Yang, S., and Abdualla, H. (2015). Electrically Conductive Mortar Characterization for Self-Heating Airfield Concrete Pavement Mix Design. *International Journal of Pavement Research and Technology*, *8*(5), 315-324. http://dx.doi.org/10.6135/ijprt.org.tw/2015.8(5).315

Ceylan, H. (2015). *Heated Pavements*. The 2015 Iowa Better Concrete Conference, Iowa State University, Ames, IA, November 12, 2015.

Ceylan, H. (2015). *Innovative Materials Technology—Airport Pavements*. The 2015 ASCE Iowa Transportation Conference, Iowa State University, Ames, IA, November 4, 2015.

Sassani, A., Ceylan, H., Kim, S., Gopalakrishnan, K., and Taylor, P. C. (2015). *Optimization of Electrically Conductive Concrete (ECC) Mix Design for Self-Heating Pavement Systems*. Mid-Continent Transportation Research Symposium, Iowa State University, Ames, IA, August 19-20, 2015.

Ceylan, H. (2015). *FAA PEGASAS COE Project 1: Heated Airport Pavements*. The FAA PEGASAS COE 3rd Annual Meeting, Purdue University, West Lafayette, IN, May 27-28, 2015.

Sassani, A., Ceylan, H., Kim, S., and Gopalakrishnan, K. (2015). *A Functional Electrically Conductive Concrete (ECON) for Heated Pavement Systems*. Poster presentation at the FAA PEGASAS COE 3rd Annual Meeting, Purdue University, West Lafayette, IN, May 27-28, 2015.

Ceylan, H., Kim, S., and Gopalakrishnan, K. (2015). *Snow and Ice Preventive Pavement Systems: PEGASAS FAA COE Project No. 1 Heated Airport Pavements*. The 2015 Purdue Road School Transportation Conference and Expo, March 10-12, 2015, West Lafayette, IN.

Ceylan, H. (2014). *PEGASAS FAA COE Project No. 1: Heated Airport Pavements*. the FAA PEGASAS COE 2nd Annual Meeting, June 3-5, 2014, Georgia Institute of Technology, Atlanta, GA.

Yang, S., Ceylan, H., Kim, S., and Gopalakrishnan, K. (2014). *Conductive Concrete for Heated Airport Pavement Systems*. Poster presentation at the FAA PEGASAS COE 2nd Annual Meeting, June 3-5, 2014, Georgia Institute of Technology, Atlanta, GA.

Gopalakrishnan, K., Ceylan, H., Kim, S., Yang, S., and Abdualla, H. (2014). *Self-Heating Electrically Conductive Concrete for Pavement Deicing: A Revisit*. Proceedings of the 94th TRB Annual Meeting, Transportation Research Board, Washington, D.C.